EFFECT OF BOLT LAYOUT ON THE MECHANICAL BEHAVIOR OF BOLTED JOINT

BY

HASSAN KHURSHID

A Thesis Presented to the

DEANSHIP OF GRADUATE STUDIES

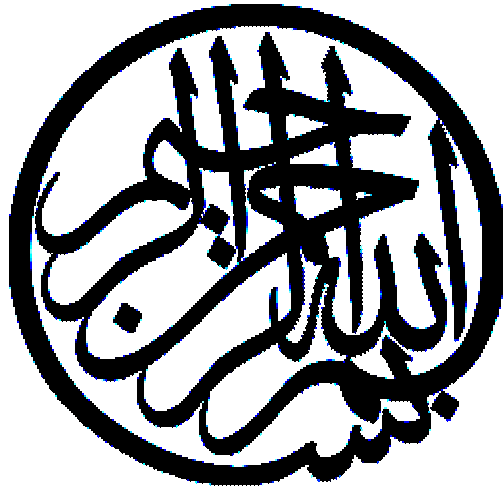## KING FAHD UNIVERSITY OF PETROLEUM&MINERALS

DHAHRAN, SAUDI ARABIA

In Partial Fulfillment of the

Requirements for the Degree of

MASTER OF SCIENCE

In

Mechanical Engineering

April, 2004

In the Name of Allah, Most Gracious, Most Merciful.

KING FAHD UNIVERSITY OF PETROLEUM AND MINERALS
DHAHRAN 31261, SAUDI ARABIA

DEANSHIP OF GRADUATE STUDIES

This thesis, written by **HASSAN KHURSHID** under the direction of his Thesis Advisor

and approved by his Thesis Committee, has been presented to and accepted by the Dean

of Graduate Studies, in partial fulfillment of the requirements for the degree of **MASTER**

OF SCIENCE IN MECHANICAL ENGINEERING.

Thesis Committee

_____
Dr. Yaagoub Al Nassar (Advisor)

_____
Dr. A.F.M. Arif (Co-Advisor)

_____
Dr. Anwar K. Sheikh (Member)

_____
Dr. Nesar Merah (Member)

_____
Dr. Khalid Al Dheylan (Member)

_____
Dr. Faleh Al-Sulaiman.
Department Chairman

_____
Prof. Osama A. Jannadi
Dean of Graduate Studies

_____
Date

Dedicated to My Beloved Mother, late Father, Dada Ji,,Chacha, Umar, Noor and Maryum whose constant prayers, sacrifice and inspiration led to this wonderful accomplishment

ACKNOWLEDGEMENTS

Table of Contents

CHAPTER 2

ONE BOLT MODEL 26

CHAPTER 3

FOUR BOLT MODEL 110

CHAPTER 4

LAYOUT FACTOR 138

CHAPTER 5

CONCLUSIONS AND RECOMMENDATIONS

LIST OF TABLES

LIST OF FIGURES

THESIS ABSTRACT

NAME:	**HASSAN KHURSHID**
TITLE:	**EFFECT OF BOLT LAYOUT ON THE MECHANICAL BEHAVIOR OF BOLTED JOINTS**
DEPARTMENT:	**MECHANICAL ENGINEERING**
DATE:	**13 APRIL, 2004**

A bolted joint is a typical connection that is widely used in machine assemblies, construction of structural components etc. Owing to the easy replacement and installation, bolted joints are very popular. Bolted joint analysis involves many variables like bolt size, diameter, member thickness, number of members, loading condition, number of bolts and their different arrangements. Due to all these factors the analysis is complex. Researchers have used different approaches like analytical, experimental and numerical techniques. The analytical method requires solution of ordinary and partial differential equations, which are not easily obtainable in actual engineering problems. Experimental work requires more resources and time and it is difficult to reproduce in case of any mistake. Because of these facts the use of numerical methods is more practical and time saving. Numerical models can be altered with ease and non-linear behavior can be included if necessary.

In the present work finite element software ANSYS is used to perform a three-dimensional analysis of a single bolt joint. Finite element modeling (FEM) of the joint is discussed with boundary conditions in shear and tensile type of loading. Non-linear effects are included by introduction of contact elements at the interfacing surfaces. The results are reported for different loads due to the applied displacements of 0.06 mm, 0.08 mm and 0.1 mm, different clearances of 0.01 mm, 0.05 mm and 0.5 mm, different pretension of 500 N, 9000 N and 30000 N and different coefficient of friction of 0.1, 0.2 and 0.3. The same three-dimensional model is extended further to four bolts to see the effect of layout on the displacement pattern and stress distribution under shear type loading. Experimental verification is done for the credibility of numerical results. A tool in form of geometrical parameters to compare different layouts in terms of critical bolt is also developed.

MASTER OF SCIENCE DEGREE

KING FAHD UNIVERSITY OF PETROLEUM AND MINERALS

Dhahran, Saudi Arabia

رسالة الماجستير

الاسم: **حسن خوشيد**

العنوان: **دراسة مدى تأثير التوزيع الهندسي لبراغي التثبيت اللولبية على قوى الإجهاد الميكانيكية**

قسم: **الهندسة الميكانيكية**

التاريخ: **13-إبريل-2004**

براغي التثبيت (مسمار التثبيت اللولبي) يعتبر من الأشياء الشائعة الاستعمال في ربط وتثبيت قطع الآلات والمنشآت بعضها ببعض وغيرها وذلك نظرا لسهولة تبديلها وتثبيتها.

إن التحليل ألإجهادي الناتج عن عملية تثبيت هذه البراغي، يتأثر بعوامل كثيرة منها: حجم البرغي نفسه، وقطره، وعدد الألواح التي يراد تثبيت بعضها ببعض، وظروف تطبيق القوى وعدد البراغي المستخدم لذلك وطريقة توزيعها. لهذه الأسباب كلها تعتبر دراسة هذه الأمور من الأمور الصعبة. إن المهتمين لهذا النوع من الدراسة استخدموا عدة محاور وطرق منها النظري أو التحليل الرقمي أو بالدراسات المعملية. أما الطرق النظرية فتتطلب وجود حلول للمعادلات التفاضلية الاعتيادية والجزئية منها والتي في أغلبها لا يمكن إيجادها في الحقيقة.أما الطرق المعملية فتتطلب وقتا طويلا و موارد مالية كبيرة وليست من السهولة إعادة التجارب نفسها وبظروفها فيما لو حدث أي خلل. لهذه الأسباب المتعلقة تصبح الطرق الرقمية أكثر فعالية واختصارا للوقت والجهد فمن خلال الطرق الرقمية يمكن تغيير أو اعتبار أي من العوامل المؤثرة في التحليل بسهولة ويسر.

في هذه الدراسة استخدمت طريقة العنصر المحدود بأبعاده الثلاثة وذلك من خلال برنامج (ANSYS) لتحليل الإجهادات في براغي التثبيت. ولقد تم شرح النموذج المستخدم في هذه العملية وطريقة تأثير القوى عليها والتي تتضمن القوى الشدية والقوى القصية . كما أضيف التأثير الغير خطي في هذا النموذج من خلال تمثيل للأسطح المتقابلة والمتلامسة فيه بالعناصر المحدودة المناسبة.

إن نتائج هذا البحث تضمنت الإجهادات المترتبة نتيجة تأثير عدة إزاحات هي 0.6 ملم و 0.8 ملم و 0.1 ملم وعدة فروقات الخلوص في الأقطار وهي 0.01 ملم، 0.05 ملم ،0.5 ملم وقوى شدية أولية هي 500 نيوتن، 9000 نيوتن و 30000 نيوتن كما تضمنت عوامل احتكاك مختلفة هي 0.1، 0.2 ، 0.3 .

بعد هذه الدراسة المركزة على واحد من البراغي تم توزيع النموذج ليشمل أربعة براغي تثبيت لدراسة تأثير توزيعها على اللوحين المراد تثبيتها تحت تأثير قوى القص. وأخيرا تم خلال هذه الدراسة بإجراء تجارب معملية للتأكد من صحة وسلامة النموذج الرقمي. كما انتهت الدراسة بإيجاد علاقة تربط بعض العوامل الهندسية لمقارنة بعض نماذج توزيع البراغي بعضها ببعض وذلك من خلال تحديد أكثر البراغي حرجا (أكثر إجهادا).

CHAPTER 1

INTRODUCTION

1.1   BACKGROUND

Bolted joints are extensively used in most modern machines since more than 65% [6] of all parts in machines are assemblies. The key feature of bolted joints is that they can be dismantled comparatively easily. In the assembly of machines threaded fasteners are immensely important, as the links of the interacting parts, they are the ones that transmit forces, created by the load, to joined parts. In recent years, however a series of newsworthy events, many of them tragic, have made the designers realize that the threaded fasteners play major role in our life. Oil drilling platforms have tipped over, airplane engines have failed, roofs have collapsed and astronauts have died due to the bolted joint failures. The nuclear regulatory commission of US has declared *Bolting* to be an unresolved generic safety issue with number one priority, even though no bolt related accidents or equipment failures have occurred in that industry. The basic problem in the design of bolted joint is the number of variables involved like shapes, materials, dimensions, number of bolts, working loads and working environment also. Since the fasteners become loci of concentrated forces within the machine, we focus on threaded fasteners and there different types.

1.2 TYPES OF THREADED FASTENERS

In the assembly of machines threaded fasteners are immensely important. They are the ones that transmit forces, created by the a load, to joined parts and are the loci of concentrated forces within the machine. Sizes of the threaded fasteners mainly depend upon the availability of space for parts. The forms of the fasteners are dictated by the constraints on the design. Commercially three forms are available as shown in the figure 1.1.

1.   Fasteners comprising a bolt and nut

        The connected parts are clamped between the bolts head and the nut

2.   Fasteners that are screws in the form of a bolt without a nut

        The fastener is introduced into one of the parts, pulling the other part to create the connection

3.   Fasteners having a headless bolt and nut

        A stud is introduced permanently into one of the parts, while a nut clamps the part together.

1.3 PARTS OF A BOLTED JOINT

The study involves the analysis of threaded fastener comprising head and nut more often called as bolted joint. Bolted joints are generally made up of the bolt group, which consists of head, stud nut and top and bottom flanges (members) as shown in the figure 1.2. Bolted connections are designed to hold two or more flanges or members together to form an assembly. In case of liquid flowing in the pipes, gaskets are added in between the flanges to avoid the leakages. Because of the different loading conditions especially high loads, bolted connections can separate. In a bolted joint the thing that interconnects the

parts are the bolts. Their sole function is to clamp the members together. The behavior and life of the joint usually depends on the correctness of the clamping force holding the parts together. Bolted joint is not a passive object, it responds to the forces and pressures and environment to which it is subjected.

1.4 FORCES IN THE BOLTED CONNECTIONS

The forces in the bolt are mainly axial forces. Subsequently the bolt elongation is the dominant deformation. Because of the prevailing axial action, one-dimensional bolted joint is considered. Bolts installed in machine components undergo two-stage loading: preloading at the assembly and the subsequent loading caused by the acting forces in the working parts.

1.4.1 Preloading

The preloading force is caused by the application of torque in tightening the nut. An estimate of the force can be derived by established of an empirical relation,

$$T = C F_i d \tag{1.1}$$

Where T is the torque and F_i denotes the axial force (preload) in the bolt, C is an empirical coefficient that can be assumed to be 0.2, based on experience [1] and d is the outer diameter of the bolt. There are ways of getting more accurate measurement of T using, for instance, a special torque wrench or measuring the nut displacement.

The preloading is also called in some literature pretension. This insures that the connection will not separate, provided the load remains under the pretension already applied. Figure 1.3 shows that on applying pretension, force in axial direction is produced in the bolt. Process of preloading is illustrated on the working of a bolted joint comprising two members, bolt and nut.

By applying one-dimensional analysis assuming that all the forces and displacements act in the axial direction of the bolt. The preloading causes a bolt extension, as shown in figure 1.4

$$\delta_b = \delta_b' + \delta_b'' \qquad (1.2)$$

where, δ_b = absolute value of the bolt displacement (tension or compression)

δ_b' = bolt displacement at nut side of the bolt (see figure 1.4)

δ_b'' = bolt displacement at bolt head side (see figure 1.4)

and causes compression of the plates.

$$\delta_c = \delta_c' + \delta_c'' \qquad (1.3)$$

where, δ_c = absolute value of displacement of members (tension or compression)

δ_c' = upper member compression (see figure 1.4)

δ_c'' = lower member compression (see figure 1.4)

Figure 1.4 shows that together these absolute displacements form a grip displacement that equals

$$\Delta_{bc} = \delta_b + \delta_c \qquad (1.4)$$

The grip displacement amounts to the difference between the dimensions of the unloaded bolt and members. Assuming the bolt and member deflections δ_b and δ_c, to be a linear function of preloading force, then condition for equilibrium to be hold is,

$$F_b = F_c = F_i \qquad (1.5)$$

$$\delta_b = \frac{F_i}{k_b} \quad \text{and} \quad \delta_c = \frac{F_i}{k_c} \qquad (1.6)$$

Where, k_b and k_c are the stiffness of the bolts and the members respectively. Consequently the grip displacement equals,

$$\Delta_{bc} = F_i \left(\frac{1}{k_b} + \frac{1}{k_c} \right)$$ (1.7)

1.4.2 Bolted Joints under Tensile Load

Axial tension loads are always present due to the preloading of the bolts when they are tightened. These bolts dominate the behavior of the joint even when other types of loads are present. Consider the bolt flange connection of a pressure vessel. The final bolt loading is defined after initial tightening and an outer applied force F_p, caused by the internal pressure in the vessel. For simplicity, assume that only part of the flanges is participating. Let F_b be the tensional force in the bolt while applying pressure in the vessel, while F_c is the resulting compressive force acting on the flanges. The condition of equilibrium states that

$$F_b = F_p + F_c$$ (1.8)

The compatibility condition requires that grip displacement which is the difference between the dimensions of the unloaded bolt and flange (member) remains unchanged i.e,

$$\Delta_{bc} = \Delta_{bc+p}$$ (1.9)

$$\Delta = \left(\frac{F_b}{k_b} + \frac{F_c}{k_c} \right) = F_i \left(\frac{1}{k_b} + \frac{1}{k_c} \right)$$ (1.10)

Combining the Equations 1.7 and 1.8, we obtain the expression for F_b and F_c as follows,

$$F_b = F_i + \left(\frac{k_b}{k_b + k_c} \right) F_p$$ (1.11)

$$F_c = F_i - \left(\frac{k_c}{k_b + k_c} \right) F_p$$ (1.12)

1.4.3 Bolted Joints under Shear Load

In a shear joint the external loads are applied perpendicular to the axis of the bolt. A joint of this sort is called a shear joint because external load tries to slide the joint members past each other and/or to shear the bolts. The strength of such a joint depends on (1) the friction developed between the joint surfaces and/or (2) the shearing strength of the bolts and the plates. Joints loaded in shear are formally classified as either friction type or bearing type.

In friction type no slip occurs therefore there are no shearing forces on the bolts and all the bolts are essentially loaded equally. As long as the joint does not slip, the tension in one set of plates is transferred to the others as if the joint are cut from a solid block.

In bearing type joints, the external loads, rise high enough to slip a friction type joint. As a result the joint plates will move over each other until prevailed form further motion by the bolts. The stress patterns in bearing type joints are more complex than those in friction type joints. The tension in one set of the plates is transmitted to the others in concentrated bundles through the bolts. Each row of the bolt transmits a different amount of load. The outermost fasteners always see the largest shear loads

1.5 BOLT AND FLANGE STIFFNESS

Stiffnesses k_b and k_c are functions of geometry and the elastic constants of the bolt and flange. Assuming a one-dimensional condition the bolt stiffness k_b is defined as follows

$$k_b = \left(\frac{A_b E_b}{l_b} \right) \tag{1.13}$$

where, A_b = major diameter area of the bolt of the bolt

l_b = length of unthreaded portion of bolt in grip

A one-dimensional model of the flange used in machine design is shown in figure 1.5. It is assumed that the flange is made up of two truncated cones, with their stiffnesses equal to that of the flange. The stiffness of the member can be defined as

$$k_c = \left(\frac{A_c E_c}{l_c} \right) \tag{1.14}$$

where A_c is the nominal cross section which is equal to the mean cross section of the two cones. Disregarding the thickness of the washer, l_w and assuming that $l_b = l_c$, then the coefficients in the equation 1.10 and 1.11 take the form

$$\kappa_b = \left(\frac{k_b}{k_b + k_c} \right) = \left(\frac{A_b E_b}{A_b E_b + A_c E_c} \right) \tag{1.15}$$

$$\kappa_c = \left(\frac{k_c}{k_b + k_c} \right) = \left(\frac{A_c E_c}{A_b E_b + A_c E_c} \right) = 1 - \kappa_b \tag{1.16}$$

1.6   BOLTED JOINT ANALYSIS

1.6.1   Purpose

Bolted joints when put in use encounter one or more types of working loads. These include tension loads, shear loads, cyclic loads or combination of these. These loads are produced by factors as diverse as snow on a roof, pressure change in a pipeline or vibration in a lawn mower engine. Purpose of bolted joint analysis is to identify the failure modes like end tear out, bearing, net section fracture and bolt shear. This analysis also involves the identification of critical bolt in a connection and the critical region in the
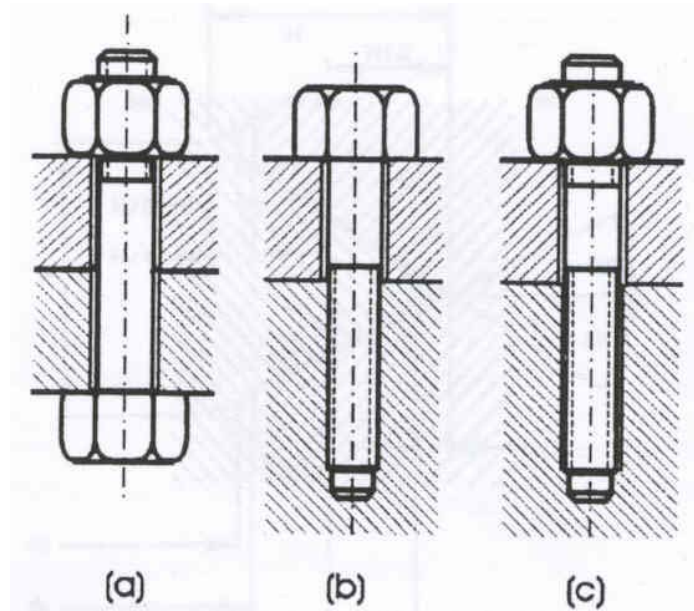
Figure 1.1: Threaded fasteners: (a) bolt with nut, (b) screw and (c) stud with nut
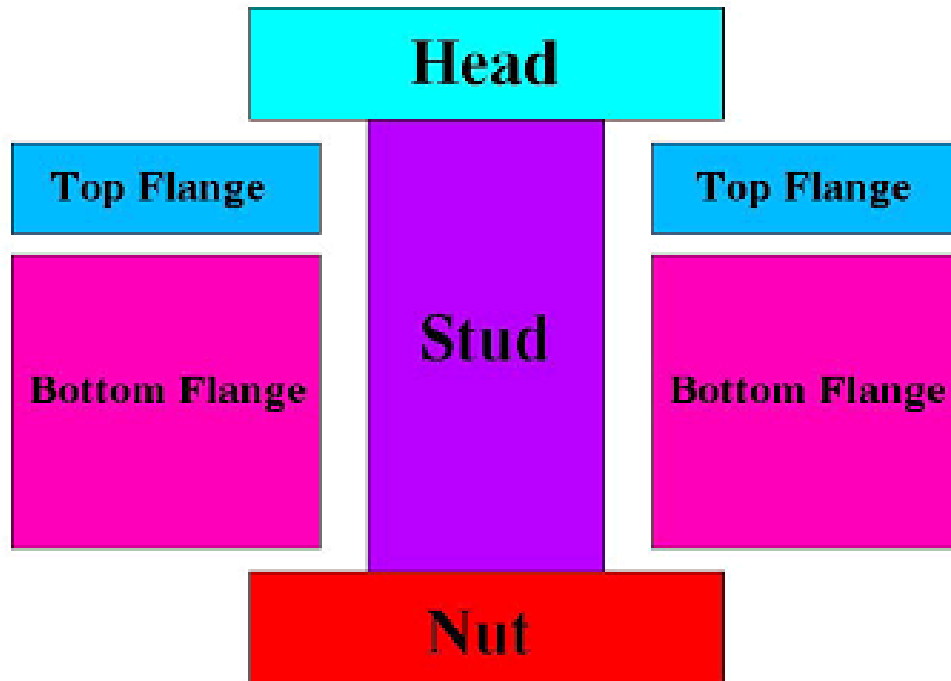
Figure 1.2: Bolted joint basic parts
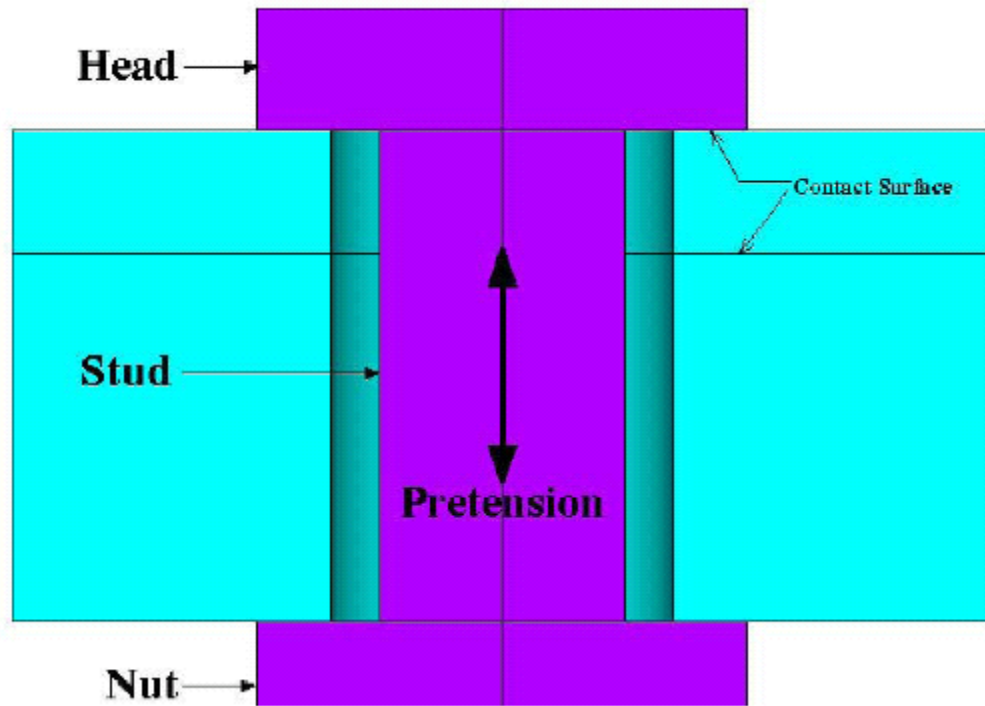
Figure 1.3: Pretension in axial direction of the bolt
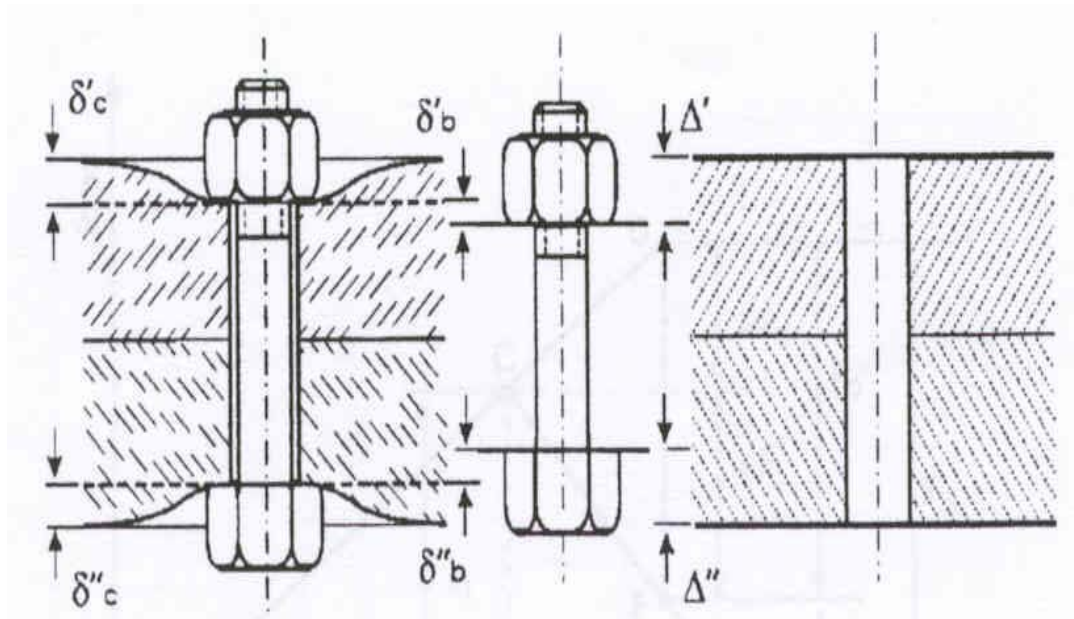
Figure 1.4: Preloading of bolt and nut
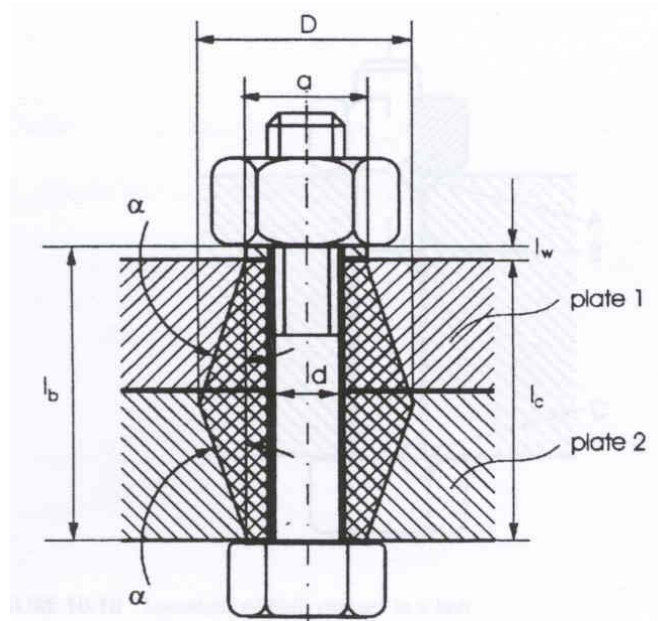
Figure 1.5: One-dimensional model of a bolted joint

member. Bolted joint analysis is of a diverse complexity thing as it involves number of factors. Some of which are given below:

- Bolt pretensioning

- Contact between plates

- Bolt deformation

- Bolt size

- Clearance between the flange and the bolt

- Number of bolts used

- Loading conditions

- Supporting conditions

- Number of plates or flanges

- Bolt layout when more than one are used

- Friction between the clamped plates or flanges

1.6.2   Analysis Approach

Researchers have used analytical, experimental and numerical techniques to analyze the bolted connections. Analytical solution requires solution of ordinary and partial differential equations, which are not usually obtainable in actual engineering problems. Analytically first step of bolted joint analysis is to calculate the stiffness of the bolt and the member. For the stiffness of the bolts formula contains the tensile stress area, major diameter area of the bolt, length of threaded portion and unthreaded portion in the grip. But for the members situation is somewhat different. There may be more than two members in the grip of a connection. All together these act like compressive springs in

series. Stiffness of the member is difficult to obtain, except by experimentation. Because the compression spreads out between the bolt head and the nut and hence the area is not uniform. Some analytical methods exist for approximating the stiffness. Ito [2] suggested the use of Rotscher's pressure cone method with a variable cone angle. This method is quite complicated so there are others such as method of Mischke [3] with cone angle of 30 and method of Motosh [4]. These methods overestimate the clamping stiffness. Once the stiffness is calculated the resultant bolt load and resultant load on members can be calculated with the help of equation 1.10 and 1.11. Another shortcoming in the existing analysis of bolted joint is when bolted joint is loaded in shear. That is, if there is more than one bolt in a connection, generally the shear is divided equally among the bolts so that each bolt takes equal force. This is not true. So there is a limitation of the analytical methods to predict the stress in a member. Experimental work requires more resources and time and it is difficult to reproduce incase of any thing go wrong. Time and cost are always a restriction of doing extensive experimentation.

Because of these facts the use of numerical methods are more useful and time saving. Model can be altered with ease and non-linear behavior can be included if necessary. Numerical methods that are of concern in this study are the finite difference method and finite element method. Finite difference method usually employs the solution of differential equations where as finite element method involves the solution of integral equations. In this study, finite element method is employed to carry out analysis. Finite element analysis can be divided into two branches, linear and non-linear finite element analysis. The standard formulation for the finite element solution of solids is the displacement method, which is widely used and effective. The basic process is that the

complete structure is idealized as an assemblage of individual structural elements. The element stiffness matrices corresponding to the global degrees of freedom of the structural idealization are calculated, and the total stiffness matrix is formed by the addition of the element stiffness matrices. The solution of equilibrium equations of the assemblage of elements yields the nodal displacement of the model. With the availability of fast machines and powerful finite element softwares that carry wide spectrum of elements degree of freedom, it is now easy to use this technique. Finite element method now provides a more realistic and workable solution technique for wide and diverse engineering problems, as it has the capability of handling somewhat complicated and irregular geometries, non-linear properties and no homogenous load distribution. Existing finite element analysis of bolted joint usually consists of linear modeling without considering the contact behavior between the thread and the bolt interface.

1.7   LITERATURE SURVEY

This section gives us a brief over view on the work done by different researchers on bolted joints analysis. From earlier discussion it is clear that use of numerical technique is suitable to analyze the bolted connection. The literature survey that is reported here is aimed in that direction highlighting, mainly, the different methods used to model the bolts and bolted joints numerically followed by the experimental work contributed in this line of study.

1.7.1   Axisymmetric Model

Effects of bolt threads on stiffness of bolted joints are studied by Lehnhoff et al [5]. They did axisymmetric linear study on the threads in order to   determine their effects

on the bolt and member stiffnesses. Different materials for the members were used. Stiffness was measured by first applying no load and then increasing the external load. 24, 20, 16 and 8-mm-dia bolts were used for the analysis. Comparison was made to published results that did not include the influence of the threads.

Also Lehnhoff et al [6] have studied the stress concentration factors for the threads and the bolt head fillet in a bolted connection. The FEA models consisted of axisymmetric representations of a bolt and two circular steel plates each 20 mm in thickness. The bolts studied were 8, 12, 16, 20, and 24-mm-dia grade 10.9 metric bolts with the standard thread profile. A comparison was made to stress concentration factors typically used in bolted connection design. Thread stress concentration factors were highest in the first engaged thread and decreased in each successive thread moving toward the end of the bolt.

A study that examined the stress analysis of taper hub flange with a bolted flat cover was carried out by Sawa et al [7]. They have done numerical and experimental work. The model that they considered was an axisymmetric and elastic limit is not crossed. A bolted connection consisting of a cover on a pressure vessel flange with a metallic flat gasket on raised faces was analyzed as a four-body contact problem using axisymmetric theory of elasticity. The contact stress distribution, the load factor, and the gasket properties were examined. In their analysis, the cover was replaced with a finite solid cylinder. The metallic flat gasket, the flange, and the hub were replaced with finite solid cylinders. The effects of the stiffness and the thickness of various size gaskets on the contact stress distribution were obtained by numerical calculations. The analytical results obtained are shown to be consistent with the experimental results.

M. Tanaka et al [8] used finite-element analysis method to incorporate the plasticity theory and the von Mises yield criterion. The model used was axisymmetric considering the geometry of the threads. In their study, they discussed the behavior of bolted joints tightened in plastic region. Moreover, in the previous analyses, very idealized models of cylinder have been used assuming the uniformly distributed axial stress and a state of pure shear. In this study, the finite element method was successfully applied to the elastoplastic analysis of bolted joints. The method proposed by them was applicable to the case with complicated geometry of bolt and was superior to the conventional one taking into account the simple yield criterion based on rigid-plastic model. The numerical results agree with the experimental ones obtained by other researcher.

1.7.2   Two Dimensional Model

Mechanical Behavior of Bolted Joints in various clamping configurations is examined by Fukuoka et al [9]. They made use of two-dimensional model but not considering yielding. In their work, mechanical behaviors of bolted joints in various clamping configurations were analyzed using FEM as multi-body elastic contact problem, and the effects of nominal diameter, friction and pitch error upon stress concentrations were evaluated for through bolts, studs, and tap bolts. In addition, the tightening process and strength of a bottoming stud, which have seldom been studied despite favorable performance in preventing stress concentration at the run out of threads, were also investigated.

A non-linear finite element model with contact elements was developed by Varadi et al [10] to evaluate the contact state of a bolt-nut-washer-compressed sheet joint system. Applying the proper material law the non-linear behavior of the members of the joint was

studied in terms of the clamping force. Based on their finite element results the load distribution among the threads in contact and the real preload diagram of the system was evaluated. They advised to use heat-treated washers to produce required clamping force.

Again, Fukuoka et al [11] studied the mechanical behavior of bolted joint during tightening such as variations of axial tension and torque. They investigated this issue both experimentally and numerically. The model they used was two-dimensional and non-linear analysis was carried out. The friction coefficients on pressure flank of screw thread and the nut-loaded surface were estimated by measuring the total torque applied to nut, axial tension and thread friction torque. A comparison between the axial tension and torque variation had been performed.

Lin et al [12] did two-dimensional linear analysis of a simple bolted joint. Finite element results were compared with theory [3]. Here the stiffness of the clamped member was calculated. The model is simple that is one bolt with two plates. It was assumed that the bolt head load was applied through a washer. They changed the bolt aspect ratio d/L to observe its effect on the stiffness.

Andreason et al [13] used the stress results of a two-dimensional finite element analysis to understand failure modes of a bolted joint in low-temperature cure woven (CFRP) laminates loaded in tension, and to predict the bearing strength. It was a non-linear analysis. Maximum stress and point stress failure criteria are employed to determine the loads for damage initiation and final fracture.

1.7.3   Three Dimensional Model

Abdel Hakim Bouzid et al [14] studied the effect of flange rotation and radial distribution of the gasket contact stress in non-linear gasket. Three-dimensional FE model of flange and bolts were made. Gasket axial displacements and contact stresses were studied against gasket width ratio. Different types of flanges were used. Their results of finite element were compared to experiment ones.

The three-dimensional finite element analysis of bolted joints with finite sliding deformable contact has been studied by Chen et al [15]. The helical and friction effect on the load distribution of each thread was analyzed. They showed that the analytical analysis by Yamamoto's method reaches a lower value of load ratio than the finite element analysis at the first thread. The load distribution on each thread between axisymmetric model and three-dimensional model were provided. Elastic limit was assumed.

The nonlinearity in compression stress-strain relationship of the gasket is considered by Cao et al [16]. The model was a parameterization model so that the geometry, material properties and loads can be easily changed to study their effects on the joint behavior. They applied two types of loads, the tightening torque and the pressure applied to the flange. In their study the bending of flange, the extension and bending of bolt, and the non-uniform distribution of gasket compression were also simulated.

The authors Al Jefri et al [17] have done a comprehensive investigation for the characteristics of bolted joints under different static tightening loading conditions. Various geometrical conditions with different bolt head diameter/bolt diameter ratios, different plates thickness ratios, different plates width/bolt head diameter ratios, different plates length/plates width ratios were considered during the investigation. The results were presented on the basis of non-linear analysis of the problem.

Part of the results reported by Bose et al [18] was devoted to the analysis of unstiffened flush end-plate steel-bolted joints by means of the finite-element technique. The flush end-plate joint represents an extremely complex and highly indeterminate analytical problem with a large number of parameters affecting its structural behavior. A three-dimensional quarter model was considered and non-linear analysis was performed using a finite element package. The variables in this study were the two beams, bolt sizes and columns. The results were compared to an experimental result.

The three dimensional fatigue analysis of a simple beam model is carried out by Kerekes et al [19]. For checking of their model, the Steyr-Daimler-Puch AG, Technologie Zentrum Steyr and the Department of Steel Structures of the Technical University of Budapest carried out a fatigue test and a numerical calculation of flange plate connections with prestressed bolt joints. Bolted joints were studied in three different positions under static and dynamic loading. They had made use of the symmetry of the problem and load was applied in steps.

A very interesting study was done by Wheeler et al [20]. A three dimensional finite element analysis of bolted end plate connection was carried out. But here four bolts are considered in the connection. Loading was also done in five steps and von Mises stress distribution was obtained in this case. The results were compared to the experimental results.

In the area of bolted joints researchers have made use of finite element packages in order to improve the existing equations. One such effort is being made by Rogers [21]. He showed that the load-capacity formulations presented in the American Iron and Steel Institute (AISI) Specification cannot be used to accurately predict the failure modes of thin cold-formed sheet-steel bolted connections that are loaded in shear. A modification to

the bearing-coefficient provisions, to account for the reduced bearing resistance of the connected materials, is necessary and has been proposed. He concluded that a revision of the net-section fracture design method is also required and stated some recommendations concerning the procedure that is used to identify the net-section fracture and bearing-failure modes.

In [22], Jerome Montgomery looks at a few methods for modeling pretension bolted joints using finite element method. Pre tension is modeled using ANSYS pre tension elements, which can be used on solid and line element also. Surface to surface contact elements are used to account for varying contact distribution along flanges. Bolt head and nut behavior is modeled by coupled nodes, beam elements, rigid body elements or solids. Bolt stud is modeled by solid elements, pipe elements or link elements. The pros and cons of different simulations are also discussed.

1.7.4 Experimental Work

Some researchers have carried out experimental work on the bolted joints. Menzemir et al [23] studied block shear failures of bolted joints were studied for different arrangements of bolts. Strain distributions around the periphery of the connection were measured and then they were compared to finite element predictions.

The behavior of truss plate reinforced by single and multiple bolted connections in parallel strand lumber under static tension loading were investigated by Hockey et al [24]. Sixty single bolt connections were tested and similarly sixty multiple bolt connections were experimented. Their effect on the ultimate tensile strength of the connection was observed. It was also observed that reinforcement significantly improved the ductility in all the connections tested.

Design Criteria for Bolted connection elements in Aluminum Alloy 6061 is reported by Menzemir et al [25]. Plates of relatively thin cross section and extruded shapes held by one or more bolts were tested in tension and shear. It was observed that localized necking and shear leaves behind an orange peel like toughness on the surface of the specimens. Boltholes along both the tensile and shear planes were elongated. Also those holes located near the edge of the specimen were elongated and noticeably rotated with respect to the far filed load axis. Their finding was that block shear failure is a potential limit state for connection plates having mechanical fasteners and should be considered in the design process.

A similar type of study is done by Tan et al [26]. They studied the effect of bolts in rows. Experiments confirm that there is a reduced effective capacity per bolt with any increase in the number that is placed in a row. This is called row effect on strength. They actually gave an elasto plastic model.

Andreasson et al [27] studied CFRP woven laminates with bolted joints. They investigated both experimentally and numerically. Double lap bolted joint test fixture was used to do the experiments. The sheet was tested in the shear force. All specimens were tested to failure by applying load through the bolts. It was observed that failures were either in net tension or bearing modes. In all specimens failure initiated at both edges of the hole in the net section due to a high local stress concentration factor and final fracture occurred in a single shear mode.

1.7.5   Geometric Factors

Many researchers in different discipline are very much motivated to develop or establish empirical relations interrelating the geometric aspect of the model under consideration because they are easy to control and adopt. Establishing such geometrical factors is very handy and fast for design and safe operations.

Arif et al [30] have developed a shape complexity factor in hot extrusion of aluminum alloys. In their study, they presented results about the relationship between die profile and modes of die failure. A total of 616 die failures involving 17 different die profiles were studied, in collaboration with a local industrial setup. All dies were made of H-13 steel, while the billet material was Al-6063 in all the case. The analysis presented here reflects three different perspectives: (a) overall and class-wise break-up of failure modes, (b) failure analysis for dies of different complexities, and (c) shape-wise breakdown of each failure mode.

G.C.J. Bart et al [31] obtained shape factor for transient heat conduction in arbitrary objects for which no analytical solution exists. Such a shape factor is the dominant parameter in the prediction of heat transfer processes. The procedure has been applied and compares favorably with other existing methods. Some data is given for transformation between the different parameters that are in use to describe shape or geometry, including those for an equivalent one-dimensional object.

V.Sheshdari et al [32] carried out a study around a circular pipe using computational fluid dynamics (CFD) code, fluent to establish the effect of body shape on the annubar factor. It is found out that the annubar factor for elliptical shape with high

slenderness ratio has the highest annubar factor and minimum permanent pressure loss. Rounding of the edges of a standard diamond shaped annubar improves its performance. The permanent pressure loss is comparatively lower than that for the orifice meter and the annubar factor is constant above a critical Reynolds number. The annubar factor reduces with increase in blockage factor.

F Osweiller et al [33] describes rules in designing fixed tube sheet heat exchangers. The purpose of this paper is to present the rules relative to the fixed-tubesheet heat exchangers and compare them with the rules provided by the Tubular Exchanger Manufacturing Association (TEMA). The tubesheet is replaced by an equivalent solid plate for which the effective elastic constants are given by original curves depending on the ligament efficiency and on the ratio of tubesheet thickness to tube pitch. The connection of the tubesheet with the shell and the head is simulated by considering the tubesheet as being elastically clamped at its periphery: this allows one to treat, in a continuous way, simply supported and clamped tubesheets and to avoid arbitrary choices by the designer between those two extreme cases. The method enables the calculation of the maximum stresses in the tube-sheet, tubes, shell and head, which are limited to allowable stresses established according to the stress category concept of ASME VIII, division 2. These rules lead generally to thinner tubesheets than those arising from TEMA whilst still providing more overall safety due to a better representation of the tubesheet behavior. Arif [34] has studied the effect of fasteners on the joint behavior. Different configurations were analyzed. A layout effect prediction tool in terms of geometry was developed. The prediction of this tool was found to be quite effective in comparing various layouts for same shear joint.

1.8 CURRENT RESEARCH

1.8.1 Motivation

Summarizing the literature survey it is observed that the effect of factors like pre tension, clearance, layout effect etc have not been reported much. Literature on the deformation pattern and stress distribution in the member, nut and bolts is also limited. Researchers have used mostly two-dimensional and axisymmetric models. Few works are there in three-dimensional bolted joint analysis. However these models have some details ignored like head of bolt, stud etc. Due to the absence of the bolt in the finite element model, stress distribution cannot be visualized in the bolt itself and the load is not transferred through the bolts to the members.In some cases bending loads and head/nut temperatures are not accounted for. Moreover pretension effect, clearance, friction and deformation pattern cannot be investigated with the models proposed by earlier researchers. Other factors that prevent the use of simpler models are that there are localized points of high stress regions in the plates and the bolts. These critical points cannot be visualized properly. When a thick plate is loaded in shear, deformation behavior is not uniform throughout the plate thickness. In the axisymmetric and two dimensional models, the helical shape of thread is not modeled which results in less accurate analysis of the thread. In all existing approaches, it is always considered that the load sharing is equal in all the bolts. This assumption is not true. Bolts come under different loads when a bolted joint is loaded. All these limitations motivate the need of full three dimensional finite element model.

1.8.2 Objectives of Current Work

On the basis of the above mentioned short comings in finite element modeling of a bolted joint, the main objectives of the current work are as following

1. Make a three-dimensional full model of a bolted joint including the threads, pretension and the contact condition between the mating surfaces.

2. Analyze the above 3D model in shear and tension using finite element software (ANSYS).

3. Validate the FE results by comparing them to experimental data.

4. Investigate the effect of bolt layout (arrangements) on the mechanical behavior of bolted joint. It means to study the displacement pattern and stress distribution in the plates and bolts.

5. Develop a geometrical tool based on the numerical results to compare different layouts.

1.8.3 Approach

First, a one bolt joint model is developed to study the effect of clearance between the bolt and hole of the plate, the effect of friction between the adjacent plates, and for the different cases of pretension values. These effects have been evaluated by investigating the stress distribution through all the members of model assembly. For validating purpose, an experiment has been carried out for one bolt model. Strain gages are placed on the loading and supporting plates around the bolts. The work is further extended to four-bolt model. The effect of layout is studied on this four-bolt model. These investigations are based on the displacement pattern and stress distribution. Four-bolt model is also validated qualitatively by means of an experiment. Two-dimensional models of different layouts are analyzed and the results are confirmed through the three-dimensional finite element model. Same two-dimensional models are then used to derive a layout factor in terms of geometric parameters. Such studies are very common in many engineering fields.

The layout factor is helpful in comparing different layouts in terms of critical bolt. Various layouts of 2, 3, 4, 6 and 8 bolts are used in the current work.

1.8.4 Organization of Thesis

The thesis comprises of five chapters. The first chapter gives brief introduction of bolted joint analysis, literature survey and definition of problem. Chapter two consists of three-dimensional model of a single bolted joint. The effects of pretension magnitude, clearance size between the bolt and plate holes and level of friction are investigated. The displacement patterns and stress distributions are examined. An experimental verification is also reported in this chapter. Chapter three contains the study on the three dimensional model of four bolted joint. Stress distribution and displacement patterns are discussed in detail. For four-bolted joints shear type loading is considered only. Results of experiment on four-bolted joint model are also included. The development of a layout factor is reported in chapter four. The procedure in reaching a correlation that applies to different bolt layouts is discussed in detail. Chapter five gives the conclusion of overall research with the limitations and recommendations.

CHAPTER 2

ONE BOLT MODEL

2.1   INTRODUCTION

Factors like pretension, clearance and coefficient of friction are very important to consider when analyzing a bolted joint. Not much work is reported in this particular area using three dimensional finite element models. In order to see the layout effect on the behavior of joints there is certainly a need to see how these factors affect a bolted joint behavior. This chapter addresses the effect of these factors on a one-bolt joint finite element model. Finite element analysis approach is employed and software package ANSYS is used to analyze the bolted joint. The software has capabilities like modeling the pretension effect easily. Special pretension element is provided. Secondly the mating surfaces of the two plates involve the relative motion of these two surfaces when load is applied. Therefore the amount of friction level can be incorporated in ANSYS. All these features are very helpful in modeling the joint realistically. In this chapter one bolt joint is analyzed first under shear load. Pretension, clearance, and coefficient of friction values are investigated. Their effects are examined by looking through the displacement patterns and stress distributions. To support the numerical finding an actual experiment of one bolt model set up under shear loading is conducted. Again one bolt model is further analyzed using tensile type of loading. The results of displacement and stress are then evaluated and discussed.

2.2   GENERAL FEATURES OF FE MODEL

The model is three-dimensional and the load is applied in shear. The displacement and the stress distribution in the members, bolt and nut are studied. Elastic analysis with contact elements placed at the contacting surfaces is performed. Contact elements predict the real situation by taking into account the effect of the coefficient of friction between the two mating surfaces. Assembly of a bolted joint model is shown in the Figure 2.1.

Where LP stands for loading plate, displacement is applied on the upper surface of this plate while SP stands for supporting plate; lower area of this one is being constrained Side of SP towards the bolt head is called as bolt side of SP and the side of LP towards the nut is called as nut side of LP. The interface surfaces are named as interface side of SP and LP. Same terminologies are used when the results are discussed.

2.3   FE MODEL BUILDING

The first step in carrying out a finite element analysis is to build the geometry. The two plates are easily modeled with the help of ANSYS command (BLC4). For modeling the nut and bolt head, ANSYS command (RPR4) is used. This command is used to make the three dimensional hexagon. The main task was to make the thread of the bolt. There is no built-in command or function in ANSYS that automatically generates the thread on the bolt. To model the threads equation of helix (*acos(t) +asin(t) +ct*) is used in order to get the keypoints. *a* is the radius, *t* is the angle between 0° to 360° and *c* is the parameter that controls the height of the helix. It is this parameter by which helix can be made course or fine. Total of thirty-eight keypoints are generated and are joined together in ANSYS program with the help of splines. Once having the pattern of helix, a small triangle is being made at one corner of the helix line. This triangle is oriented in the YZ plane. This

triangle is then dragged along the helix line to form one cycle of thread. The command (VDRAG) is used for this purpose. Figure 2.2 shows the steps followed to generate series of threads in ANSYS. The dimensions of SP and LP used in the model are same i.e. *70mm x70mm x10mm*. Bolt and nut of *M16 x 2* are used Figure 2.3 shows the individual parts of the bolted joint.

2.3.1   Type of Element

The first step is to define right element for the finite element modeling of the bolted joints. For this problem visco 107 is chosen. Visco107 is used for 3-D modeling of solid structures. It is defined by eight nodes having three degrees of freedom at each node: translations in the nodal x, y and z directions. The shape of the element can be seen in the Figure 2.4.

2.3.2   Material Properties

Most element types require material properties. Depending on the application, material properties can be linear or nonlinear. As with element types and real constant, each set of material properties has a material reference number. The table of material reference numbers versus material property sets is called the *material table*. Linear material properties can be constant or temperature-dependent, and isotropic or orthotropic. Nonlinear material properties are usually tabular data, such as plasticity data (stress-strain curves for different hardening laws), magnetic field data (B-H curves), creep data, swelling data, hyper elastic material data, etc. The model under study is linear and material non-linearity is not considered. It means that the loads are applied in such a way that the parts of bolted joints are not going in plastic deformation. It is also a fact that the bolt, nut and the joint behave as elastic bodies under the high loads. So bolted joint acts as

Figure 2.1: Solid model

Step1 Generating Keypoints   Step2 Making Splines   Step3 Small triangle
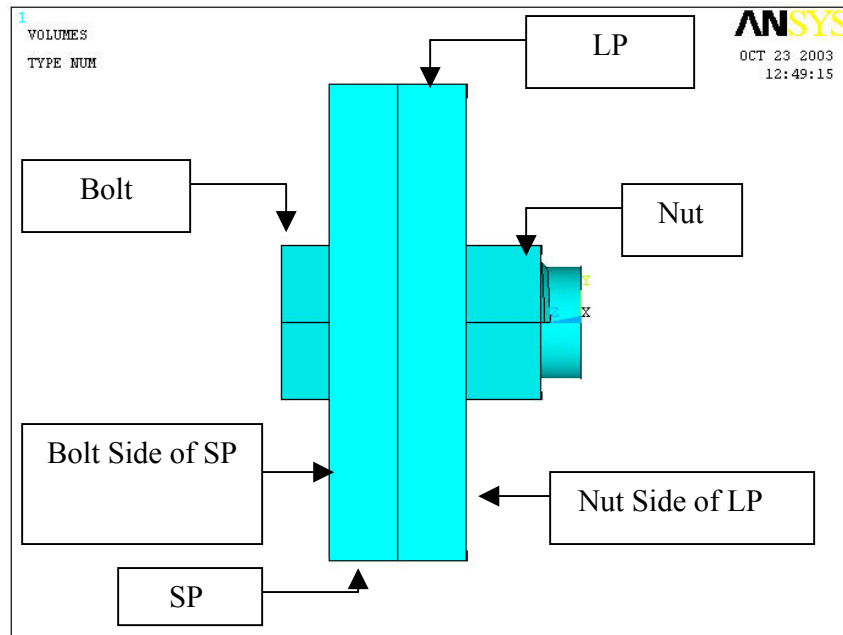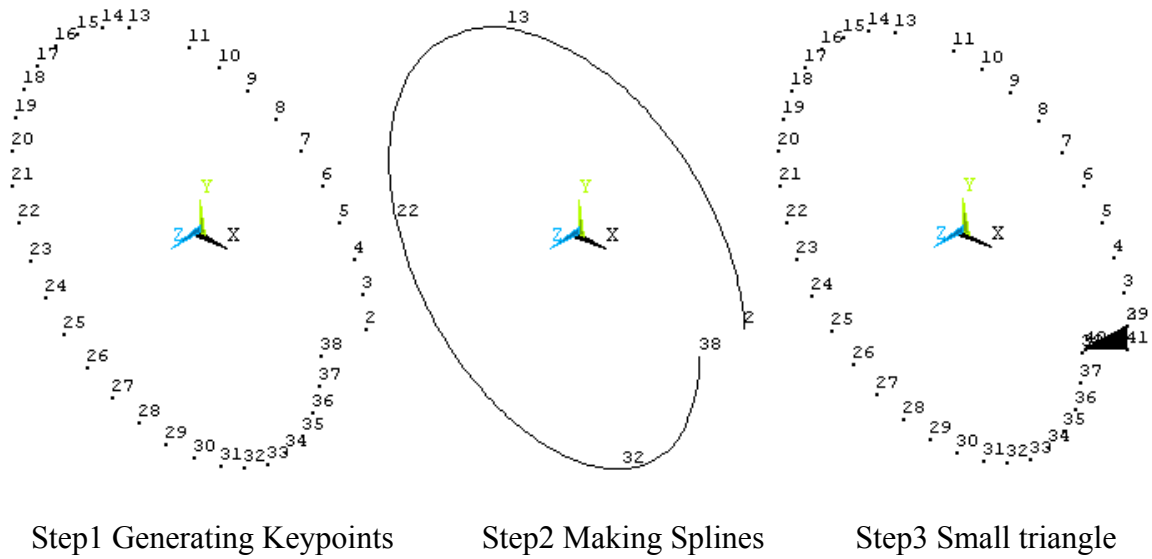
Figure 2.2(a): Steps involved in generating a thread
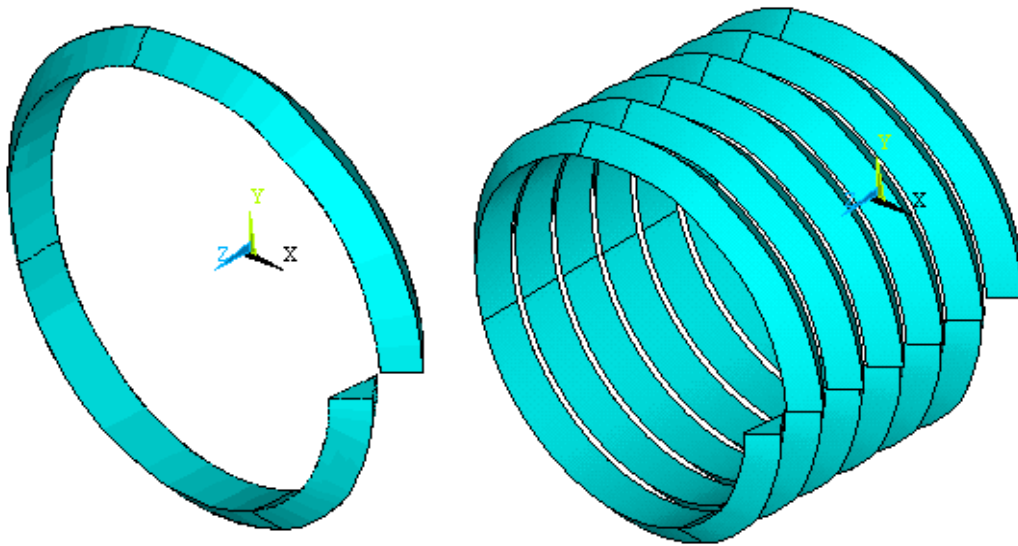
Step4 Dragging triangle along the spline   Step5 Copying one thread to form series of threads

Figure 2.2(b): Steps involved in generating a thread

Bolt

Nut

LP

SP
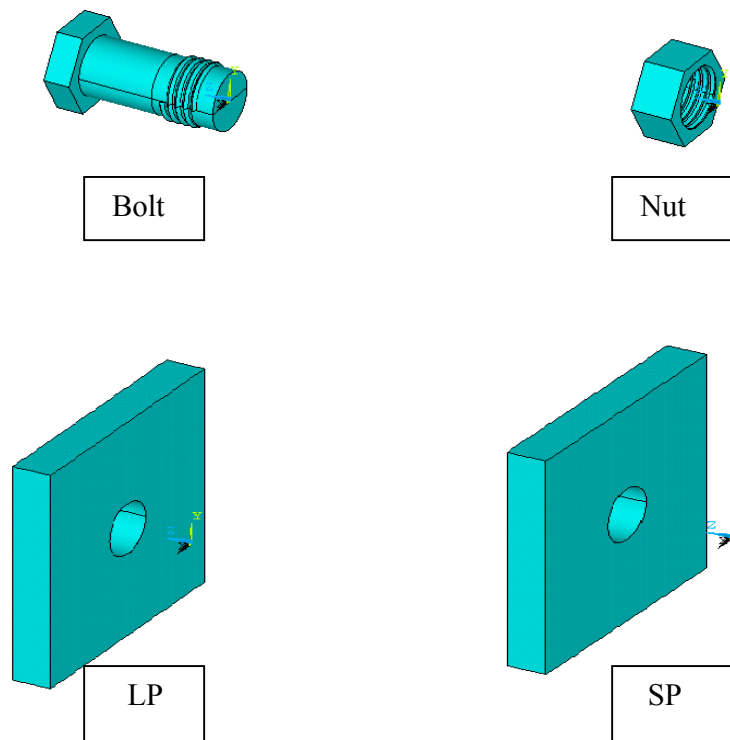
Figure 2.3: Individual parts of a bolted joint
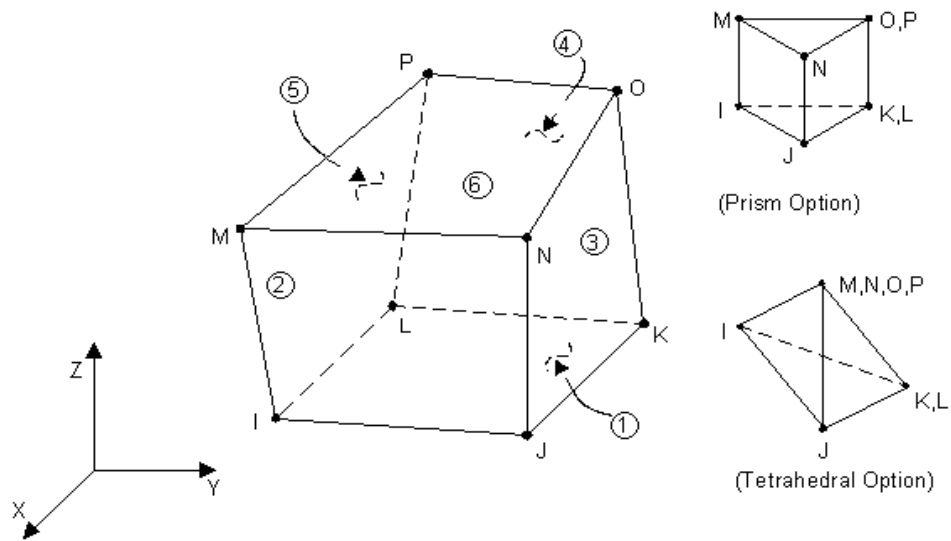
Figure 2.4: Visco 107 solid 3D element

a system of elastic springs and not as a system of rigid bodies. The material properties of steel that are used are defined as follows:

Material Used	Young's Modulus, E	Poisson ratio, ν
Steel	210 GPa	0.29

2.3.3 Meshing

After making the geometric model and defining the element type with material properties, the next step is to mesh the model. This means to divide the solid model into nodes and elements. There are two methods to create the finite element mesh: one is solid modeling and the other one is direct generation. With *solid modeling,* the geometric shape of the model is described, and then instruction is given to the ANSYS program to automatically *mesh* the geometry with nodes and elements. The size and shape in the elements that the program creates can be controlled. With *direct generation,* the location of each node and the connectivity of each element are defined manually. The method used here is the solid modeling. This method is more appropriate for large or complex models, especially 3-D models of solid volumes. Modifications to geometry can be readily executed resulting in time saving. Direct generation on other hand is useful when the model is small and simple. But once it is made changes cannot be done easily in the geometry. To mesh one bolt model smart sizing is used. The mesh is refined to such level where after further refinement of the mesh the results converge to same values. Figure 2.5 shows a typical finite element mesh of a single bolted joint. The number of nodes and elements in the single bolted models analyzed under different conditions are around respectively 70,000 and 30,000.
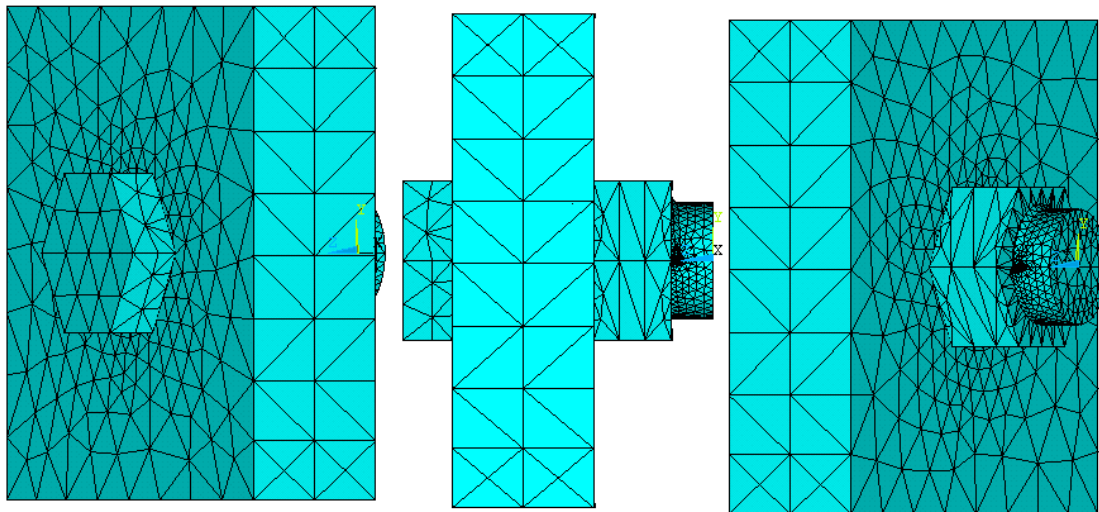
Figure 2.5: A typical finite element mesh of a single bolted joint (three views)

2.3.4   Contact Modeling

There is relative motion at the interfaces of the bolted joint model when the load is applied. This refers to contact condition and contact elements are to be used at these interfaces. In studying the contact between two bodies, the surface of one body is conventionally taken as a contact surface and the surface of the other body as a target surface. The "contact-target" pair concept has been widely used in finite element simulations.

Contact problems fall into two general classes. These are rigid-to-flexible and flexible-to-flexible. For rigid-flexible contact, the contact surface is associated with the deformable body; and the target surface must be the rigid surface. For flexible-flexible contact, both contact and target surfaces are associated with deformable bodies. The contact and target surfaces constitute a "Contact Pair". In rigid-to-flexible contact problems, one or more of the containing surfaces are treated as rigid (i.e., it has a much higher stiffness relative to the deformable body it contacts). In general, any time a soft material comes in contact with a hard material, the problem may be assumed to be rigid-to-flexible. Many metal forming problems fall into this category. The other class, flexible-to-flexible, is the more common type. In this case, both (or all) contacting bodies are deformable (i.e., have similar stiffnesses). An example of a flexible-to-flexible contact is bolted flanges. ANSYS supports three contact models: node-to-node, node-to-surface, and surface-to-surface. Each type of model uses a different set of ANSYS contact elements and is appropriate for specific types of problems. The contact type that is used in this problem is surface-to-surface contact. *Targe 170* and *Contac 174* elements are sued to define the contact between surfaces. *Targe170* is used to represent various 3-D target

surfaces for the associated contact elements. The contact elements themselves overlay the solid elements describing the boundary of a deformable body that is potentially in contact with the rigid target surface, defined by *Targe170*. Hence, a "target" is simply a geometric entity in space that senses and responds when one or more contact elements move into a target segment element. *Conta174* is an 8-node element that is intended for general rigid-flexible and flexible-flexible contact analysis. In a general contact analysis, the area of contact between two (or more) bodies is generally not known in advance. *Conta174* is applicable to 3-D geometries. It may be applied to contact of solid bodies, or shells, to static or dynamic analyses, to problems with or without friction. *Conta174* contact element is associated with the 3-D target segment elements via a shared real contact set number. This element is located on the surface of 3-D solid, shell elements (called underlying element). It has the same geometric characteristics as the underlying elements. The contact surface can be either/both side of the shell or beam elements. Figure 2.6 shows how the target and contact elements interact with each other. After choosing the element types for the target and contact next step is to define the real constants and the co efficient of friction for the problem. ANSYS uses a set of 20 real constants and several element key options to control contact behavior using these surface-to-surface contact elements. Of the 20 real constants, two (R1 and R2) are used to define the geometry of the target surface elements. The remaining are used by the contact surface elements. The real constants are for example, normal contact stiffness factor, initial closure factor, pinball" region, maximum contact friction, cohesion sliding resistance etc. ANSYS uses default values for these. For friction model Coulomb Model is used. The Coulomb friction model is selected for the friction case. In the basic Coulomb friction model, two contacting surfaces can carry shear stresses up to a certain magnitude across their interface before

Figure 2.6: Surface-to-surface contacts in ANSYS program (Contac 174)

they start sliding relative to each other. This state is known as sticking. The Coulomb friction model defines an equivalent shear stress τ, at which sliding on the surface begins as a fraction of the contact pressure p (τ = μp + COHE, where μ is the friction coefficient and COHE specifies the cohesion sliding resistance). Once the shear stress value exceeds, the two surfaces will slide relative to each other. This state is known as sliding. The sticking/sliding calculations determine when a point transitions from sticking to sliding or vice versa. ANSYS provides an option for defining a maximum equivalent shear stress so that, regardless of the magnitude of the contact pressure, sliding will occur if the magnitude of the equivalent shear stress reaches this value. To specify the maximum allowable equivalent shear stress across the interface, the real constant shear stress τ_{max} is set. This shear stress limit is usually used in cases where the contact pressure stress may become very large, causing the Coulomb theory to provide a critical shear stress at the interface that exceeds the yield stress in the material beneath the surface. A reasonable upper estimate for τ_{max} is $\sigma_Y/\sqrt{3}$, where σ_y is the von Mises yield stress of the material adjacent to the surface. Figure2.7 shows the contact elements that are being generated;. One contact element pair is between the bolt head and the supporting plate. One between the two plates. One between the loading plate and the nut surface. Rests of the two are between the bolt shank and the inner surface of the hole of the two plates.

2.3.5   Boundary Condition

There are two types of boundary conditions when analyzing the bolted joints. As discussed these are the external constraints, applied force or pressure and the pretension in the bolt internally. One type is due to tightening of the bolt. This tightening produces a
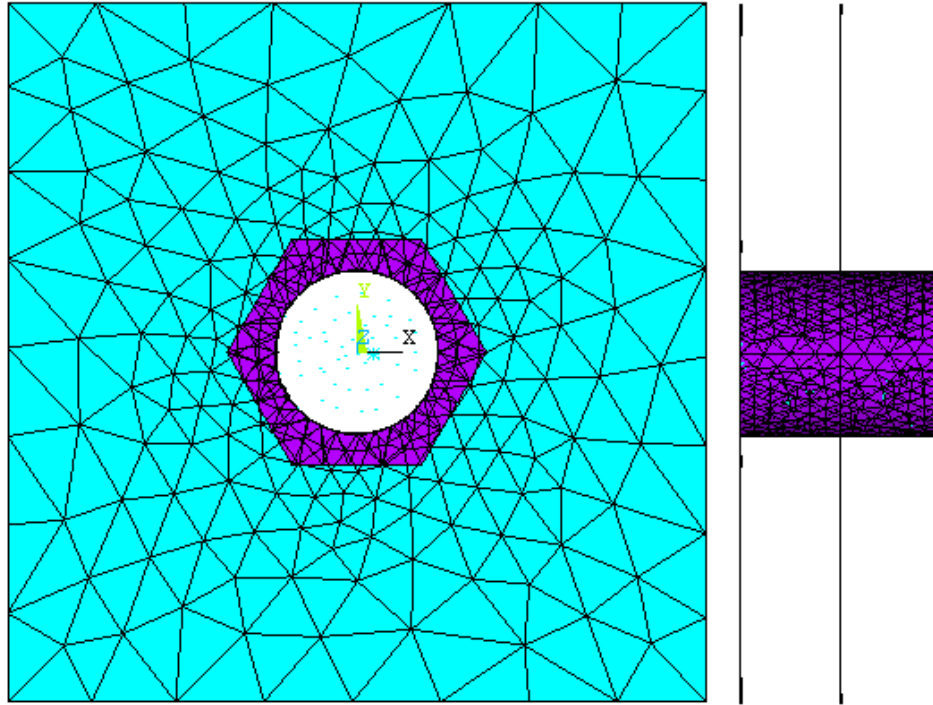
Figure 2.7: Contact elements at the interfaces (front and right side view)

pretension force in the axial direction of the bolt. This force causes the bolt to be elongate. Here, the pretension force is represented by a special element *PRETS 179*. The easiest way to apply pretension condition is through the use of *PSMESH* command. This command can be used only if the fastener is *not* meshed in separate pieces. The command defines the pretension section and generates the pretension elements. It automatically cuts the meshed fastener into two parts and inserts the pretension elements. Figure 2.8 explains the phenomena of pretension element in ANSYS. Nodes I, J are the end nodes, usually coincident. Node K is the pretension node which location is arbitrary. It has one degree of freedom. Actual line of action is in the pretension load direction, which is constant. It does not update for rotations. Figure 2.9 indicates the meshed pretension section on the bolt.

The other type of boundary condition is the constraints and the applied force. Loading is given in the form of displacement in this model. The lower bottom area of the supporting plate is constrained in the Y direction only where as the upper area of the loading plate is given displacements in the Y direction respectively. The boundary conditions are clear from the Figure 2.10.
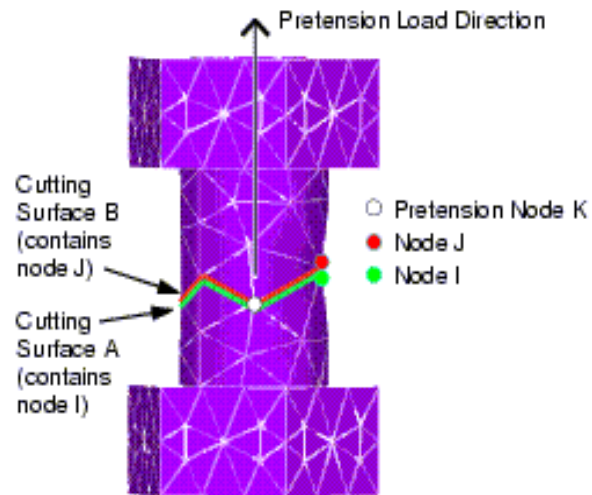
Figure 2.8: Pretension definitions
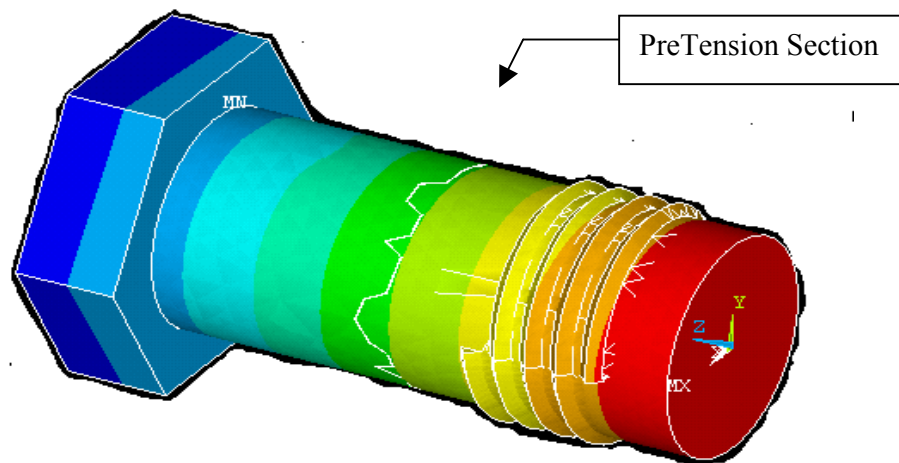
Figure 2.9: Pretension mesh section in the bolt

Displacement. in
y-direction

Fixed Surface
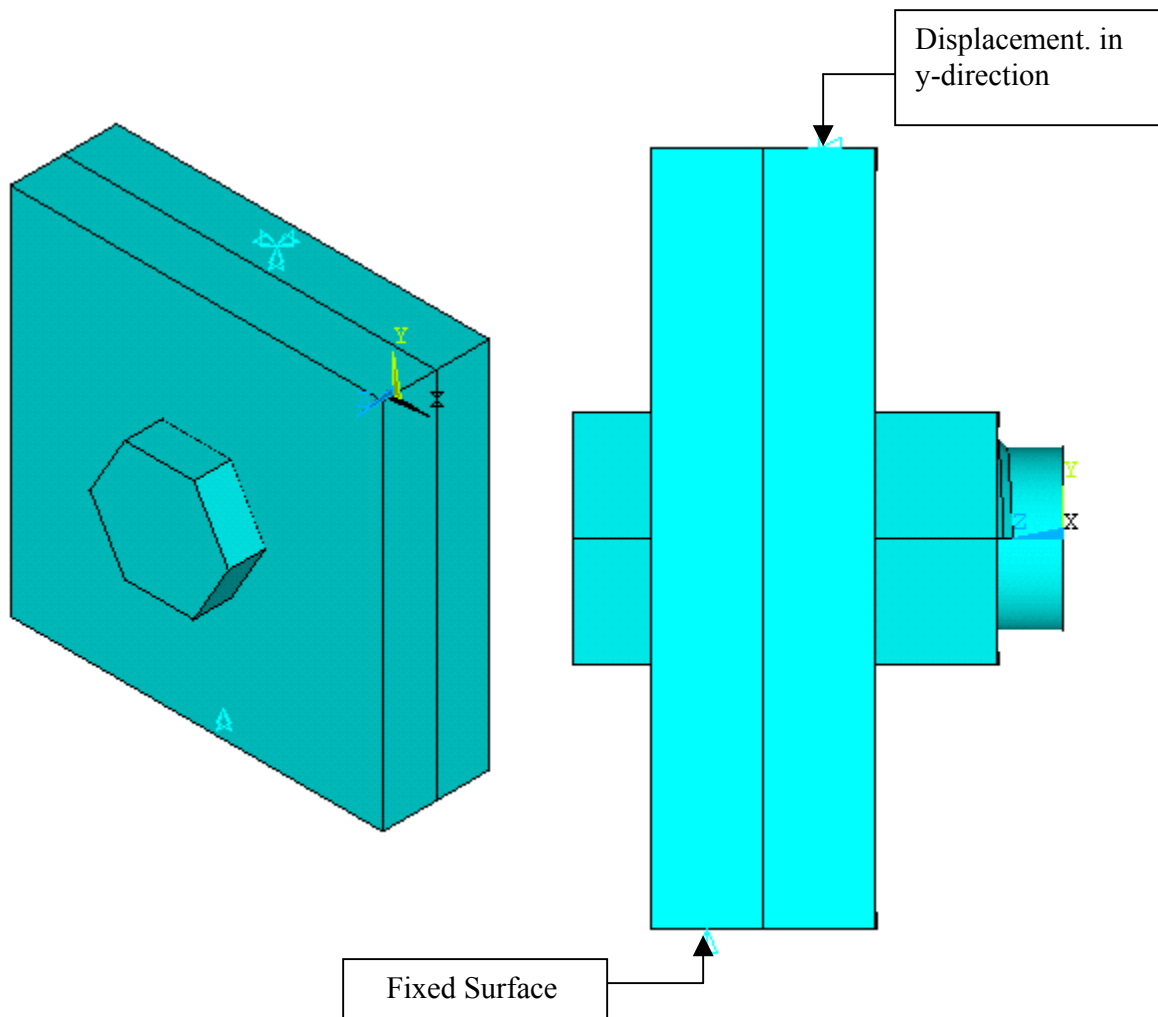
Figure 2.10: Boundary condition

2.4   RESULTS AND DISCUSSIONS

There are many variables that affect the behavior of a bolted joint. Some of these are the force or pressure applied, value of pretension, level of clearances between the bolt and the hole and also the coefficient of friction between the contact two surfaces. On the basis of these variables four cases of shear loading and one case for tensile loading is considered using one bolt model.

	Displacement	Pre Tension	Coefficient of Friction	Clearance
Study A1 (Shear)	0.06 mm, 0.08 mm and 0.1 mm	500 N	0.1	0.05 mm
Study A2	0.06 mm	500 N, 9000 N and 30000 N	0.1	0.05 mm
Study A3	0.06 mm	500 N	0.1,0.2 and 0.3	0.05 mm
Study A4	0.06 mm	500 N	0.1	0.01 mm, 0.05 mm and 0.5 mm
Study B1 (Tensile)	0.06 mm	2500 N, 5000 N and 30000 N	0.1	0.05 mm

2.4.1   Study A1: Deformation under Increasing Load

y-displacement

To illustrate the deformation pattern, displacement load values of 0.06,0.08 and 0.1mm are applied to the loading plate top face in the finite element model and the results are obtained. The results for displacement load of 0.08 mm are not shown in the figures 2.11-18 but are given in the tables afterwards. The friction coefficient between steel-to-steel is 0.75 but for the fast iteration and convergence low value is used in the model. It is also important to mention that qualitative results are more important here than the quantitative precision. The same boundary condition is verified through an experiment. Details of this are given in the section after this. Some numerical results are compared with experimental results.

ANSYS uses Coulomb friction model between the contacting surfaces. Two contacting surfaces can carry shear stresses up to a certain magnitude across their interface before they start slidin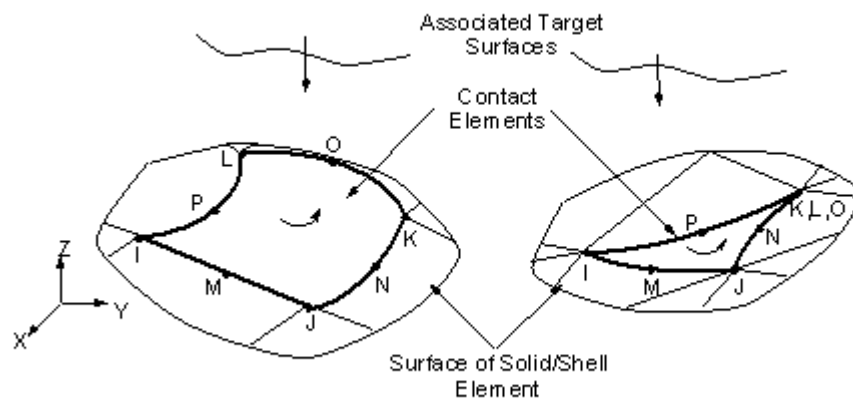g relative to each other. This state is known as sticking. Once the shear stress is exceeded, the two surfaces will slide relative to each other. This state is known as sliding. The sticking/sliding calculations determine when a point transitions from sticking to sliding or vice versa. Figure 2.11 shows the (a) SP bolt side, (b) LP nutside, (c) SP interface side and (d) LP interface side. Figure 2.11(a) shows that the region near to the lower edge is not moving due to the constraint applied. Figure 2.11(b) shows the LP nutside displacement pattern. Most of the surface is sliding and moving. Figure 2.11(c) shows that there is a maximum displacement region just above the bolt hole. Actually this is the point where the bolt is coming in contact with the supporting plate. Sliding is obvious due to the different displacement bands on the plate. Figure 2.11(d) shows the surface is sliding and the region near the top edge is moving to the maximum displacement load of 0.06 mm. The minimum value of displacement is greater than the radial clearance value of 0.05 mm used. The radial clearance serves as a lower bound value for the displacement in the loading plate.

Figure 2.12(a and b) show the displacement pattern in the Y direction on SP bolt side. and LP nut side due to 0.1 mm load. The maximum displacement vale and the pattern are changed with the increase in the load. Figure 2.12(c and d) show the displacement pattern on SP and LP interface side As the load is increased there is an increase in the spread of the region above the bolt hole in Figure 2.12(c) and the region below the bolt hole in Figure 2.12(d). The regions are pointed out with the help of arrows. So there is a change in the displacement pattern with increasing load.

Figure 2.13 and 2.14 show the displacement pattern in bolt and nut in Y direction at load of 0.06 and 0.1 mm respectively. When displacement of 0.06 mm is applied it is observed in the bolt that the part after the threads is displaced more than the given load. This means that there is bending in the bolt. Similar behavior is for the other load condition in which the displacement at the free end is more pronounced because of the high load value with which the plate is moved in the upward direction. The value of displacement at the bolt head region is negative thus giving an indication of the downward movement while the region at the free end has positive value meaning that that part is moving upwards. Same behavior is for the nut in both cases. Table 2.1 gives the results of maximum displacements in bolts, nut, SP and LP. Values for 0.08 mm test are also included. This confirms the pattern that as the load is increased the displacement values also increase.

z-displacement

Figure 2.15 to 2.18 show the displacement pattern in the z-direction of the bolt, nut and the two plates at two different applied loads. Figure 2.15 and 2.16 show the SP and LP plate movement in z-direction at two displacement values of 0.06 mm and 0.1 mm. For SP the upper half region till the bolt hole has positive values and the lower half has negative. This means that the upper half part is moving in the positive z-direction For LP most regions above the bolt has almost zero value and the lower half has negative value indicating that the plate exhibits bending. For both case the pattern is similar. In figure 2.17 and 2.18, the region at the upper left corner of the bolt shows that there is some positive movement in z-direction of the bolt. The region of the lower left corner of the bolt has negative value giving an indication that there is some bending in the bolt. The results are in harmony with the applied set of boundary conditions and loads.
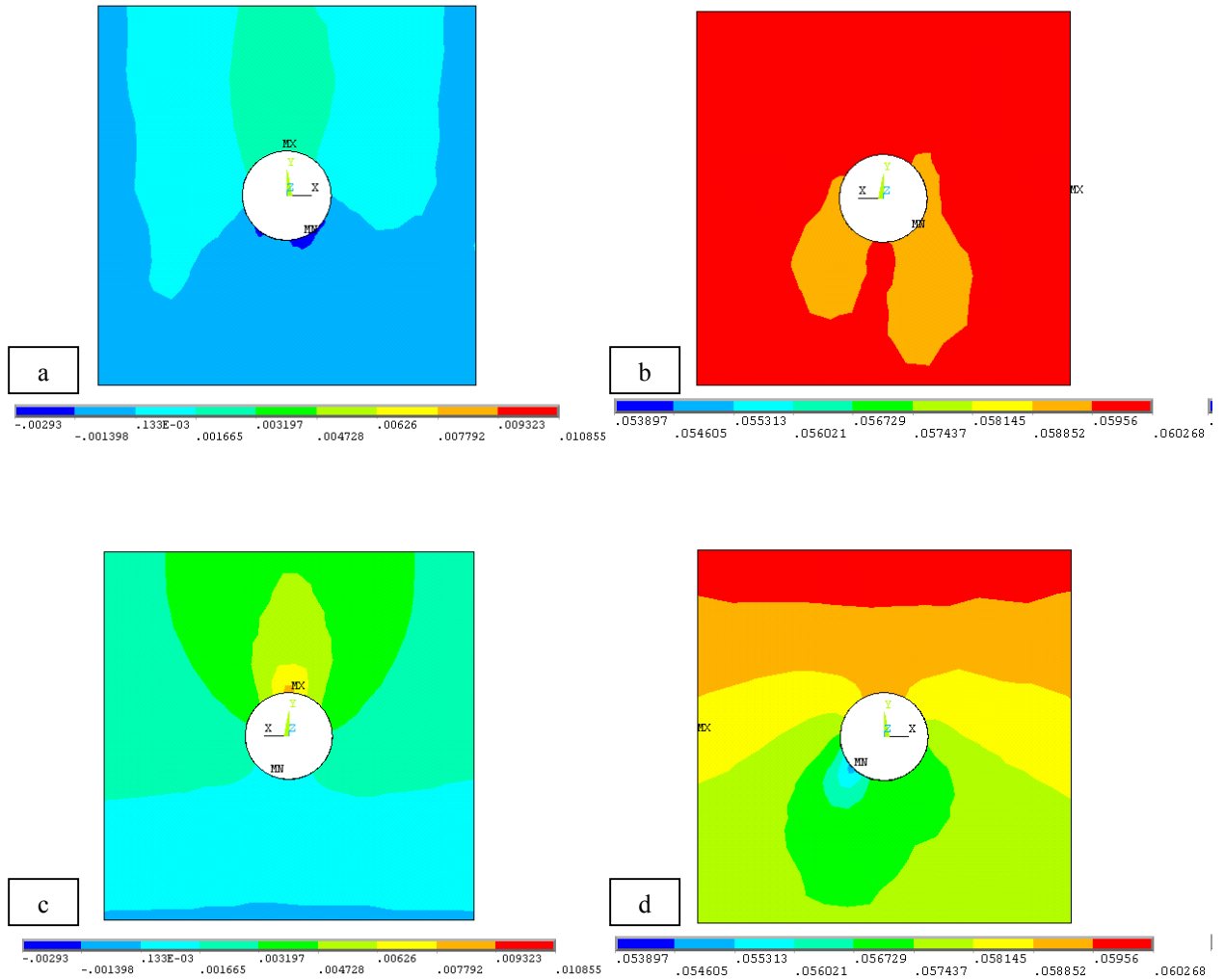
Figure 2.11: *y*-displacement of (a) SP boltside (b) LP nutside (c and d) SP and LP interface
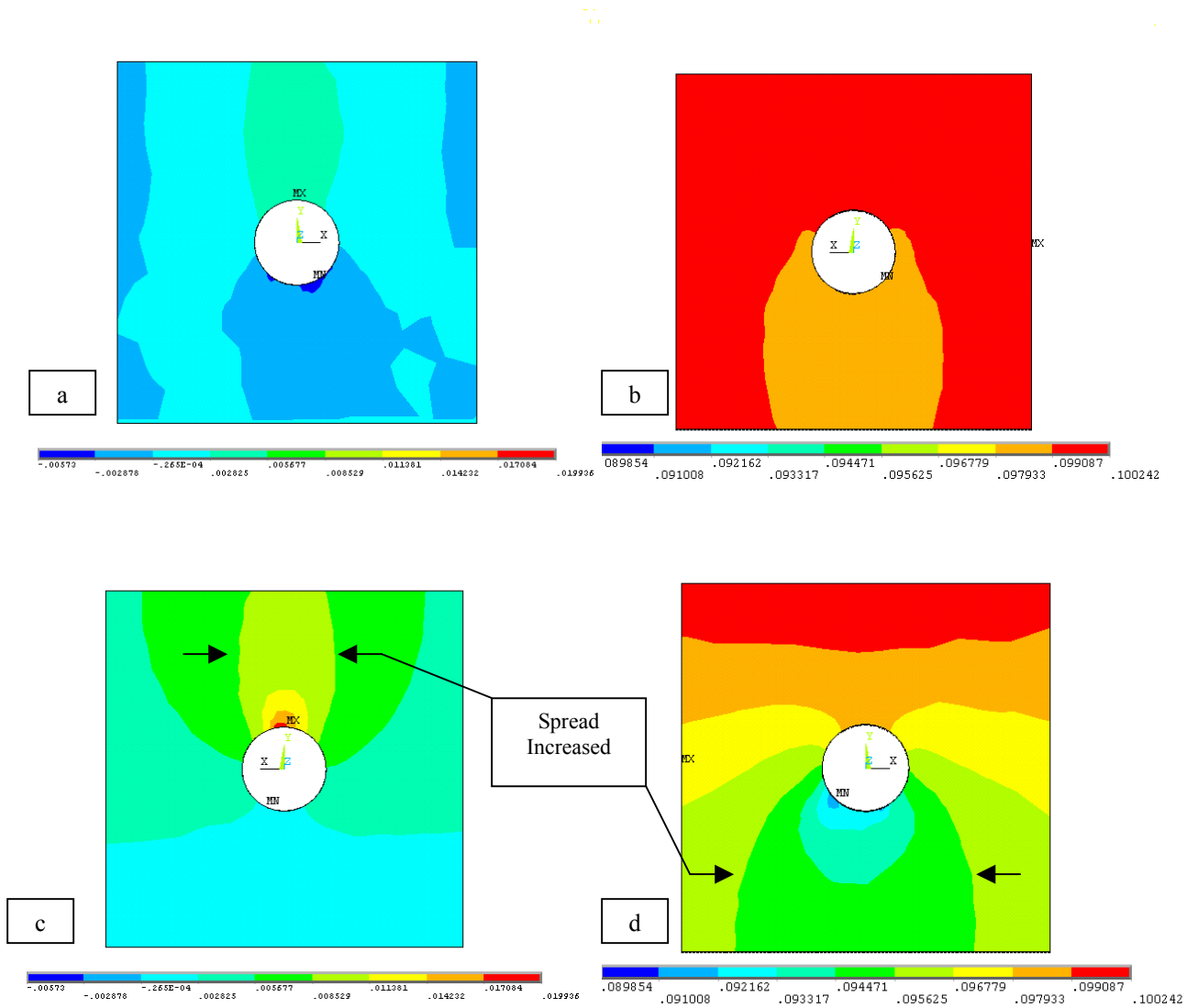
side at 0.06 mm

Figure 2.12: *y*-displacement of (a) SP boltside (b) LP nutside (c and d) SP and LP interface

side at 0.1 mm

Figure 2.13: *y*-displacement of bolt and nut at 0.06 mm
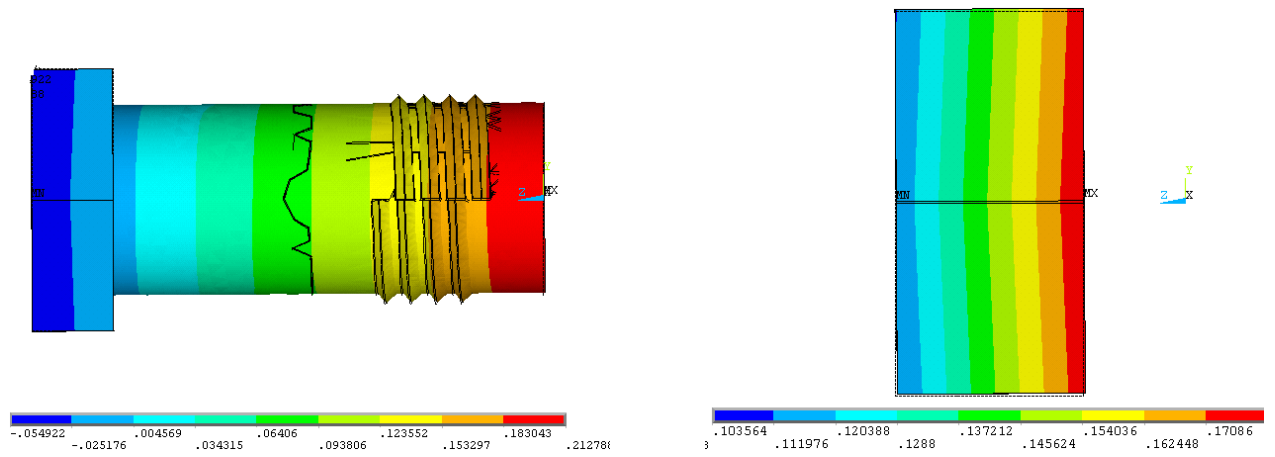
Figure: 2.14: *y*-displacement of bolt and nut at 0.1 mm

Table 2.1: Maximum *y*-displacement values under increasing load

Displacement loads (mm)	Bolt (mm)	Nut (mm)	SP (mm)	LP (mm)
0.06	0.11804	0.099302	0.010855	0.060268
0.08	0.165409	0.138756	0.014845	0.080259
0.1	0.212788	0.17086	0.019936	0.100242
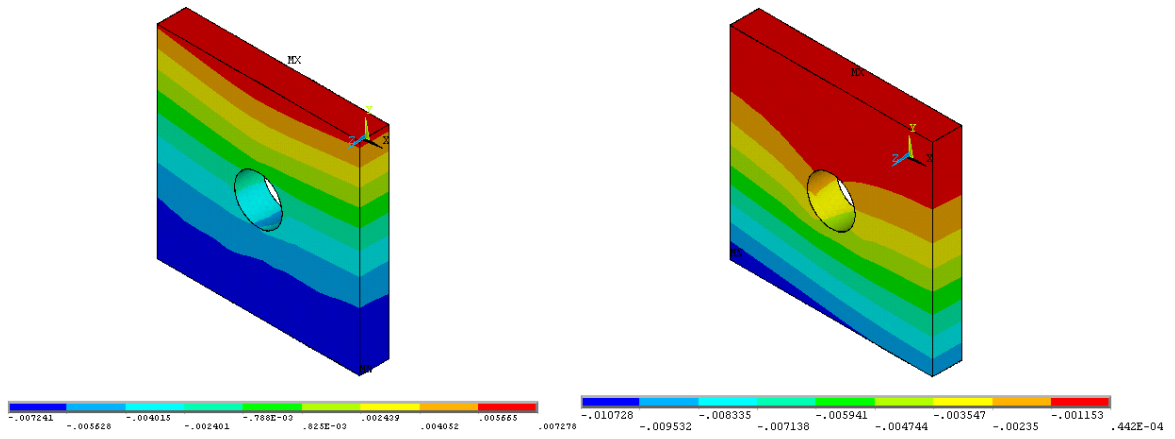
Figure 2.15: *z*-displacement of SP and LP at 0.06 mm
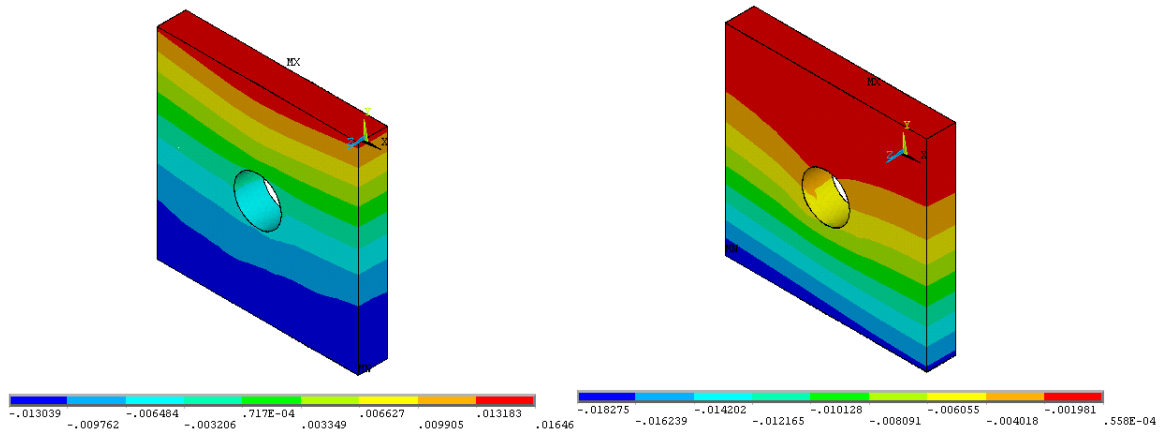
Figure 2.16: *z*-displacement of SP and LP at 0.1 mm
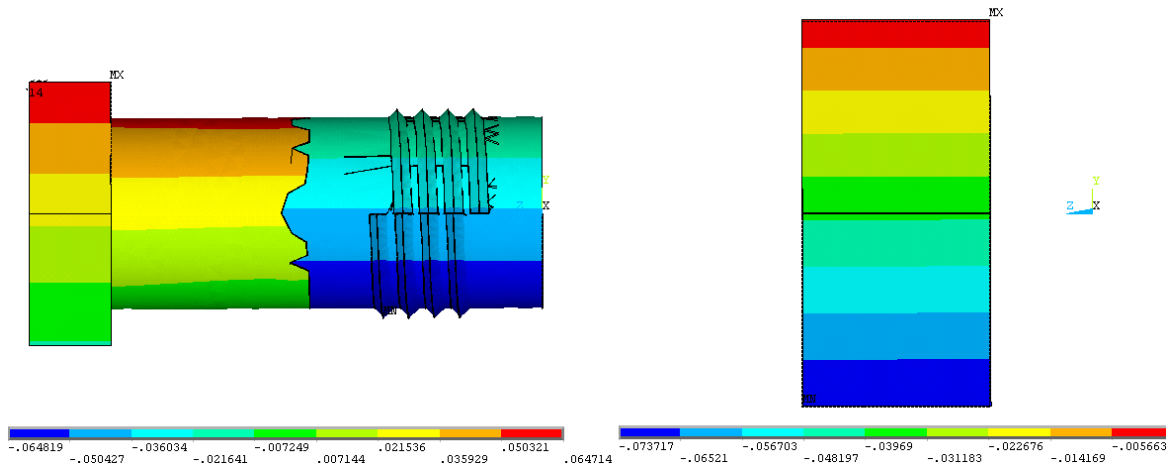
Figure 2.17: *z*-displacement of bolt and nut at 0.06 mm
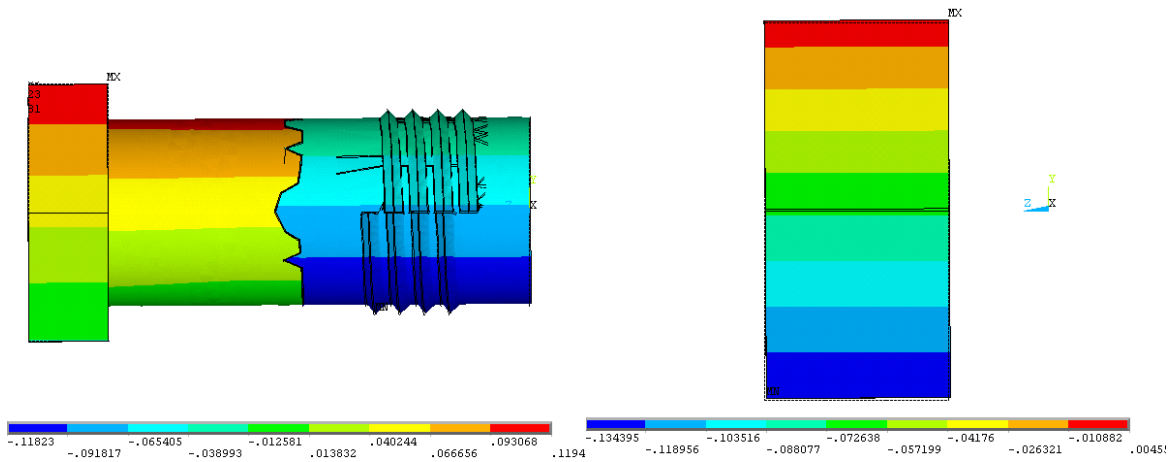
Figure 2.18: *z*-displacement of bolt and nut at 0.1 mm

Stress σ$_y$

The positive value of stress σ$_y$ in the Figure 2.19 and 2.20 corresponds to tension and negative values of stress to compression. This is expected, as when the external load is applied in upward direction, the bolt will strike the lower surface of the loading plate first. The bolt will resist the upward motion of the loading plate thus putting the lower half region of the plate in compression. Consequently the upper half region of the plate will go in tension. The effect is opposite in the case of supporting plate.

Figure 2.19 shows the stress σ$_y$ distribution in (a) SP boltside, (b) LP nutside, (c) SP interface side and (d) LP interface side at the displacement load value of 0.06 mm. Figure 2.19(a) shows that most of the region is in compression. This is because; this surface is taking most of the compression if the two plates are seen together. Figure 2.19 (b) shows that stress is distributed uniformly all over the plate because there is not much relative movement on this side. Figure 2.19(c) shows that the upper half region of the supporting plate is in compression where as the lower half region is in tension. Highly compressive stress regions (marked by arrow) are located above the bolt hole because of the contact of the bolt at that point. Figure 2.19(d) shows that the upper half region is in tension and the lower half is in compression. The explanation is already given in the beginning of this discussion. Region (marked by arrow) below the bolt hole is highly compressed due to the bolt contact at that point.

Figure 2.20 shows the stress σ$_y$ distribution on (a) SP boltside, (b) LP nutside (c) SP interface side and (d) LP interface side at displacement load of 0.1 mm. Figures show that increasing the displacement load from 0.06 mm to 0.01 mm increases the stress in both plates and the pattern too.

Table 2.2 summarizes the results of maximum stresses in bolt, nut, SP and LP for the three loading cases (0.06, 0.08 and 0.1mm). The values show that as the load is increased the maximum stress σ_y, shear stress σ_{xy} and von Mises stress values increases. Von Mises stress values are helpful in the failure criterion of study. Knowing the yield stress value of components in assembly one can say whether the bolt connection part is going to plastic deformation or not. The immediate conclusion is that on applying displacement load of 0.08 mm and 0.1 mm the bolt and supporting plate are going in to plastic deformation. For 0.06mm all parts remain in elastic region. It is also observed that stress values are higher in the supporting plate as compared to the loading plate.
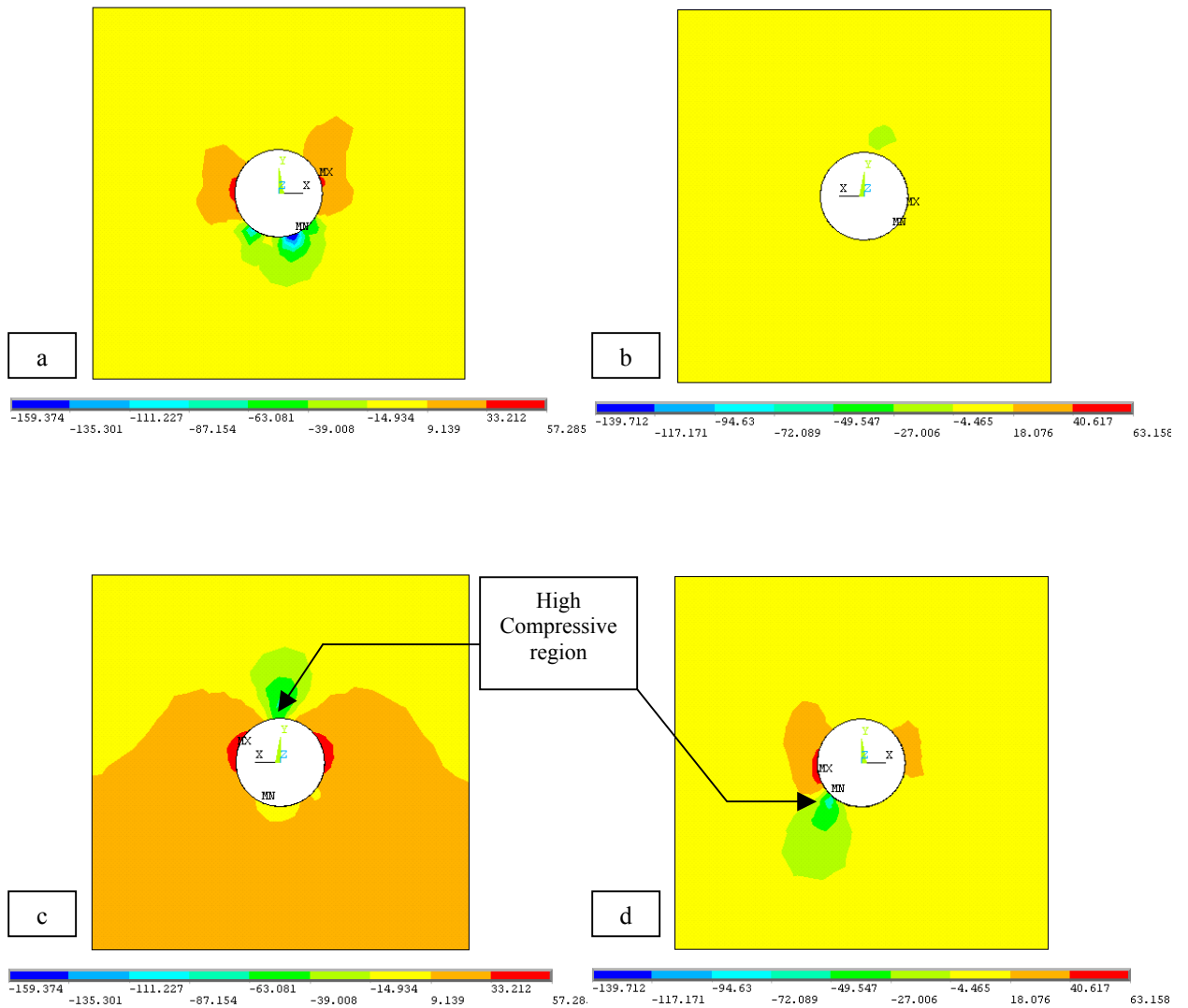
Figure 2.19: Stress σ_y of (a) SP bolt side (b) LP nutside (c and d) SP and LP interface side at

0.06 mm
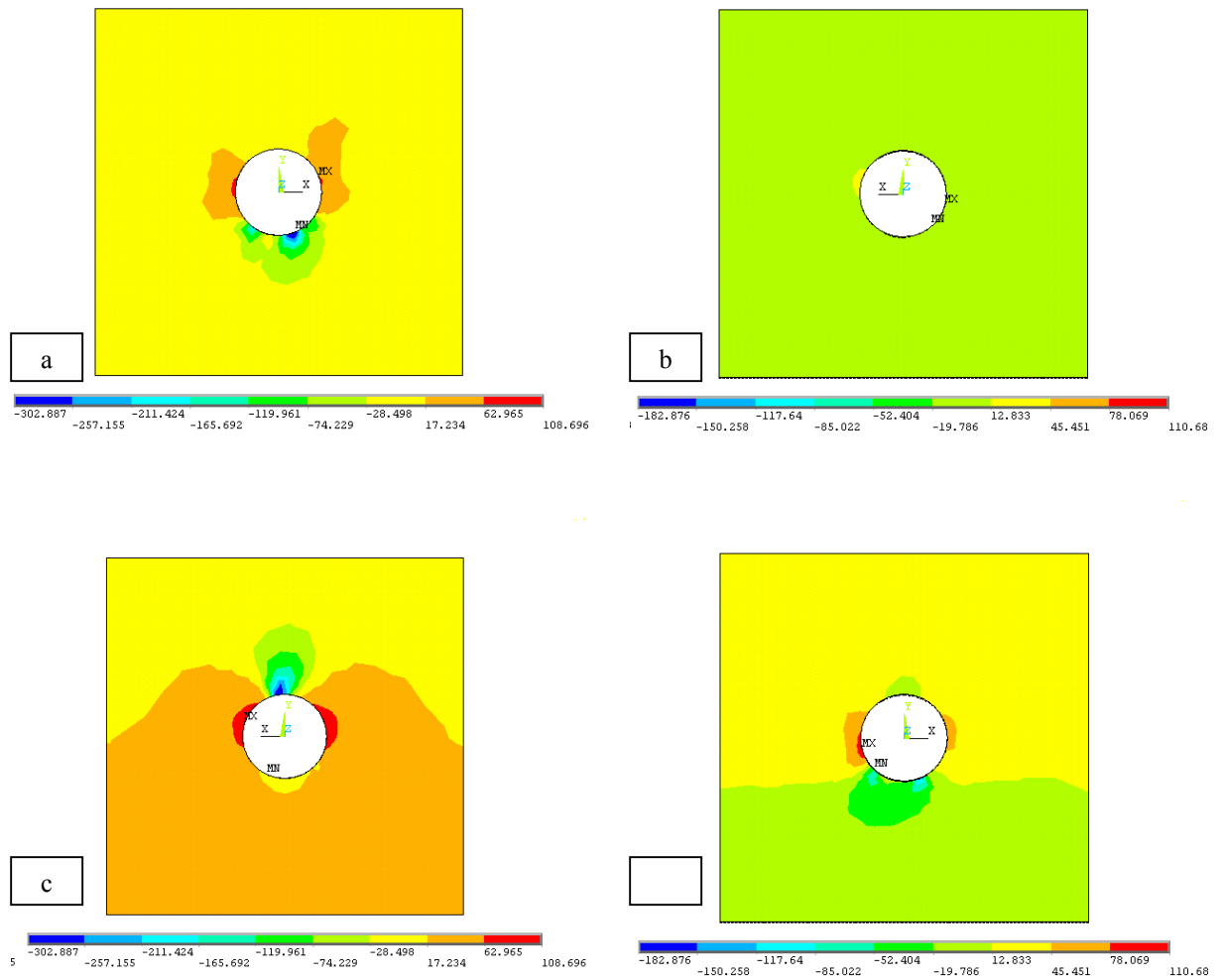
Figure 2.20: Stress σ_y of (a) SP boltside (b) LP nutside (c and d) SP and LP interface side
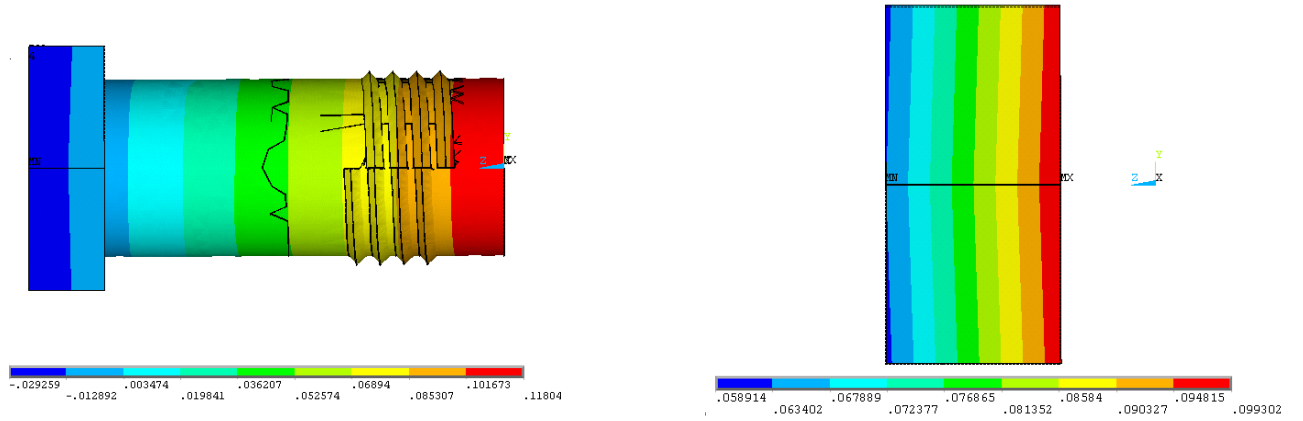
at 0.1 mm

Table 2.2: Maximum stress σ_y value under increasing load

Displacement loads (mm)	σ_y at SP (MPa)	σ_y at LP (MPa)	σ_{xy} at SP (MPa)	σ_{xy} at LP (MPa)
0.06	57.285	63.158	78.267	37.584
0.08	79.171	81.065	120.673	47.449
0.1	108.696	110.687	153.29	80.229

Table 2.3: Maximum von Mises stress value under increasing load

Displacement loads (mm)	Bolt (MPa)	Nut (MPa)	SP (MPa)	LP (MPa)
0.06	279.826	27.069	211.25	160.462
0.08	358.254	26.365	321.363	203.438
0.1	403.8	26.871	408.223	228.841

Experimental Verification

To validate the numerical model an experiment is conducted. Tensile testing machine is used for this purpose. Fixtures are prepared to apply the shear load to the one bolt joint. Figure 2.21 shows the experimental setup. The steel fixtures are designed in such a way that the upper portion of each, goes in to the top and bottom jaw of the machine. Each fixture applies a uniform pull on one surface of the plate thus producing a shearing effect. The two plates are made up of aluminum and their dimensions are 140 mm x 150 mm. Steel bolts of *M 16x 2* are used to clamp the two plates.

Three strain gages are placed on each plate. The locations (figure 2.22) of these strain gages are such that they are positioned around the bolt as closely as possible and towards the loading edge. Values of strain are recorded at displacement loads of *0.06, 0.07, 0.075, 0.08* and *0.09 mm* on each strain gage with the help of strain reader shown in figure 2.23. Figure 2.24 shows these locations on the two plates. Through ANSYS the numerical model is analyzed under the same experimental loading conditions. Material properties of aluminum *(E = 69MPa, v = 0.3* and *μ = 1.3)* for the plates and steel *(E = 210GMPa, v = 0.3* and *μ = 0.7)* for the bolts are used in the finite element model. The numerical strain values are obtained at each load. Figure 2.23 and 2.24 show the comparison between the strain values obtained from experimental work and numerical analysis for the six strain gage locations.

Figure 2.25 show that as the displacement load increases the value of strain increase at all the three locations of the loading plate. At location 2 that is closer to the loading edge and in front of the bolt, the values of strain obtained experimentally and numerically are very close to each other. The strain at this location is in the range of 60 x 10^{-6} and 80 x 10^{-6}.

The maximum value of strain at this location is higher than the maximum values at location 1 and 3, which are located on the sides of the bolt.

Same trend can be observed in Figure 2.26 for the strain values at location 5, which is located in front of the bolt on the supporting plate. There is a difference between the strain values at location 4 and 6 for experimental and numerical results. This difference is may be due to the weak response from the strain gages being placed on the side of the bolt. Also due to the clearance may be bolt is striking at one side of the bolt hole more as compared to the other side. This explains the trend of over and under estimation of the numerical values of strains at location 4 and 6.The finite element model used in the validation is used for further investigation
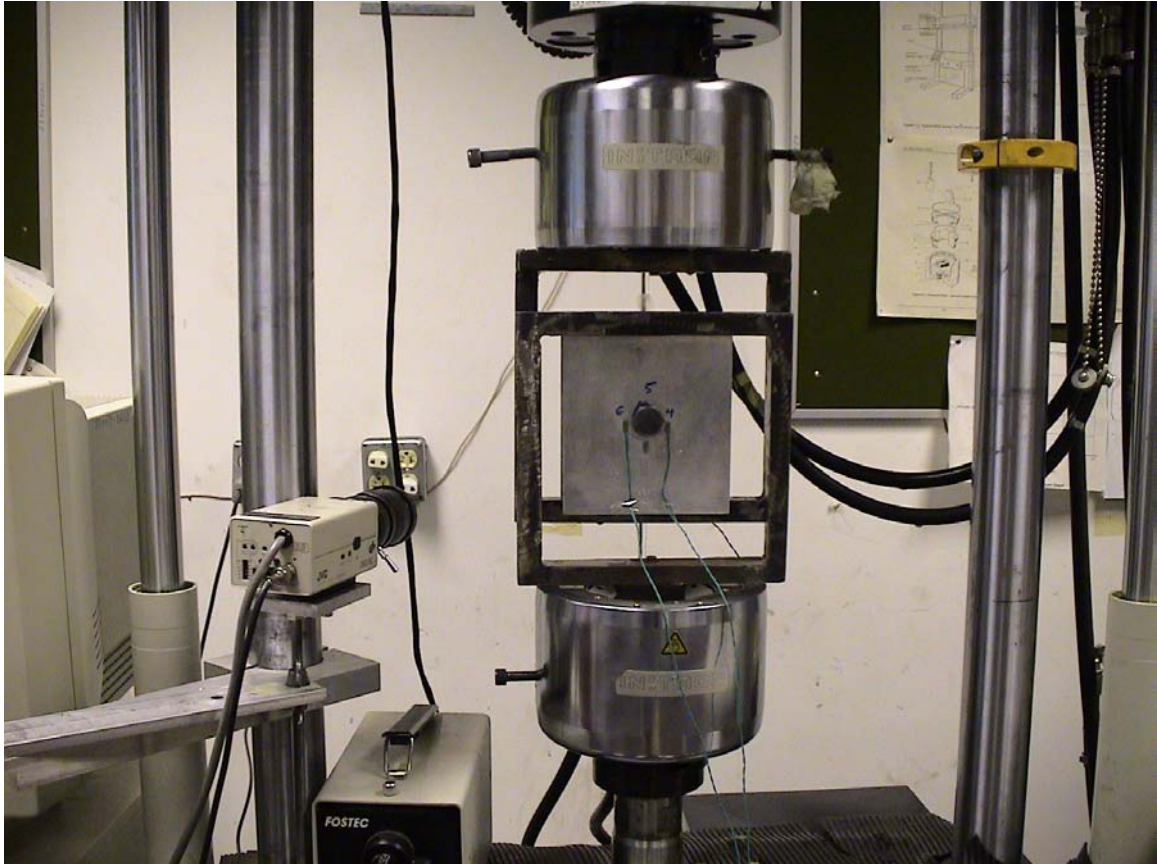
Figure 2.21: Experimental set up
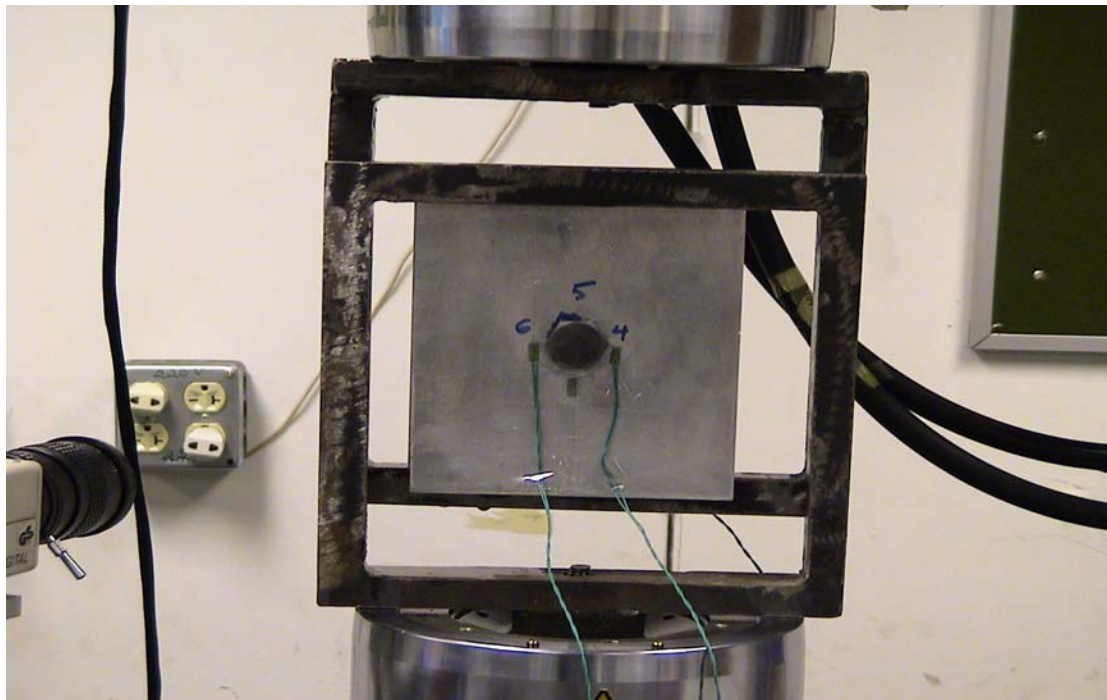
Figure 2.22: Strain gage positions on the one bolt joint

Figure 2.23: Strain indicator
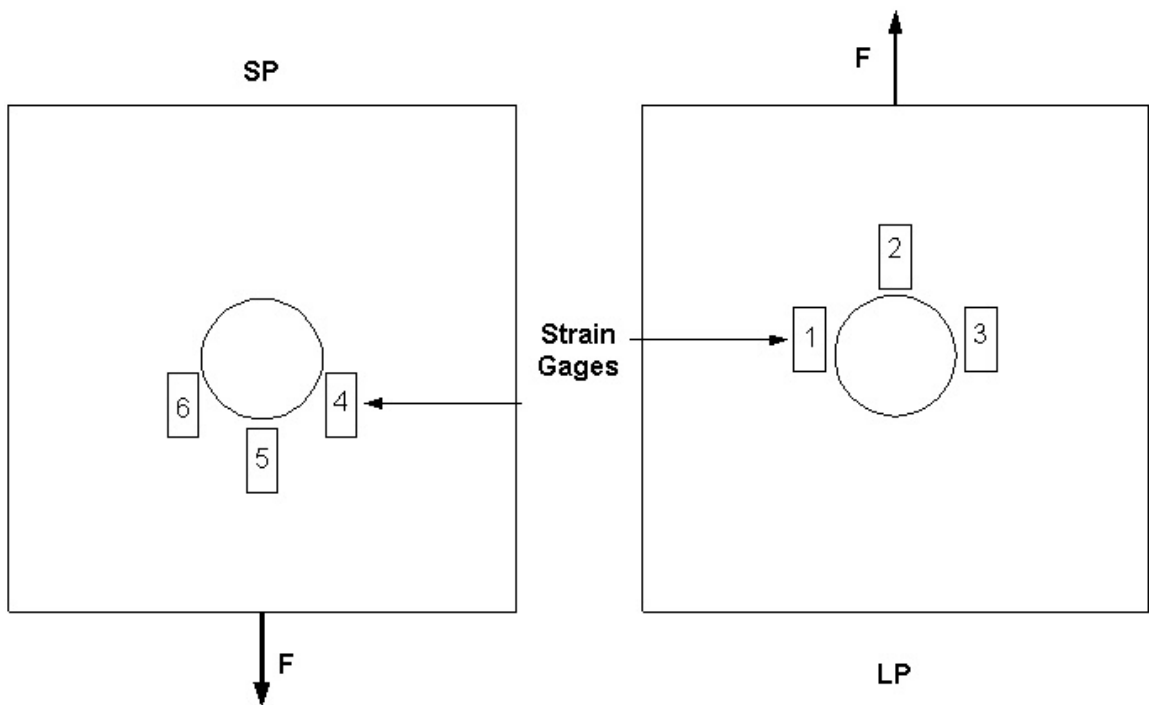
Figure 2.24: Locations and numbering of strain gages.
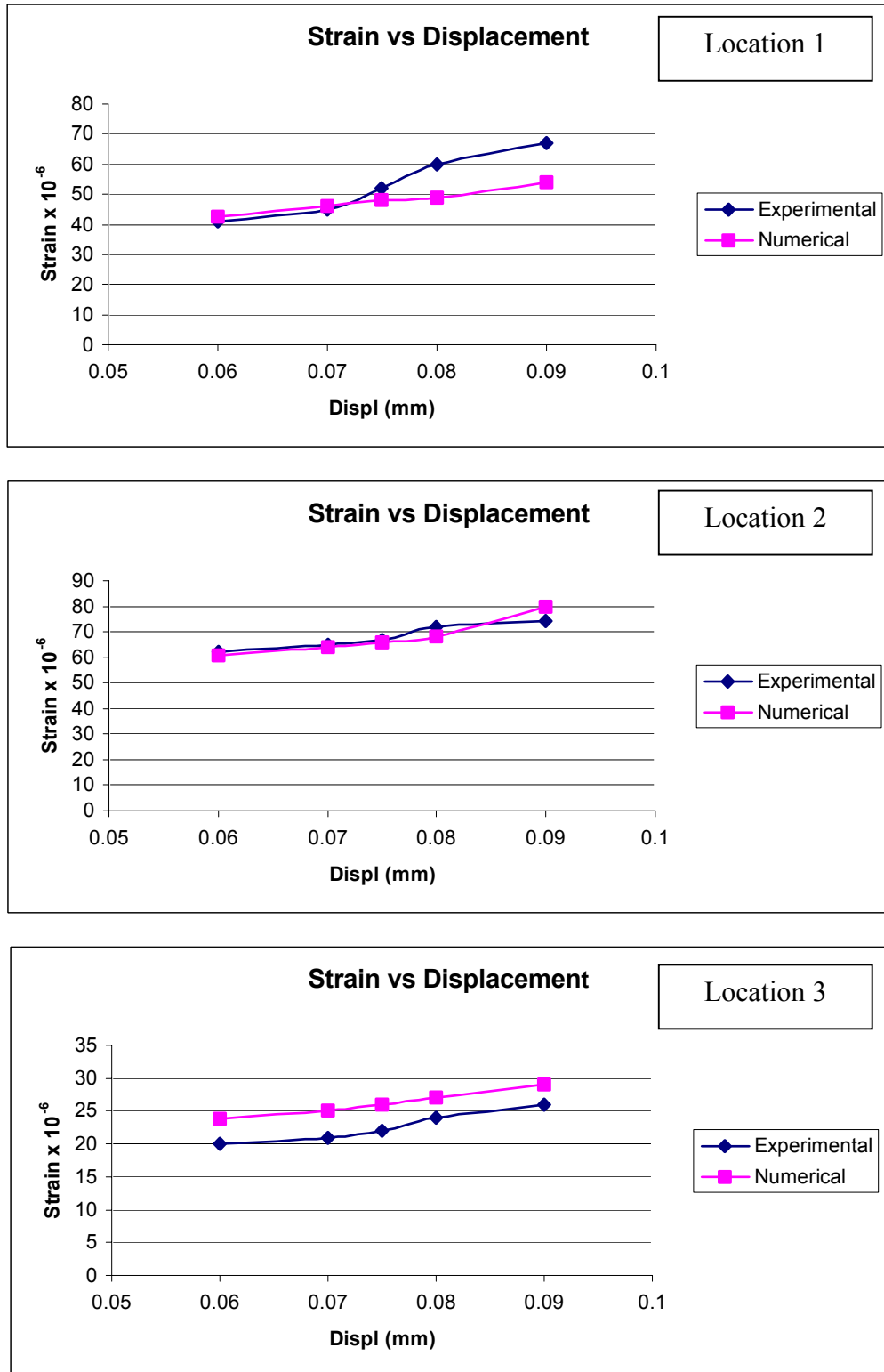
Figure 2.25: Comparison of strain values on the LP at location 1,2 and 3
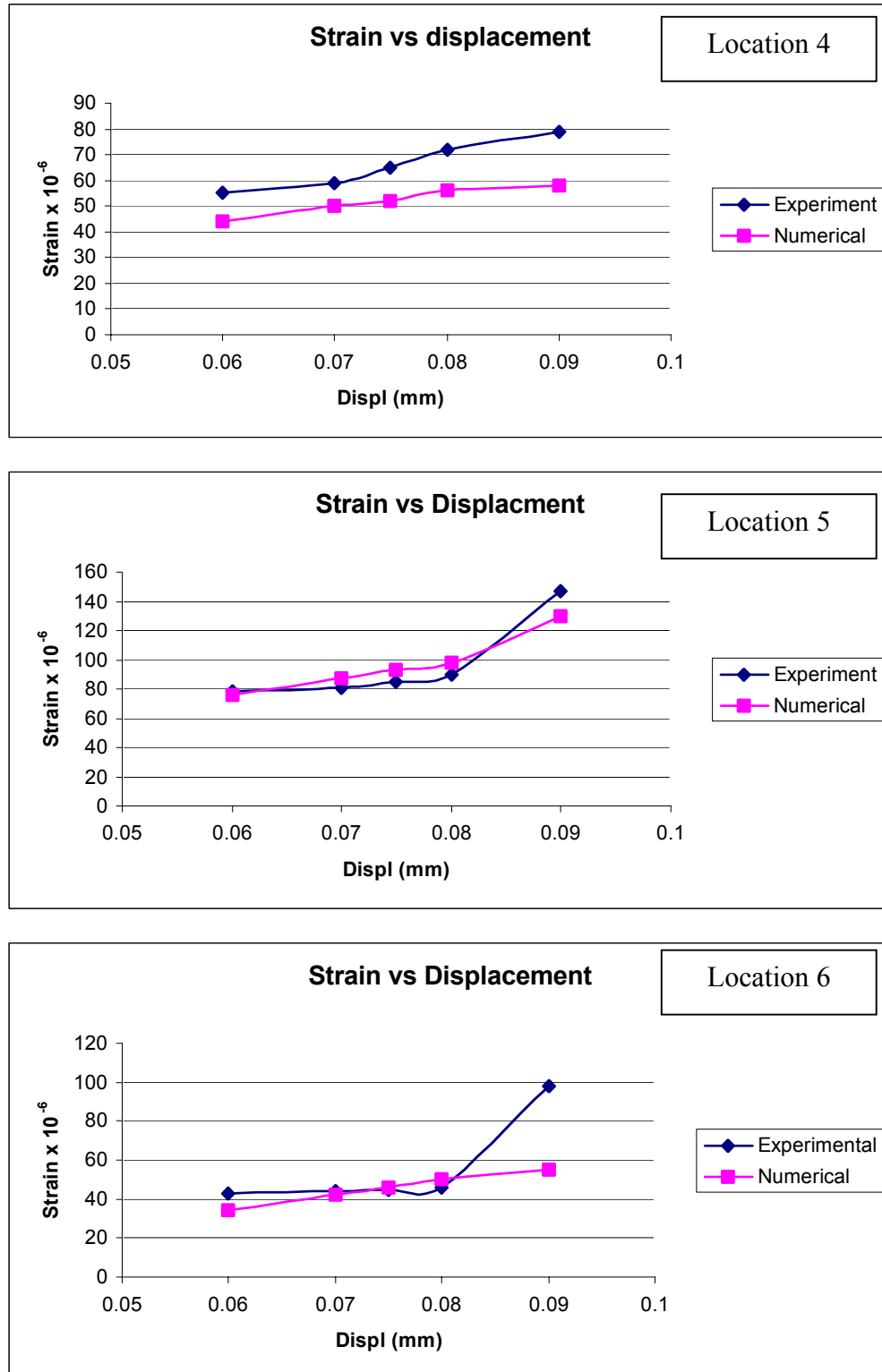
Figure 2.26: Comparison of strain values on the SP at location 4,5 and 6

2.4.2   Study A2: Effect of Pretension

y-**displacement**

In this study pretension force is increased while clearance (0.05 mm) and displacement load (0.06 mm) remains constant. Three pretension values of 500 N, 9000 N and 30000N are considered. Figures for 9000 N and 30,000 N are shown and the results for pretension 500 N are included in the table 2.4 to 2.7. Figure 2.27 shows the *y*-displacement pattern on (a) SP boltside, (b) LP nutside, (c) SP interface side and (d) LP interface side at pretension of 9000 N. Figure 2.27(a) shows that the region just above the bolt hole (marked by arrows) is displaced more as compared to the lower region on SP boltside due to the constraint applied at the lower face. LP nutside (Figure 2.21(b)) surface is moving with the applied load value. More relative movement due to the larger surface of the contact can be seen on the interface sides of SP and LP (figure 2.27 c and d) than SP boltside and LP nut side (Figures 2.27 a and b). Figure 2.28 shows the *y*-displacement pattern on (a) SP boltside, (b) LP nutside (c) SP interface side and (d) LP interface side at 30000 N pretension. Figure 2.28(c) shows that there is slightly a greater region of displacement right above the bolt (marked by arrows), which is not there in the Figure 2.27(c). Reason cause there is more movement in *y*-direction due to the increasing pretension force. This increase in displacement region can be seen on LP interface side too if figures 2.27(d) and 2.28(d) are compared. The maximum *y*-displacement band in figure 2.29 varies between 0.040 mm and 0.045 mm. As the pretension is increased the maximum *y*- displacement band now varies between 0.047 mm to 0.054 mm in figure 2.30. High pretension value elongates the bolt more as it produces more axial tension in the bolt. Table 2.4 summarizes the maximum displacement values in *y*-direction and is helpful in concluding the discussion. Maximum values obtained when pretension was 500

N is also included in the table. As the pretension is increased there is an increasing trend of maximum value in SP and LP.
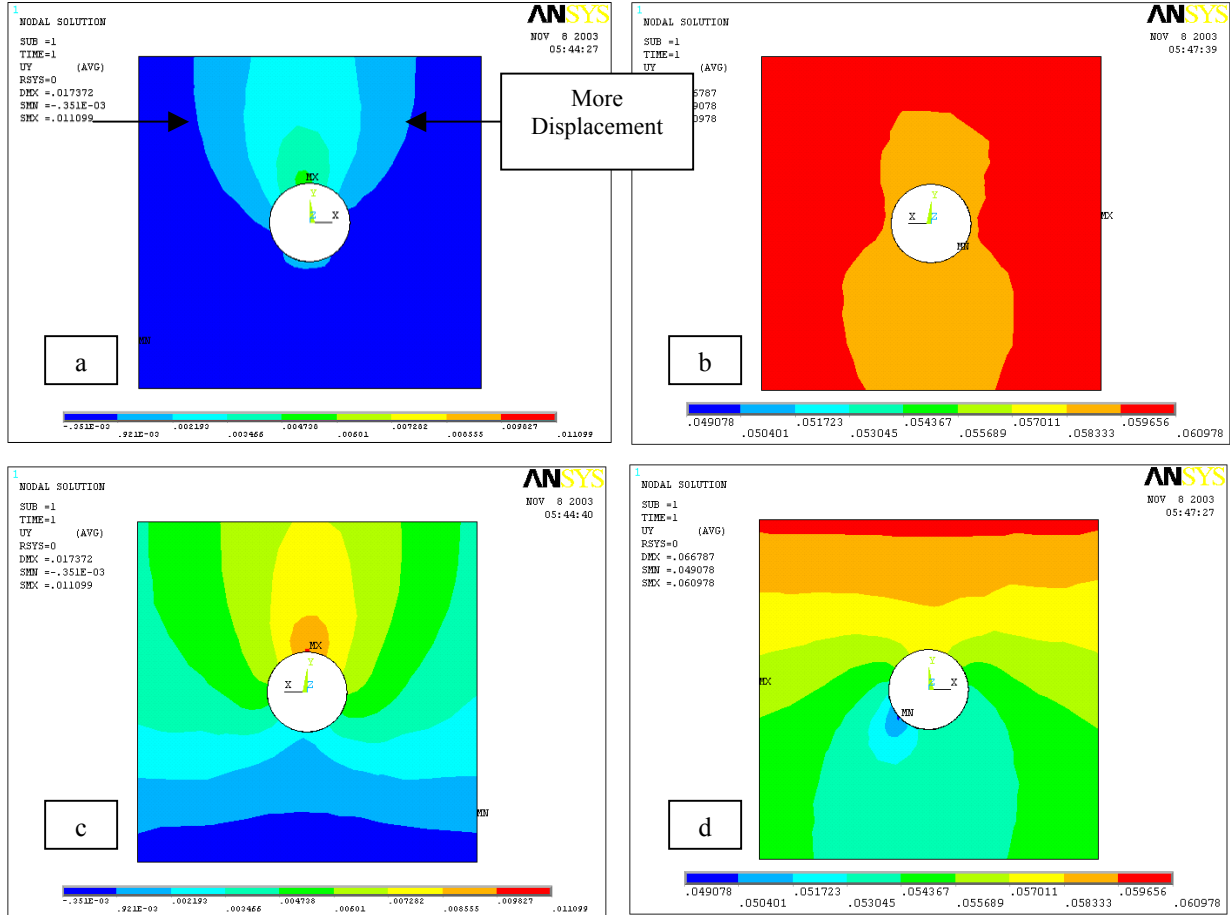
Figure 2.27: *y*-displacement of (a) SP boltside (b) LP nutside (c and d) SP and LP

interface side at 9,000 N
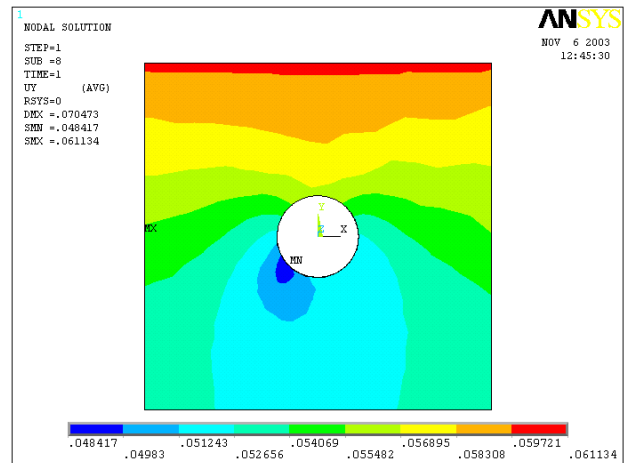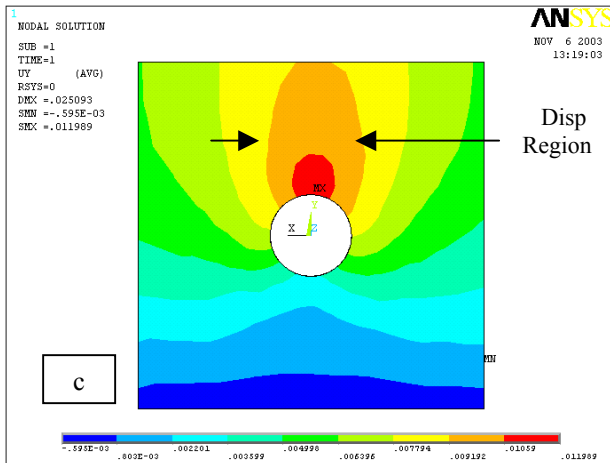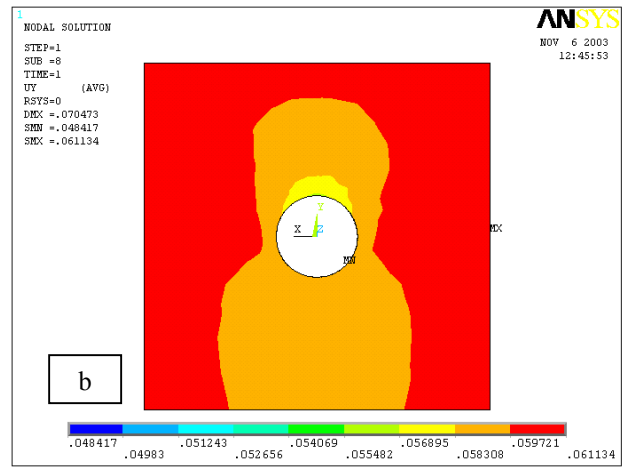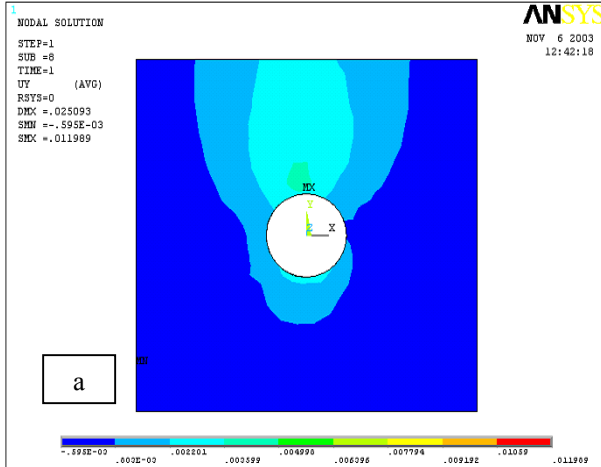
Figure 2.28: *y*-displacement of (a) SP boltside (b) LP nutside (c and d) SP and LP interface

side at 30,000 N
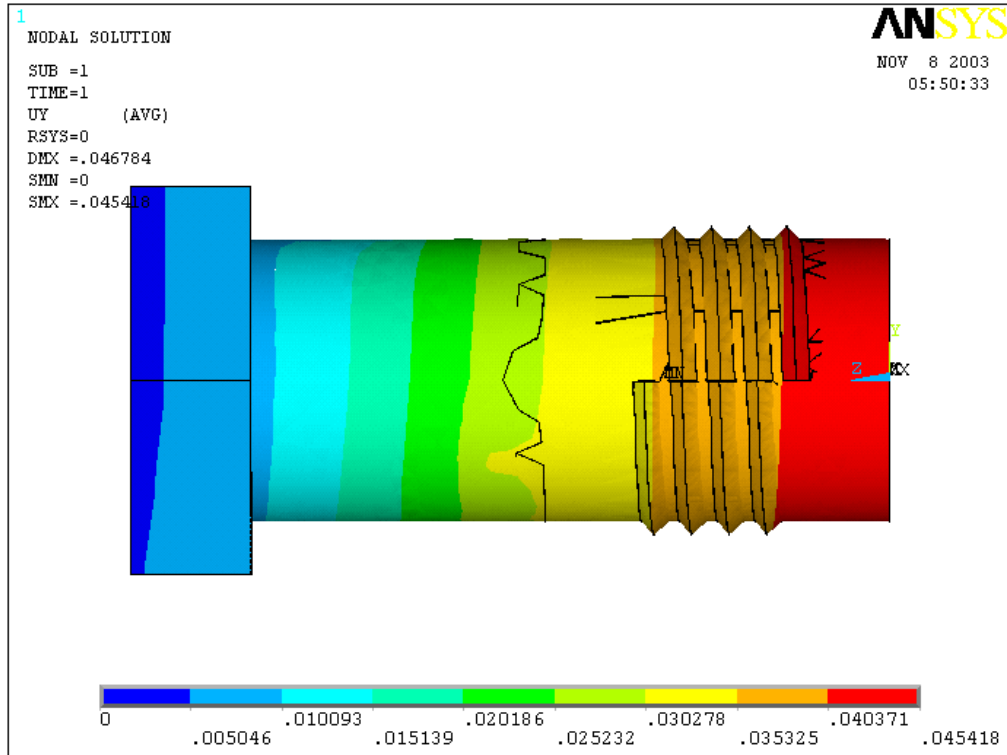
Figure 2.29: *y*-displacement of bolt at 9,000 N
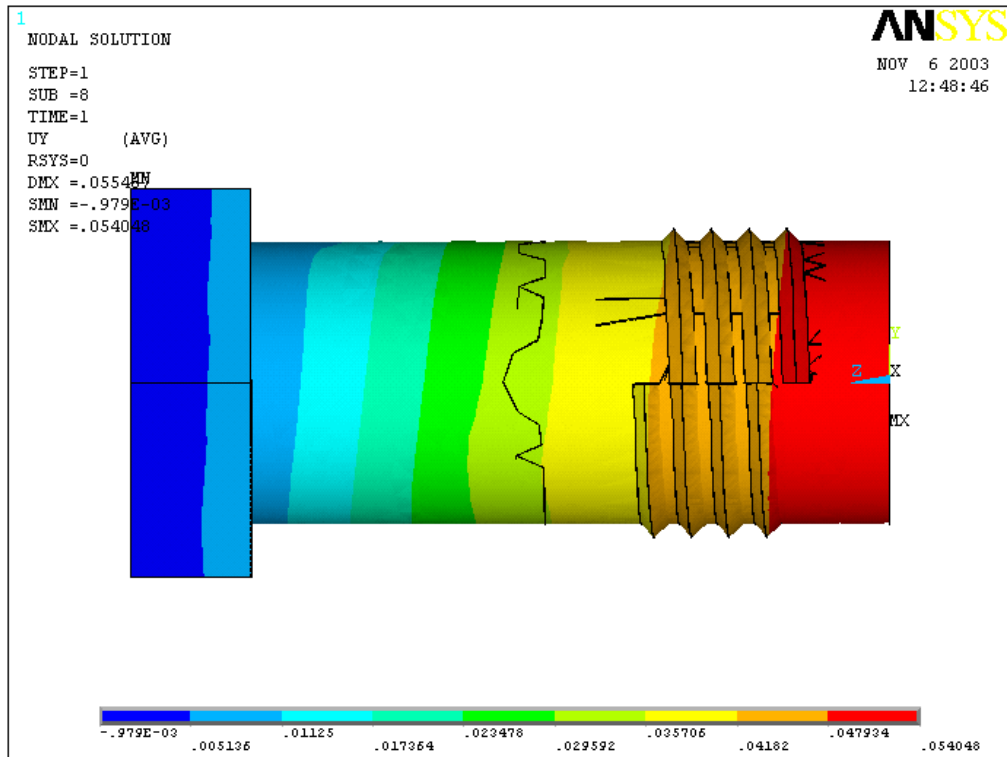
Figure 2.30: *y*-displacement of bolt at 30,000 N

Table 2.4: Maximum *y*-displacement value under increasing pretension

Pre Tension (N)	Bolt (mm)	Nut (mm)	SP (mm)	LP (mm)
500	0.11804	.099302	0.010855	0.06026
9,000	0.045418	0.041542	0.011098	0.060978
30,000	0.05405	.049001	0.01198	0.061134

Stress σ_z

The bolt preload force is in the direction parallel to the axis of the bolt. To observe the compression produced in the plates by this preload force, stress along the bolt axis, which is stress σ_z , is noted. Figure 2.31 shows the stress σ_z distribution on (a) SP bolt side, (b) LP nutside, (c) SP interface side and (d) LP interface side at pretension of 9000 N. It is noted that highly compressive stresses are present around the bolt hole. The stresses decrease in magnitude moving towards the edge of the plate from the center. The main reason of this high compressive stress is the preloading in the bolt that compresses the plate. Same trend of stress distribution can be seen in figure 2.32. Figure 2.33 shows the contour plot of stresses σ_z for the pretension values of (a) 500 N, (b) 9000 N and (c) 30,000 N on the LP interface side. The maximum value of the stress around the bolt hole is written in the center of each hole. It can be noted from the values that as the pretension is increased the maximum value of stress around the bolt hole increases. This again indicates that the plate is getting more compressed. Stress concentration around the bolt hole is also high in case of high pretension force (Figure 2.35c).

Figure 2.34 and 2.35 show the stress σ_z in the bolts at pretension 9000 N and 30000 N. The bolt having high pretension is stressed more. Table 2.5 gives the von Mises stress value. Any trend cannot be predicted by looking at these values. Table 2.6 is more useful to predict the behavior of pretension effect. As the pretension is increased the value of maximum stress σ_z is increased.
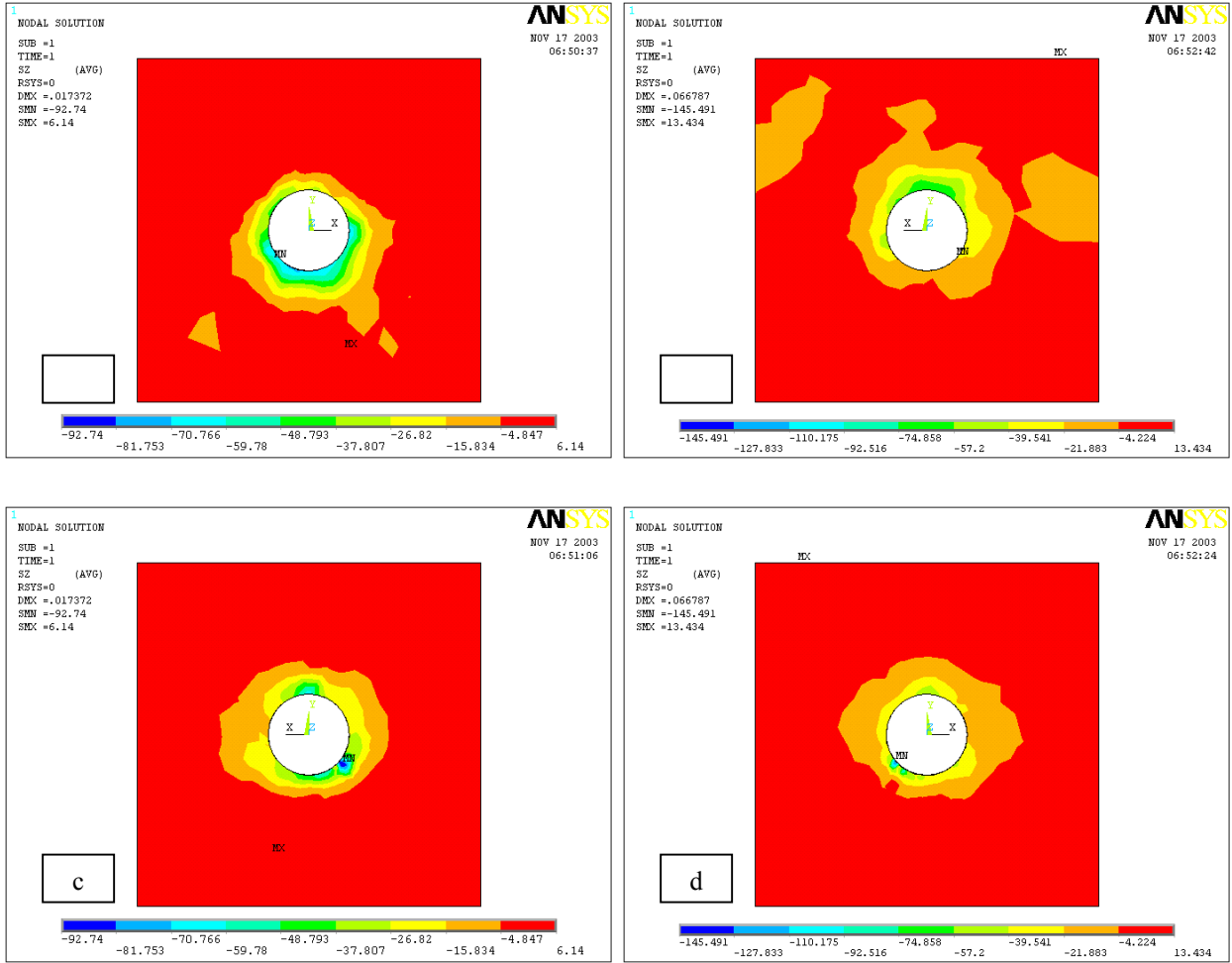
Figure 2.31: Stress σ_z of (a) SP boltside (b) LP nutside (c and d) SP and LP interface side at
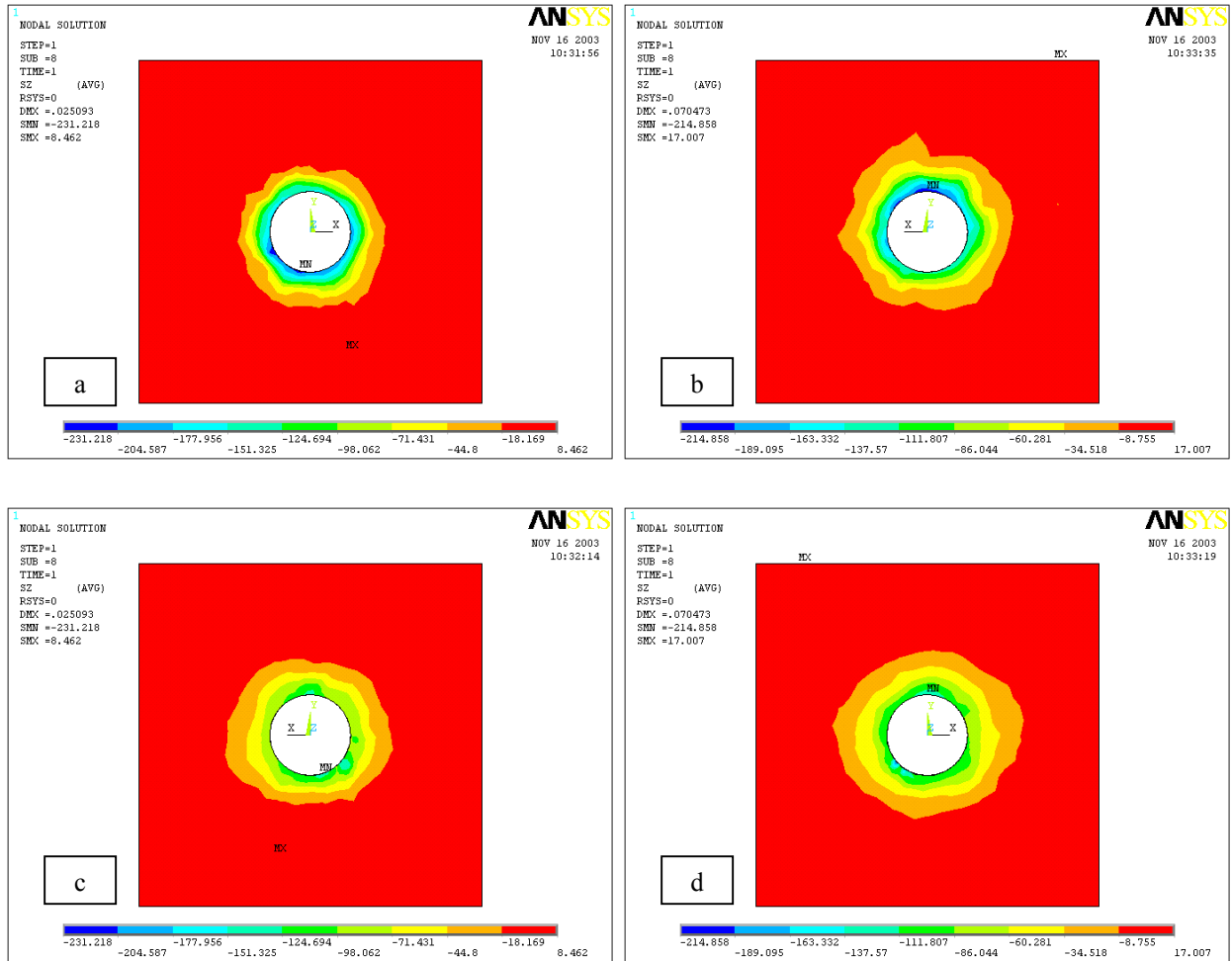
9,000 N

Figure 2.32: Stress σ_z of (a) SP boltside (b) LP nutside (c and d) SP and LP interface side at

30,000 N

(a) Pretension = 500N

(b) Pretension = 9000N

(c) Pretension = 30,000N
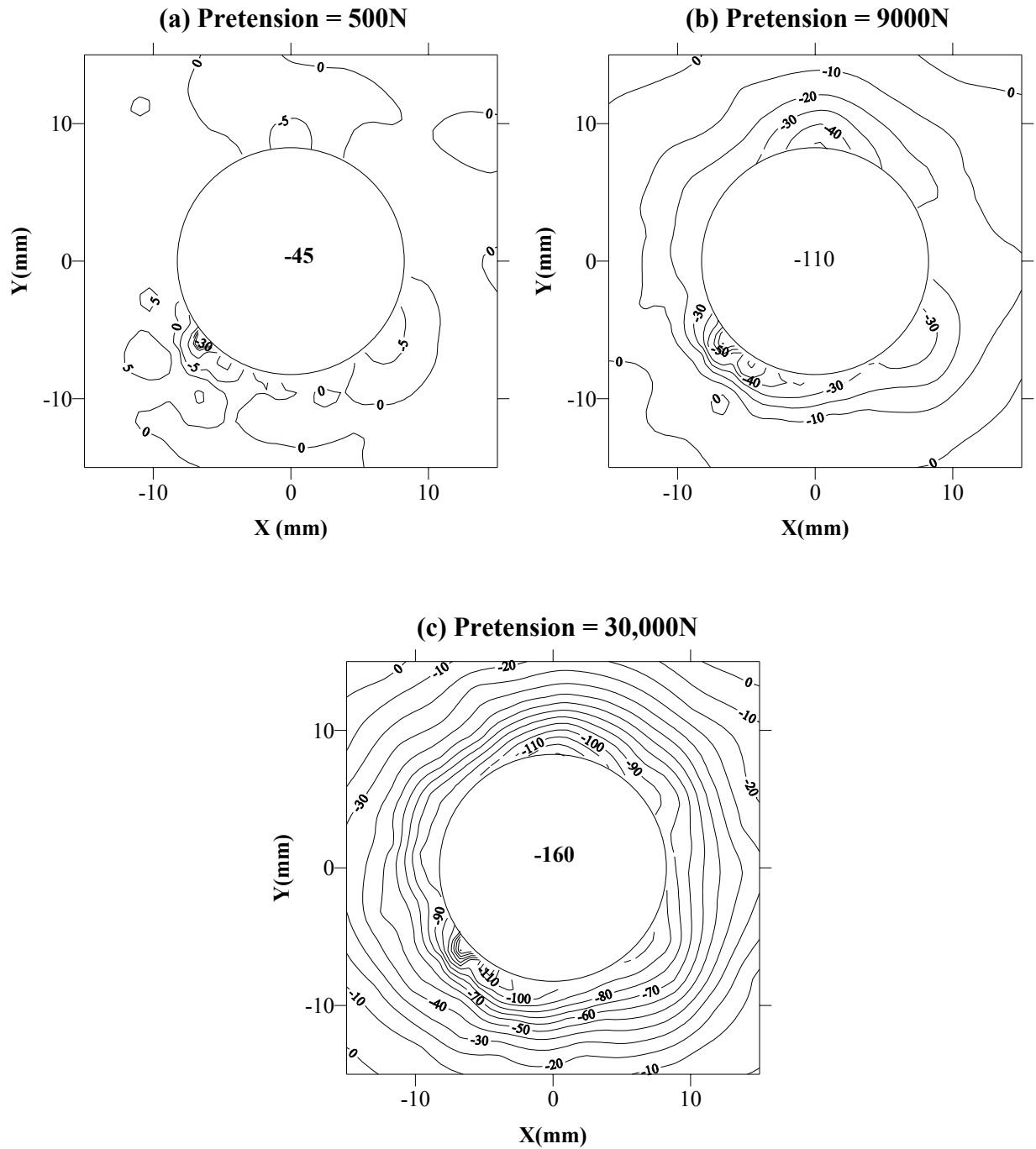
Figure 2.33: Stress σ_z contours on interface side of loading plate at pretension of

(a) 500 N, (b) 9,000 N and (c) 30,000 N
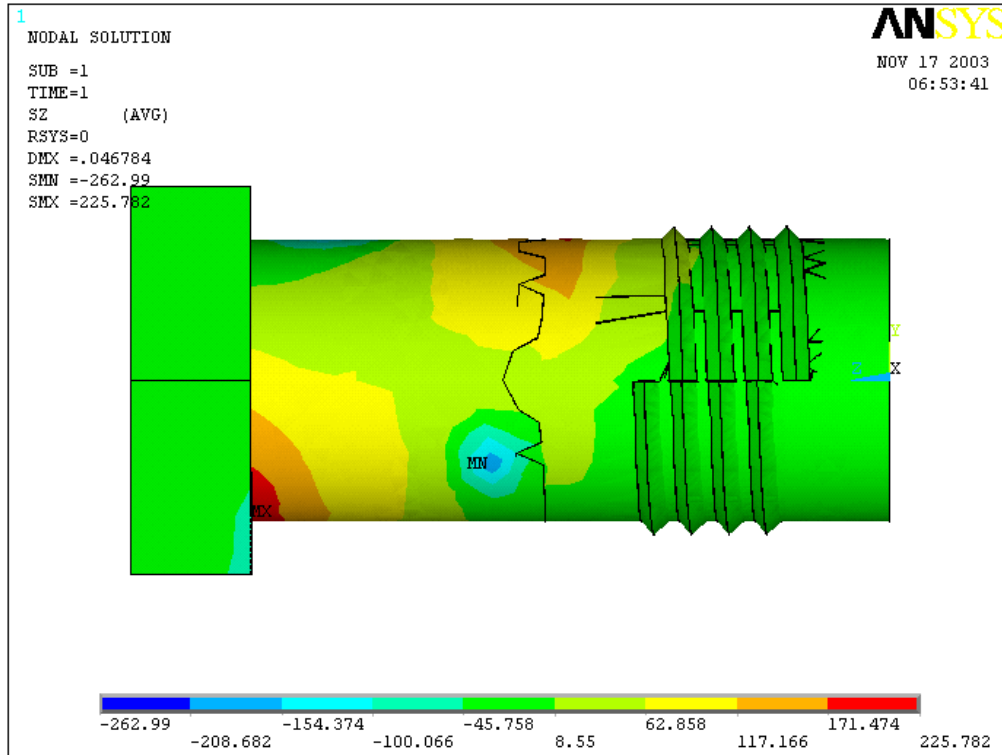
Figure 2.34: Stress σ_z of bolt at 9,000 N
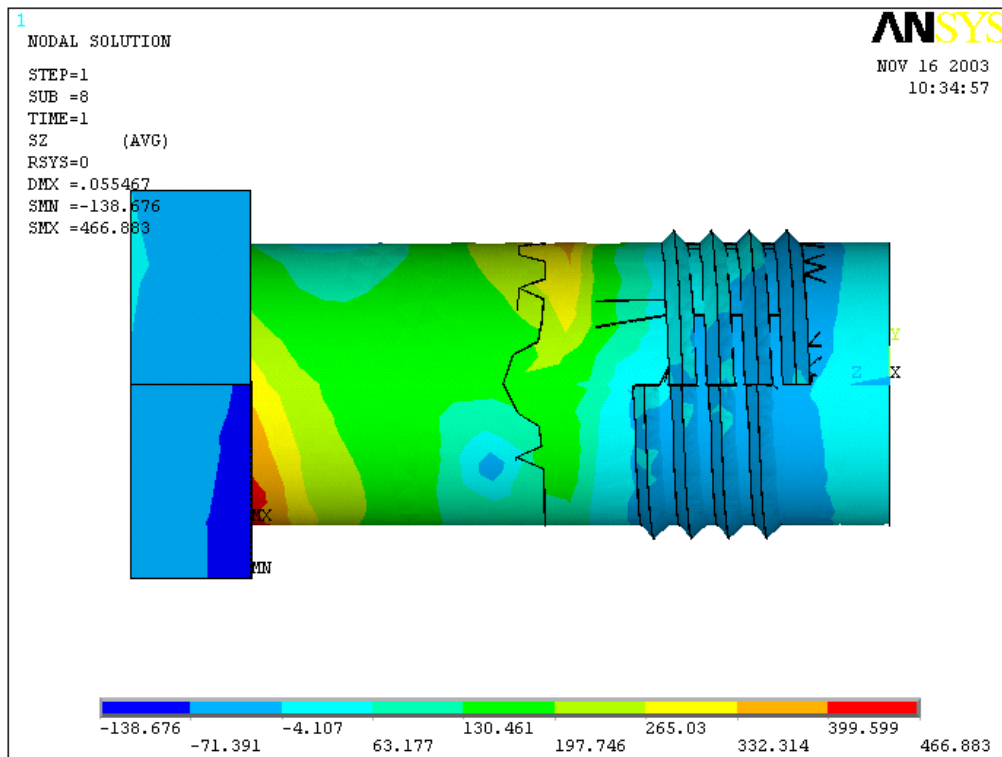
Figure 2.35: Stress σ_z of bolt at 30,000 N

Table 2.5: Maximum von Mises stress value under increasing pretension

Pre Tension (N)	Bolt (MPa)	Nut (MPa)	SP (MPa)	LP (MPa)
500	279.826	27.069	211.25	160.462
9,000	419.318	106.701	103.026	241.721
30,000	417.428	220.458	206.567	198.882

Table 2.6: Maximum stress σ_z value under increasing pretension

Pre Tension (N)	Bolt (MPa)	SP (MPa)	LP (MPa)
500	58	-51	-69
9,000	225	-92	-145
30,000	466	-231	-214

2.4.3   Study A3: Effect of Clearance

The clearance between the bolt and the hole is an important factor in a bolted joint analysis. Strength and durability of a bolted joint is partially dependent on the closeness of fit between bolt and hole. The hole should not be so small that the bolt is to be forced in to that hole. Also it should not be so large that the resulting joint is loose. A loose joint will allow relative motion (wear), will allow moisture (corrosion), will cause hardening of bearing surface (eventually cracking), will transmit load unevenly and will allow cracking under the head of the bolt or thinning of a soft material. The analysis here has examined three radial clearances of 0.01 mm, 0.05 mm and 0.5 mm. Other parameters such as pretension (500 N) and the displacement load (0.06 mm) are kept constant.

y-displacement

Figure 2.36 shows the y-displacement on (a) SP boltside, (b) LP nutside, (c) SP interface side and (d) LP interface side at 0.01 mm radial clearance value. Figure 2.37(a) shows that maximum displacement value is 0.024 mm and displacement pattern is uniform all over the region. SP and LP interface sides as in figures 2.36 c and d show relative movement due to the contact condition and applied load. Figure 2.37 shows the displacement pattern on (a) SP boltside, (b) LP nut side (c) SP interface side and (d) LP interface side at clearance value of 0.05 mm. Figure 2.37(a) shows that lower half portion of the SP is not moving, unlike the first case as in figure 2.36(a) when the small clearance is used. The maximum displacement value is 0.0108 mm hence there is a decrease in the maximum value of displacement when clearance is increased. The reason for this behavior lies in the fact that in low clearance value case bolt is striking the surface of the plate earlier than in high clearance case at same applied displacement load. Figure 2.37(c) tells that the region of displacement above the bolt hole (marked by arrows) is decreased as

compared to the low clearance case (figure 2.36c). Same decrease (marked by arrows) can be seen in region in figure 2.37(d) under the bolt hole. This result indicates that there is more deformation in the plate having low radial clearance. Figure 2.38 and 2.39 show the displacement pattern in bolts at two clearance values. There is very slight change in the displacement pattern of the bolts when clearance is increased. However the values in different displacement bands are not same. Table 2.8 is giving the maximum values of displacement in y-direction at three clearance values. As the clearance is increased the value is decreased. This reasoning is explained in the beginning of the discussion.
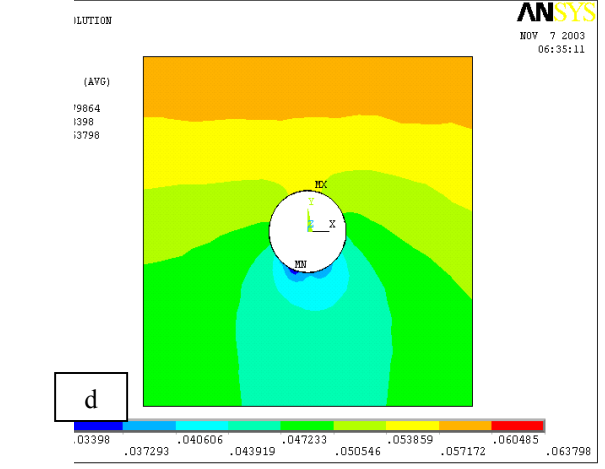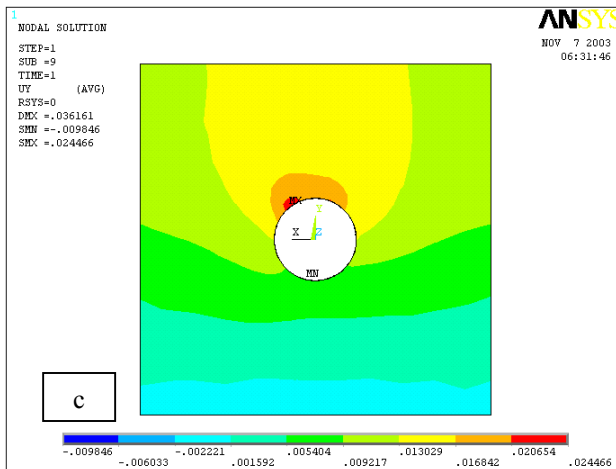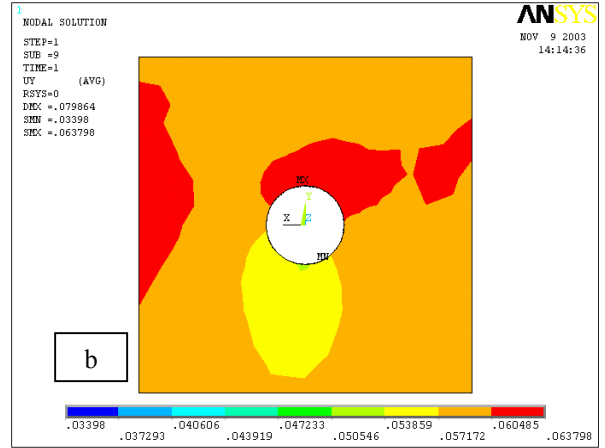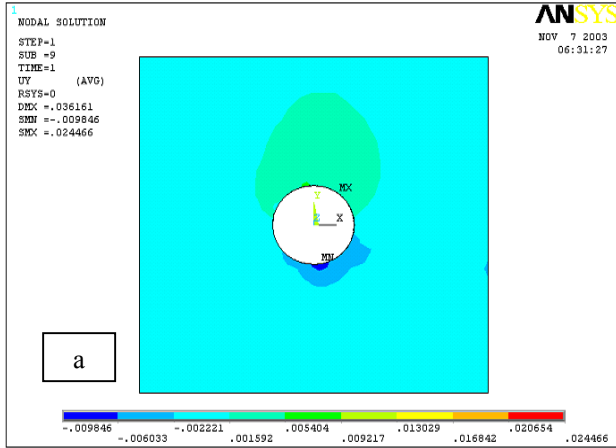
Figure 2.36: *y*-displacement of (a) SP boltside (b) LP nutside (c and d) SP and LP

interface side at 0.01 mm
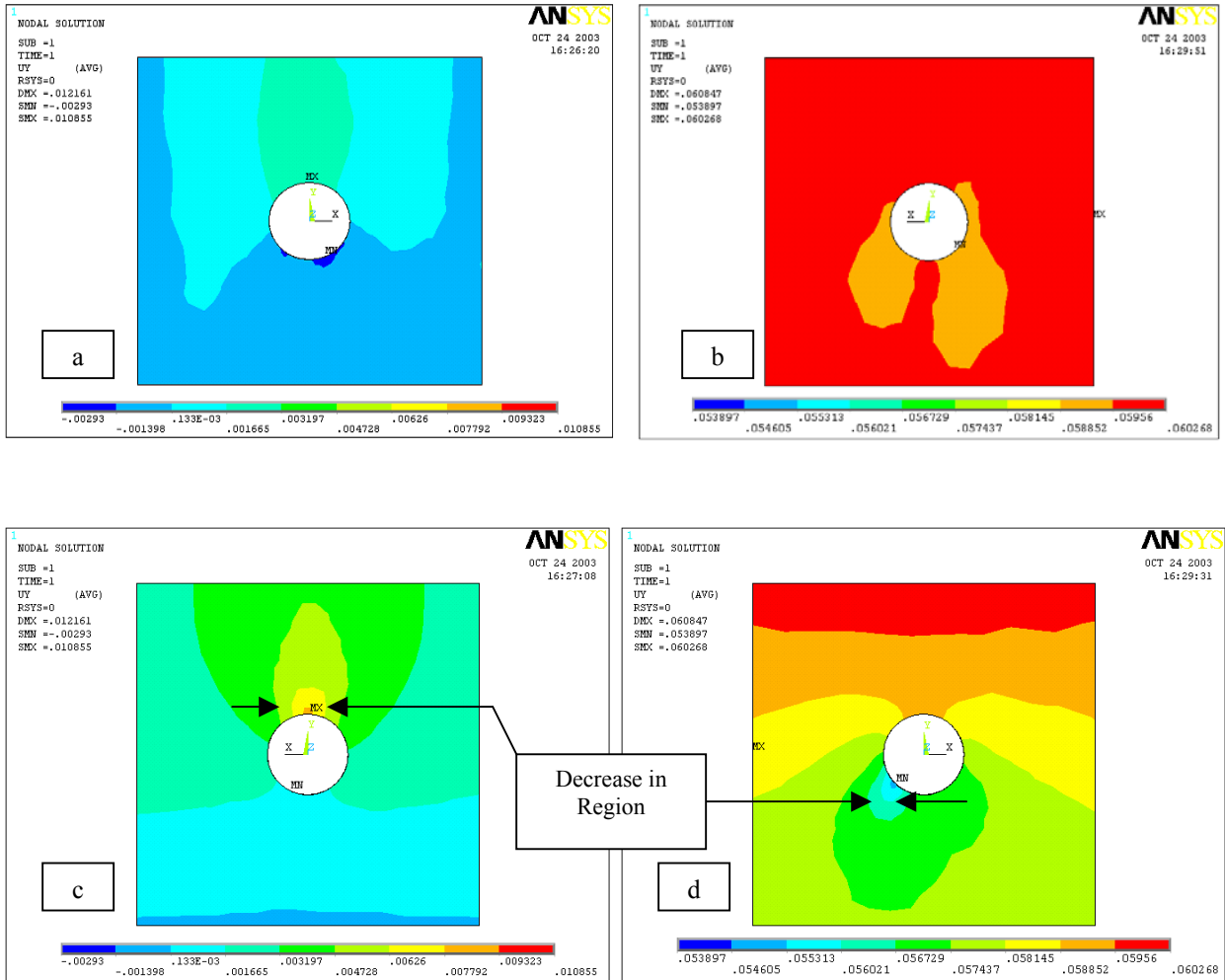
Figure 2.37: *y*-displacement of (a) SP boltside (b) LP nutside (c and d) SP and LP interface

side at 0.05 mm

Figure 2.38: *y*-displacement of bolt at 0.01 mm

Figure 2.39: *y*-displacement of bolt at 0.05 mm
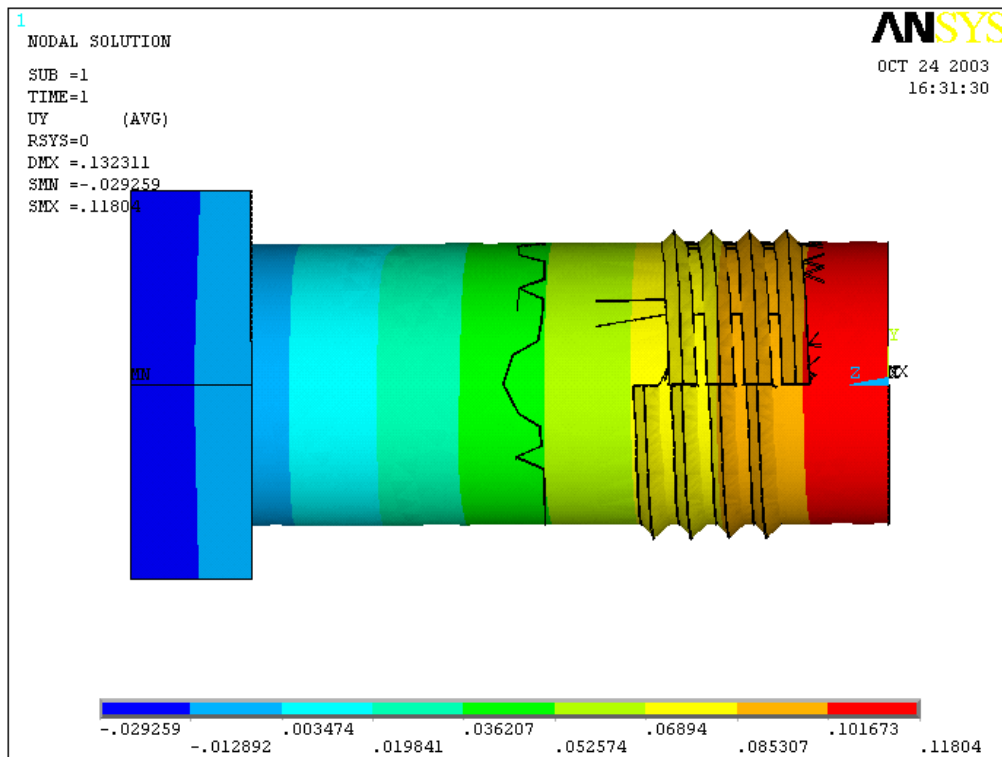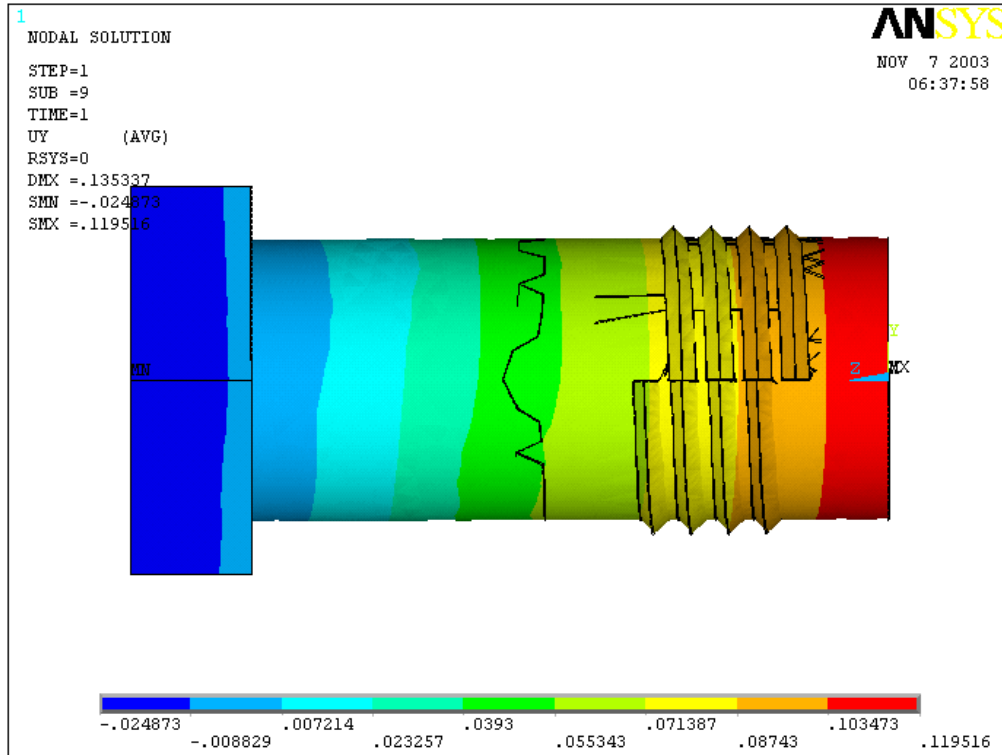
Table 2.7: Maximum *y*-displacement values under increasing clearance

Clearance (mm)	Bolt (mm)	Nut (mm)	SP (mm)	LP (mm)
0.01	0.119516	0.102175	0.024466	0.063798
0.05	0.11804	0.099302	0.010855	0.060268
0.5	0.042238	0.04282	0.00102	0.060015

Stress σ_y

Figure 2.40 shows the stress σ_y distribution on (a) SP boltside, (b) LP nutside, (c) SP interface side and (d) LP interface side at clearance value of 0.01 mm. Figure 2.40(a, b) show the stress σ_y distribution in SP boltside and LP nutside respectively. Most of the region in SP and LP is in compression with small regions (marked by arrows) of LP going in tension. In Figure 2.40(c) small regions around the bolt hole are in tension whereas in figure 2.40(d) most of the upper half surface is in tension. This is due to the striking of the bolt on loading and supporting plate at lower and upper bolt hole surface respectively. Figure 2.41 shows the stress σ_y distribution on (a) SP boltside, (b) LP nutside, (c) SP interface side and (d) LP interface side at clearance value of 0.05 mm. Figure 2.41(c) shows that as the clearance is increased more region is in tension (marked by arrow) unlike the figure 2.40(c) where most of region is in compression. Figure 2.41(d) shows that the tension region marked in figure 2.40(d) is disappeared now. The reason being that the bolt is putting more stress on the plate due to the early contact in low clearance case. These figures show that there is an effect of clearance on the behavior of stress distribution. Figure 2.42 shows the contour plot of stress σ_y on the interface side of the loading plate at radial clearance values of (a) 0.01 mm, (b) 0.05 mm and (c) 0.5 mm. The value of maximum stress in Figure 2.42(a) is 0.6 MPa. There is no contribution of the stresses on the plate coming from the bolt. The radial clearance is higher than the applied displacement load in this case. Figure 2.42(b) shows that as the clearance is decreased to 0.05 mm there is contact of bolt with the hole and the maximum value of stress is increased. In figure 2.42(c) the maximum stress around the bolt hole increases and more stress concentration around the bolt hole is seen as compared to figure 2.42(b).

Table 2.8 and 2.9 gives the values of maximum shear stress; stress σ_y and maximum von Mises stress. Value at 0.5 mm clearance is also included in the table to get some useful conclusion. As the displacement is more in the low clearance case the stress is higher. The value of stress σ_y and shear stress both are higher incase of 0.01 mm as compared to the 0.05 mm case considerably. Table 2.9 shows that the bolt, SP and LP are going in the plastic deformation region when the clearance is very less. In normal practice there is a clearance within the bolt and the bolthole. By looking at the results of clearance 0.5 mm, the stress values are very low. The reason being that the displacement as load is lesser than the clearance given. So even at the full load the bolt is not touching the plates in either case. Consequently there is no movement in the plates and very little stresses are produced. Only stresses those are present due to the frictional and sticking effect. To conclude as the clearance is increased the maximum stress σ_y value in bolt, SP and LP decreases.
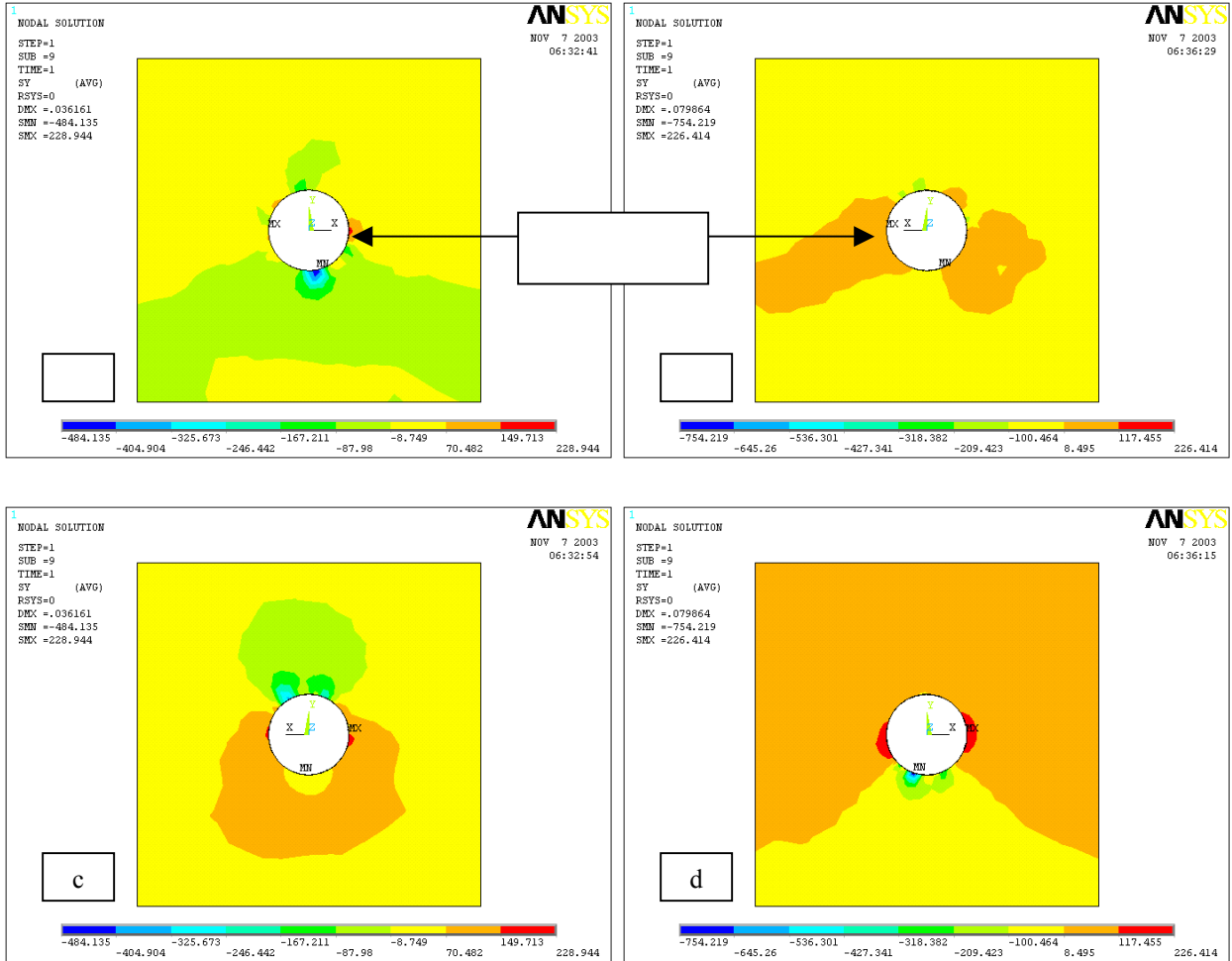
Figure 2.40: Stress σ_y of (a) SP boltside (b) LP nutside (c and d) SP and LP interface side at
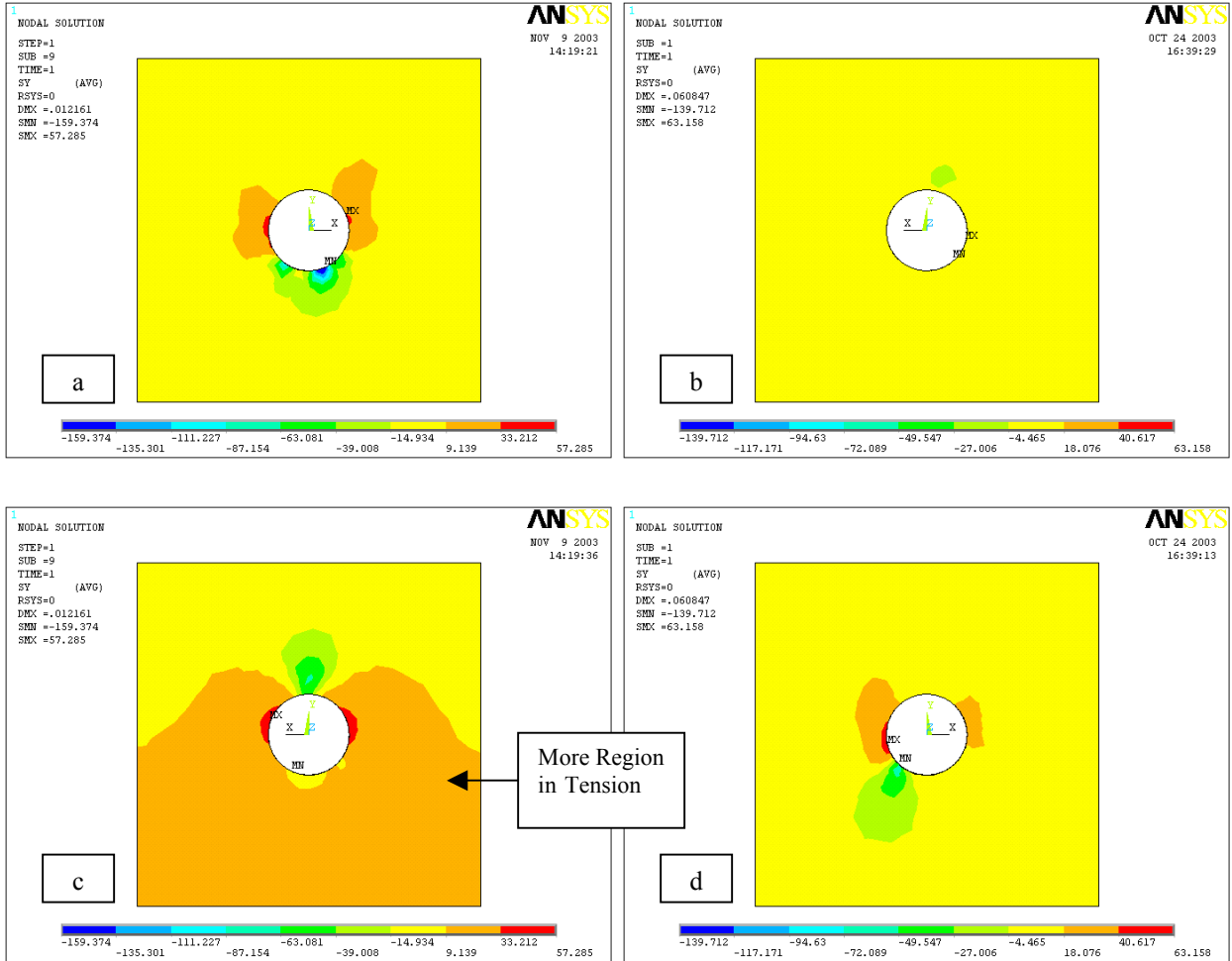
0.01 mm

Figure 2.41: Stress σ_y of (a) SP boltside (b) LP nutside (c and d) SP and LP interface side at
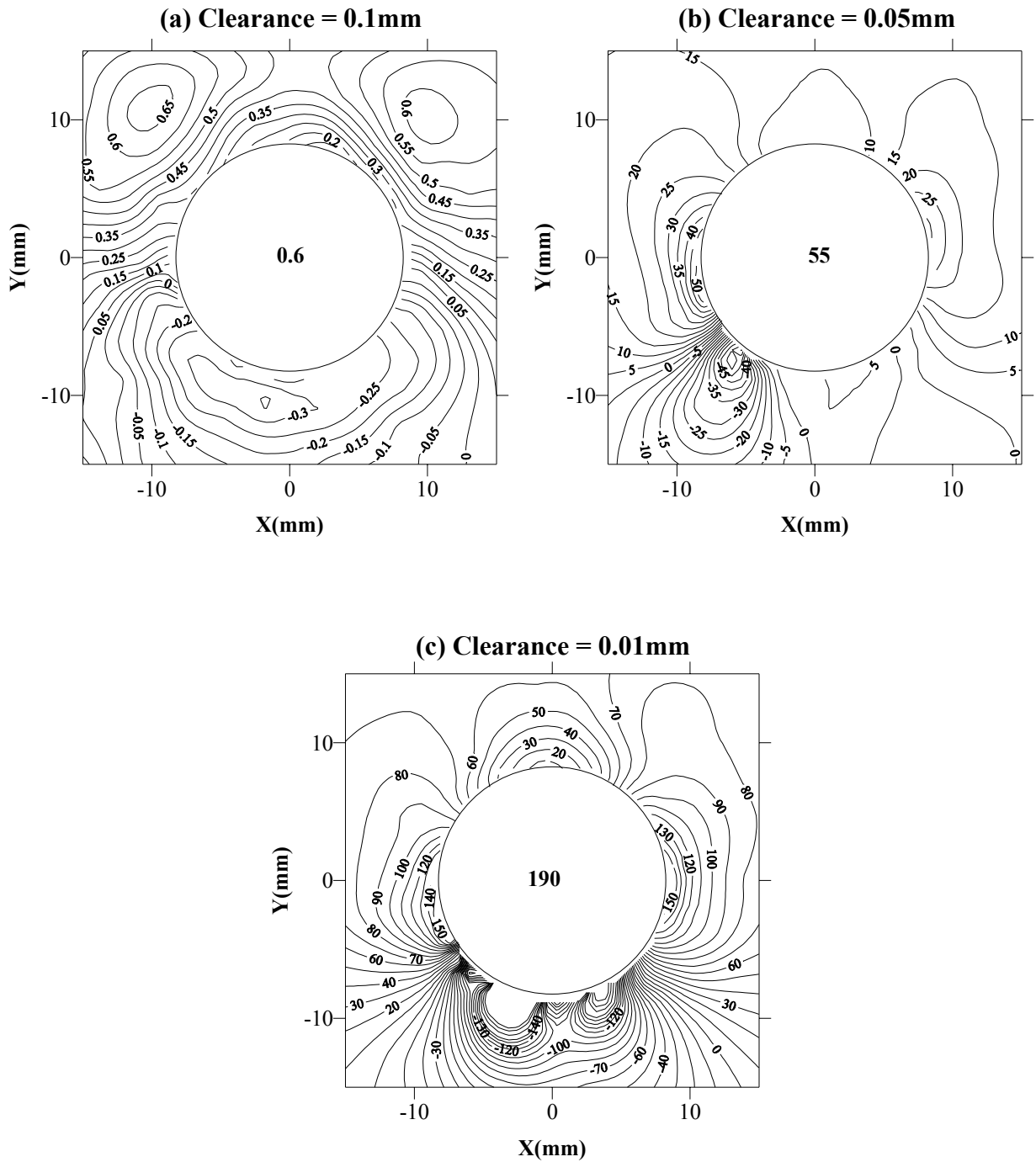
0.05 mm

Figure 2.42: Stress σ_y contours on the interface side of loading plate at (a) 0.1mm, (b) 0.05mm and (c) 0.01 mm Clearance

Table 2.8: Maximum stress σ_y and σ_{xy} value under increasing clearance

Clearance (mm)	σ_y at SP (MPa)	σ_y at LP (MPa)	σ_{xy} at SP XY (MPa)	σ_{xy} at LP (MPa)
0.01	228.944	226.414	272.098	263.693
0.05	57.285	63.158	78.267	37.584
0.5	0.6578	0.67542	1.029	0.890636

Table 2.9: Maximum von Mises Stress value under increasing clearance

Clearance (mm)	Bolt (MPa)	Nut (MPa)	SP (MPa)	LP (MPa)
0.01	434.865	112.283	755.038	837.732
0.05	279.826	27.069	211.25	160.467
0.5	5.752	3.416	3.281	2.743

2.4.4   Study A4: Effect of Coefficient of Friction

The only way to determine the coefficient of friction between two bodies is to conduct experiments. Factors, which affect the surface friction, include surface finish, lubrication, relative speed, relative pressure, temperature and environment. In this study the effect of friction coefficient on displacement and stress is studied by considering the values of 0.1, 0.2 and 0.3.

_y_-displacement

Figure 2.43 shows the displacement pattern in y direction on (a) SP interface side and (b) LP interface side for friction coefficient of 0.1. Figure 2.43(a) shows the lower region of the plate not moving due to the constraint applied to the lower face. Figure 2.43(b) shows that in the upper region of LP, the value of maximum displacement is going up to 0.06mm that is the applied load. Compare the y-displacement pattern at 0.1 and 0.3 friction coefficient values. In figure 2.43(a) the low displacement band (marked by arrow) close to the lower edge of the plate is small. This region is increased in case of high friction coefficient in figure 2.44(a). This is because when there is more resistance to movement due to frictional effect, the displacement will be less. In figure 2.43(a) the displacement band (marked by arrows) varies in between 0.0567 mm and 0.0574 mm. Figure 2.44(b) shows that this range (marked by arrows) is now in between 0.0564 mm and 0.0572 mm. Increase in friction causes a decrease in the displacement values. Figure 2.45and 2.46 show the y-displacement pattern in bolts. When the friction is higher the values of minimum and maximum values of y-displacement are smaller and vice versa. Table 2.11 tells that the displacement of bolt and SP decreases slightly with increase in the friction coefficient. High friction does not allow moving the plate freely, as it is the case in which low friction is used.
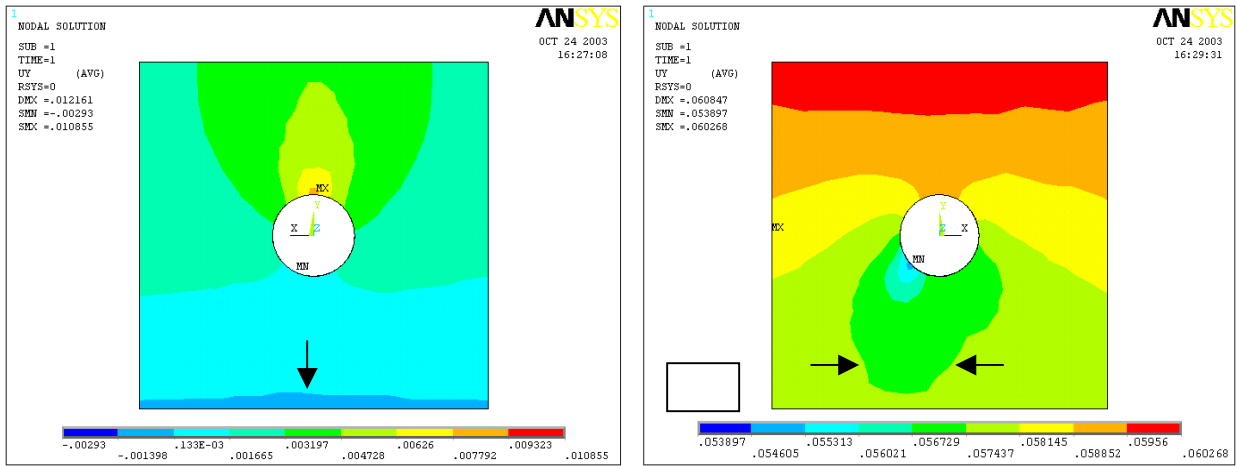
Figure 2.43: *y*-displacement of (a) SP interface side (b) LP interface side with friction
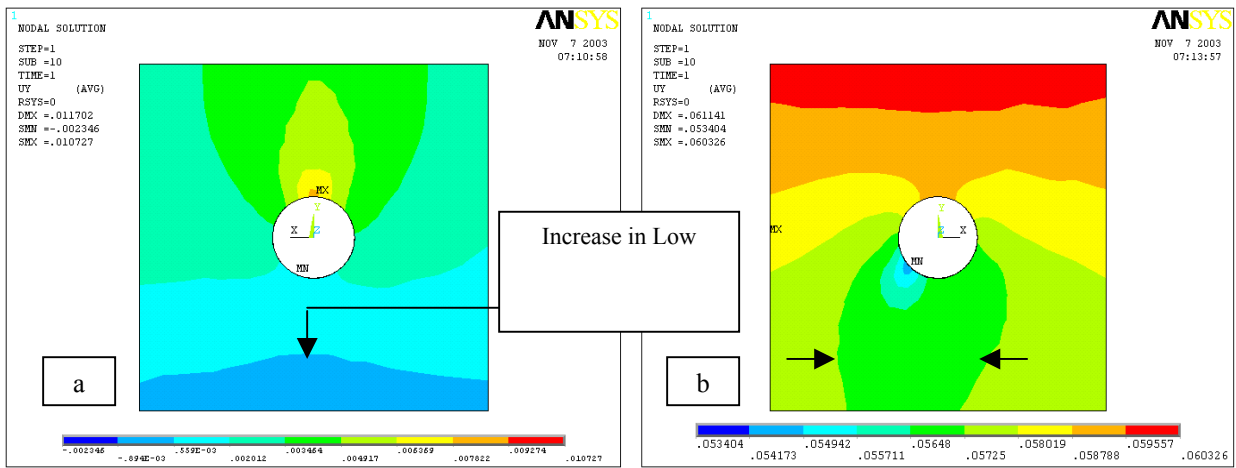
coefficient of 0.1

Figure 2.44: *y*-displacement of (a) SP interface side (b) LP interface side with friction
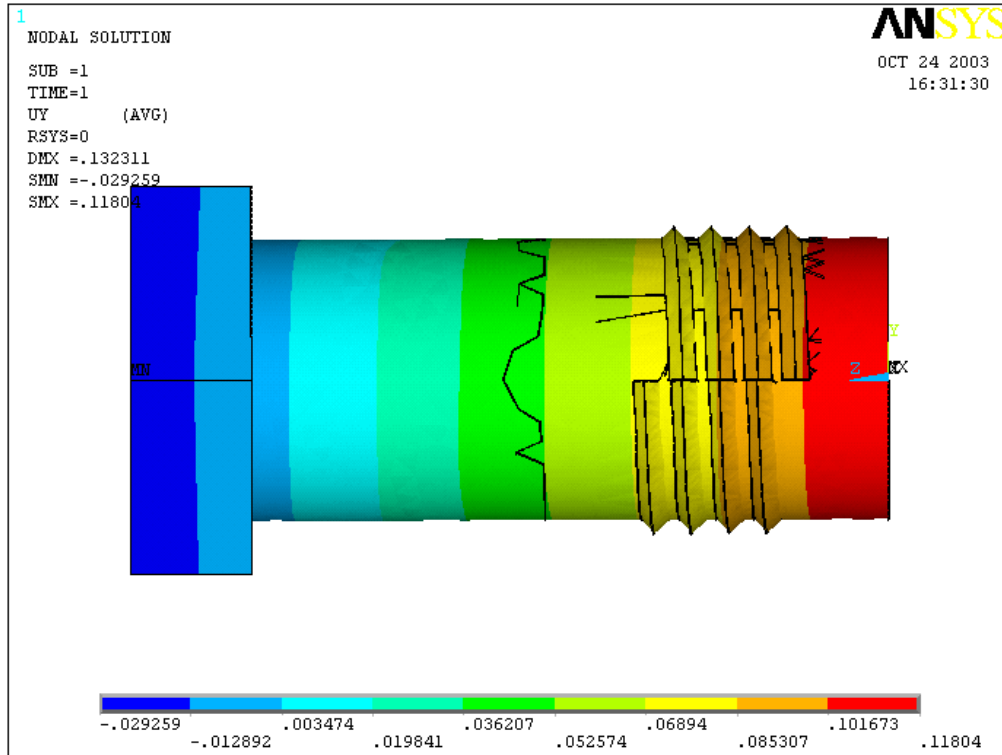
coefficient of 0.3

Figure 2.45: *y*-displacement of bolt with friction coefficient of 0.1
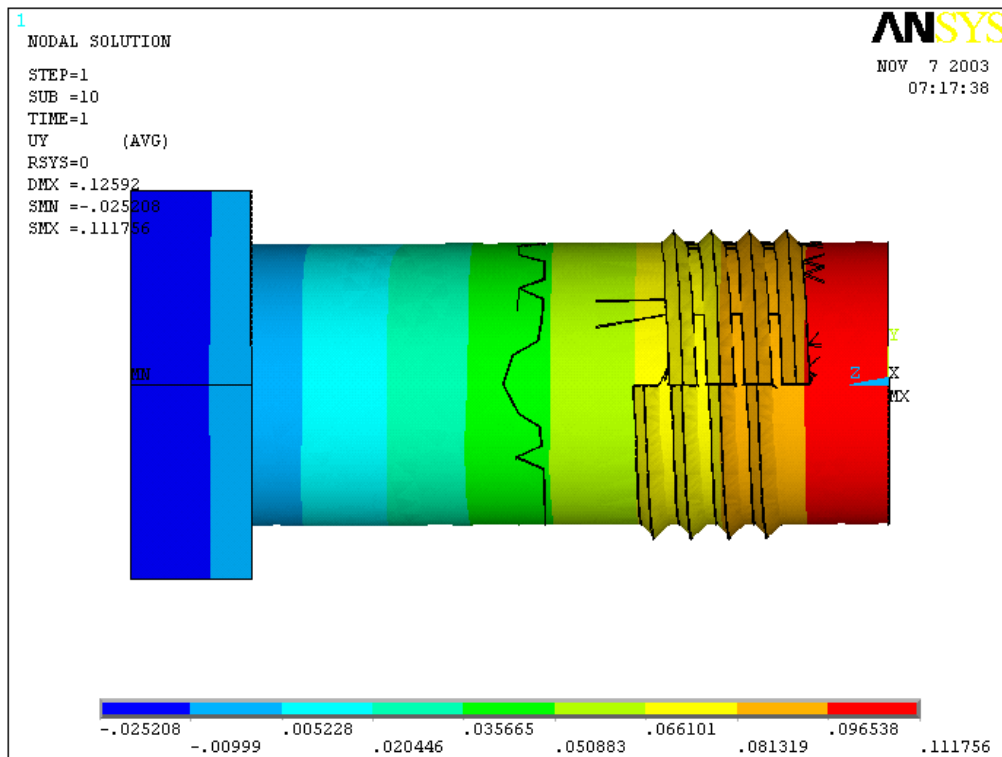
Figure 2.46: *y*-displacement of bolt with friction coefficient of 0.3

Table 2.10: Maximum *y*-displacement values under increasing friction (μ)

μ	Bolt (mm)	SP (mm)	LP (mm)
0.1	0.118040	0.010855	0.06026
0.2	0.114357	0.010771	0.0603
0.3	0.111756	0.010727	0.06032

Stress σ$_y$

Figure 2.47 and 2.48 shows the stress σ$_y$ distribution for the (a) SP interface side and (b) LP interface side friction coefficient of 0.1 and 0.3. There is a slight change in the distribution of stress on all the surfaces. The compressive stress region (marked by arrows) in figure 2.47(a) is smaller as compared to the region in figure 2.47(b). High friction coefficient resists the motion of the plate and produces more stress. The increase in the compressive region (marked by arrows) in figure 2.48(b) is obvious if it is compared with the region present in figure 2.48(a). Table 2.12 shows the results at three coefficient of friction values 0.1, 0.2 and 0.3. There is an increase in the stress σ$_y$ and shear stress value σ$_{xy}$ in LP as the friction co efficient is increased. For SP the shear stress σ$_{xy}$ decreases as μ increases. Table 2.13 tells that increase in the μ increases the von Mises stress in bolt, nut and LP and decreases in SP. The von Mises stress value remains under the yield stress value in all the cases.
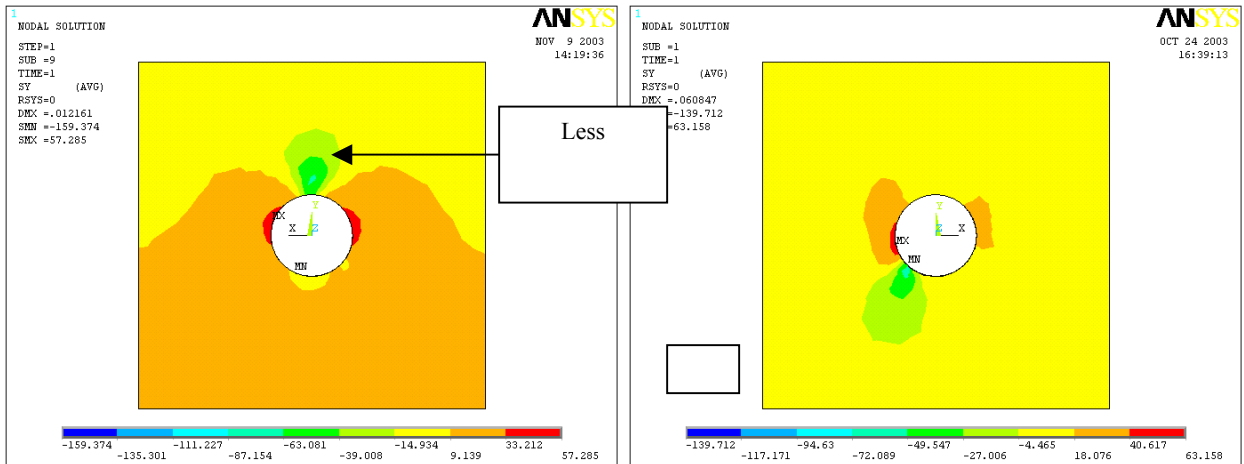
Figure 2.47: Stress σ_y (a) SP interface side (b) LP interface side with friction coefficient of 0.1
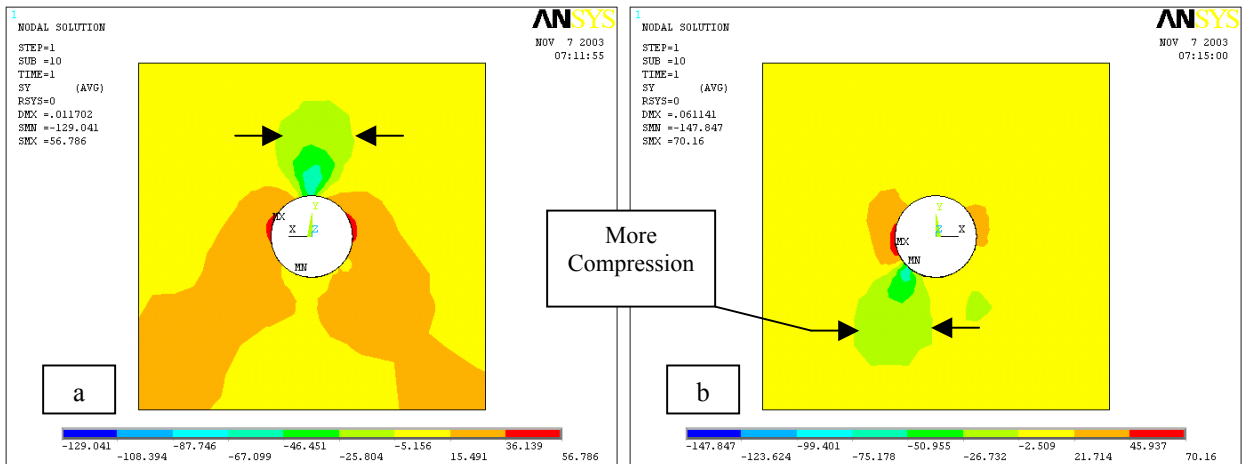
Figure 2.48: Stress σ_y (a) SP interface side (b) LP interface side with friction coefficient of 0.3

Table 2.11: Maximum stress σ_y and σ_{xy} value under increasing friction

μ	σ_y at SP (MPa)	σ_y at LP (MPa)	σ_{xy} at SP (MPa)	σ_{xy} at LP (MPa)
0.1	57.285	63.158	78.267	37.584
0.2	57.025	66.71	69.741	39.093
0.3	56.785	70.16	67.605	40.194

Table 2.12: Maximum von Mises stress value under increasing friction

μ	*Bolt* (MPa)	*SP* (MPa)	*LP* (MPa)
0.1	279.826	211.25	160.462
0.2	287.425	186.398	165.487
0.3	293.598	164.933	169.502

2.4.5   Study B1: Tensile Type Loading (Pretension Effect)

The general model for this case is the same as described in section 2.2. Same element type and material properties are used. Only half model due to the symmetrical nature of whole structure is used for this analysis. Boundary conditions are different in this case and are shown in figure 2.49. (a) The three sides of SP are constrained, (b) pressure is applied on LP nut side as load and (c) symmetry boundary condition is applied at the lower surfaces in the y-direction. The direction of applied pressure of 0.2 MPa is shown in the figure 2.50. Three different pretension values (2,500 N, 5,000 N and 30,000 N) are used. The clearance between the hole and the bolt is 0.05 mm. Additional contacts are defined in this case between the thread of the bolt and the mating surfaces of threads on the nut. Number of nodes and elements in this half model are reduced to 10765 and 3462 respectively.

z-displacement

The pressure is applied in the negative z direction thus the parameters of interest are displacements and stresses in z-direction. Figure 2.51 shows the displacement pattern in the z-direction of SP at pretension of 2,500 N. The figure shows the (a) isometric view, (b) bolt side and (c) the interface side of SP. SP is constrained at the three edges, so the displacement is minimum in the regions near the edges. Figure 2.51(b) and (c) shows that the plate tends to move more away from the edges approaching towards the bolt hole. Maximum value is just around the bolt hole on both (b) and (c) surfaces. Figure 2.52 shows the (a) isometric view, (b) bolt side and (c) the interface side of SP at pretension force of 30,000 N. displacement pattern is same but the values in different displacement bands is increased showing the effect of increasing pretension. Bolt head exerts more pressure on the surface of SP because of increased clamping force. Figure 2.53 shows the

(a) isometric view, (b) interface side and (c) nutside view of LP at a pretension force of 2,500 N. Pressure is applied at the nutside surface of LP as an external load in z-direction. Corners of LP are more displaced and the displacement of the plate is decreasing moving towards the center Central portion shows less movement because of the presence of nut that is not allowing free motion in the direction of applied pressure. Figure 2.54 shows the (a) isometric view, (b) interface side view and (c) nutside view of LP at a pretension force of 30,000 N. As the pretension is increased outer corners of the plate are displaced more as compared to the low pretension case. The value is increased from −0.002184 mm to −0.00662 mm. High pretension value produces more axial tension in the bolt thus increasing the clamping force. As a result LP is compressed more at the center due to the nut, and corners displace more (marked by arrow) in negative z direction. Figure 2.55 shows the displacement pattern in z direction at pretension force of 2,500 N of the bolt. The negative values in different displacement bands indicate that the bolt as a whole is moving in the direction of applied pressure. Figure 2.56 shows the displacement pattern of the bolt at pretension value of 30,000 N. Increase in the pretension value changes the pattern of displacement in the bolt. Two types of forces are acting on the bolt. First one is the pressure acting on the bolt indirectly and second one is the pretension force in the bolt. The high pretension force tends to move some portions of the bolt (marked by arrows) in the opposite direction of the applied pressure. Such movement is absent in Figure 2.55 when pretension is low. In that case external load is overcoming the pretension force as no displacement in opposite direction is noted.

Stress σ_z

Figure 2.57 shows the stress σ_z distribution of the SP at pretension force of 2,500 N. (a) Isometric view; (b) boltside and (c) interface side is shown in the figure. Highly compressive stresses can be seen around the bolthole. The stresses σ_z decrease (marked by arrows) moving away from the bolt hole towards the edges. . This stress is due to the pretension applied as it is pressing the plate in that region. The stress σ_z distribution is slightly different on SP boltside and interface side. Bolt head side is more stressed around the bolt hole. Figure 2.58 shows the three views of SP at pretension value of 30,000 N. The stress σ_z distribution pattern is almost the same. The values of maximum stress in different stress bands are increased. Maximum stress region is on the SP boltside. Figure 2.59 shows the (a) isometric view; (b) interface side and (c) nutside of LP at pretension force 2500 N. High compressive stresses are present around the bolthole. Pretension produces a clamping force that results in more compression on the surface of LP due to the pressure of nut. Nutside is directly in contact with the nut so it shows more stress than the interface side. Figure 2.60 shows the stress distribution at higher pretension value. The stress values are increased in different bands. Figure2.61 and 2.62 show the stress σ_z behavior of bolt when tension type loading is applied. The two regions (marked by arrows) of high stresses are the regions just below the head of bolt and around the first engaged thread. Figure 2.63 shows the graph of stress σ_z distribution at the root of engaged threads 1, 2, 3 and 4 at three pretension values. Thread 1 is the first engaged thread. Value of stress is noted at a point at the root of each thread. The graph tells that maximum stress is present in the first engaged thread i.e. 1 and the stress drops significantly in the threads 2, 3 and 4. In case of pretension 30,000 N, the first thread is

taking 47 % of the total load. This load share is decreased to 24%, 16 % and 13% in thread number 2, 3 and 4 respectively. For pretension values of 5,000 N and 2,500 N the first thread is taking 54 % and 49 % respectively. Figure 2.64 shows the graph between the stresses variations in thread 1, from root (0) to tip (h) at three pretension values. The graph tells that at the root stress is high and it decreases as we move towards the tip. At the tip there is slight increase in the stress again. From table 2.14 it is clear that as the pretension is increased the compressive stresses are increased in the bolt, SP and LP. The parts of bolted joint are going in plastic deformation in the tensile type of loading at pretension value of 30,000 N. Calculating the stiffness of the members is difficult because the compression spreads out between bolt head and the nut, hence the area is not uniform. There are however some analytical methods that predict the stiffness of the member approximately. In theory compression of a member is represented by a frustum of hollow cone. Mischke [2] uses half apex angle $\alpha = 30\,^{\circ}$ to calculate the stiffness with the help of the formula given below,

$$k = \frac{\pi E d \tan \alpha}{\ln \dfrac{(1.155t + D - d)(D + d)}{(1.155t + D + d)(D - d)}}$$

Wileman, Choudary and Green conducted a finite element study. They offer a formula for easy calculation of the stiffness of the member in this form

$$\frac{k}{Ed} = A \exp(Bd/l)$$

These formulae contain geometrical parameters like length l, diameter of washer D and diameter of the bolt d, thickness of the frusta t and angle α. In addition it contains the modulus of elasticity E.

Figure 2.65 (a,b and c) show the stress σ_z distribution on the loading plate around the bolt hole at 2500 N, 5000 N and 30,000 N in the XZ plane. Cone angle of 30° is used and by inspecting the frusta at angle $\alpha=30^o$ it can be concluded that,

1. Stress concentration region outside the frusta is significant in all cases. The concentration increases as the pretension force increases.

2. The spread of stress concentration (marked by arrows in figure 2.65 a) is increasing with the increase in the pretension force. The stress lines exceed the frusta when pretension of 30,000 N is used.

3. The pretension force must be incorporated in the formulae 2.1 and 2.2, in order to predict the accurate value of stiffness of the member.
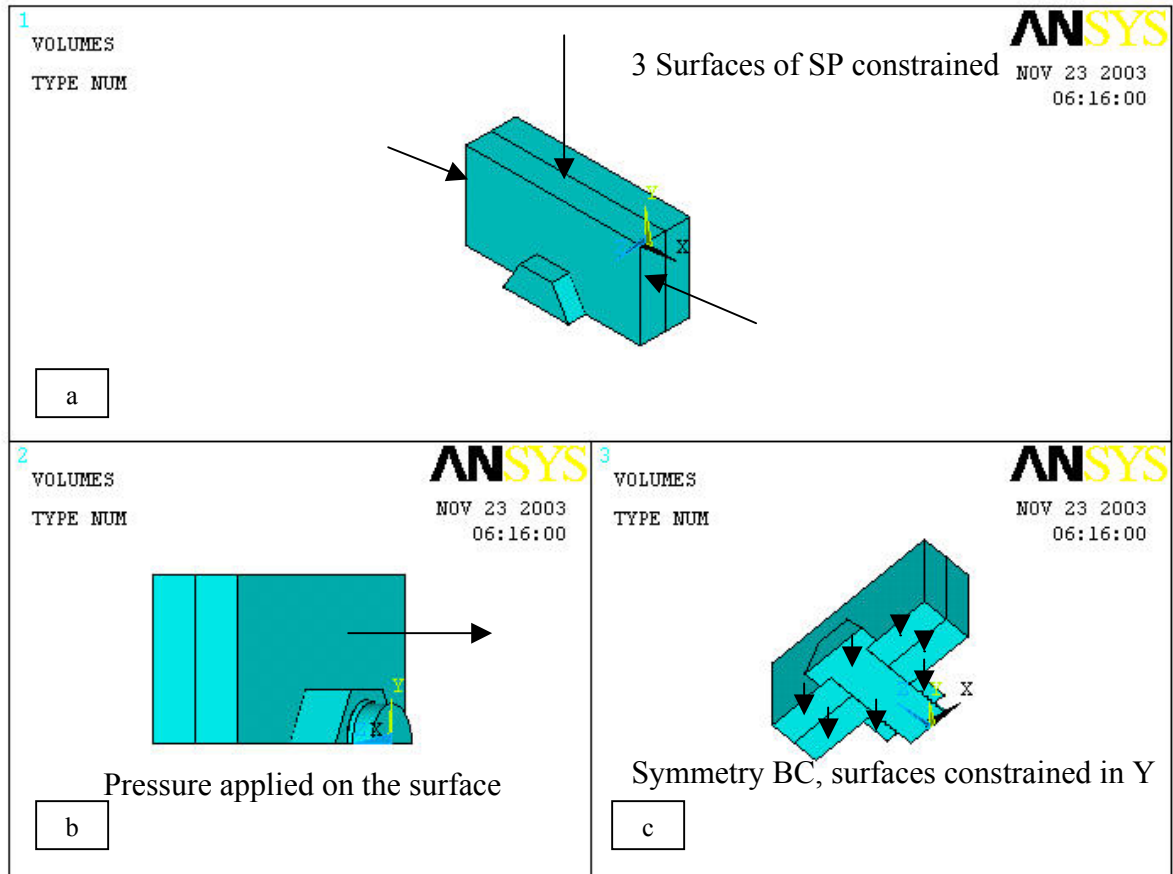
Figure 2.49: Applied boundary condition
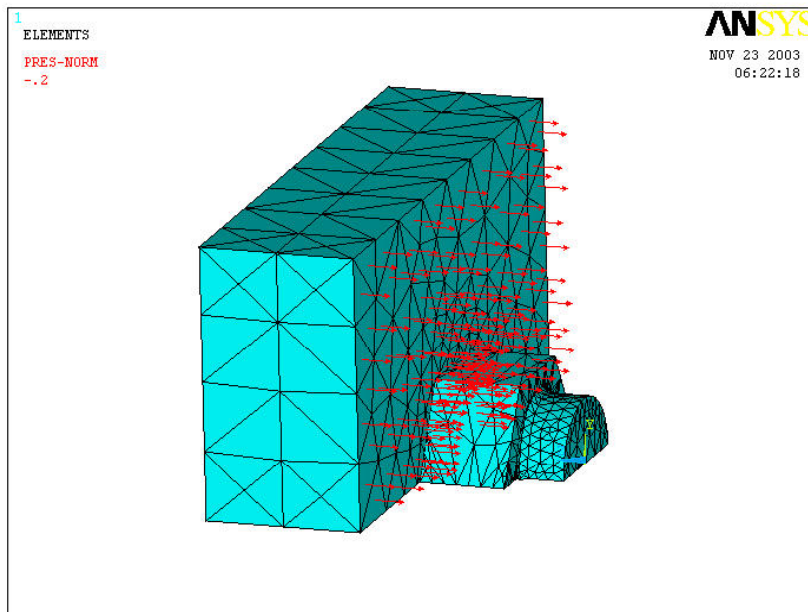
Figure 2.50: Direction of applied pressure
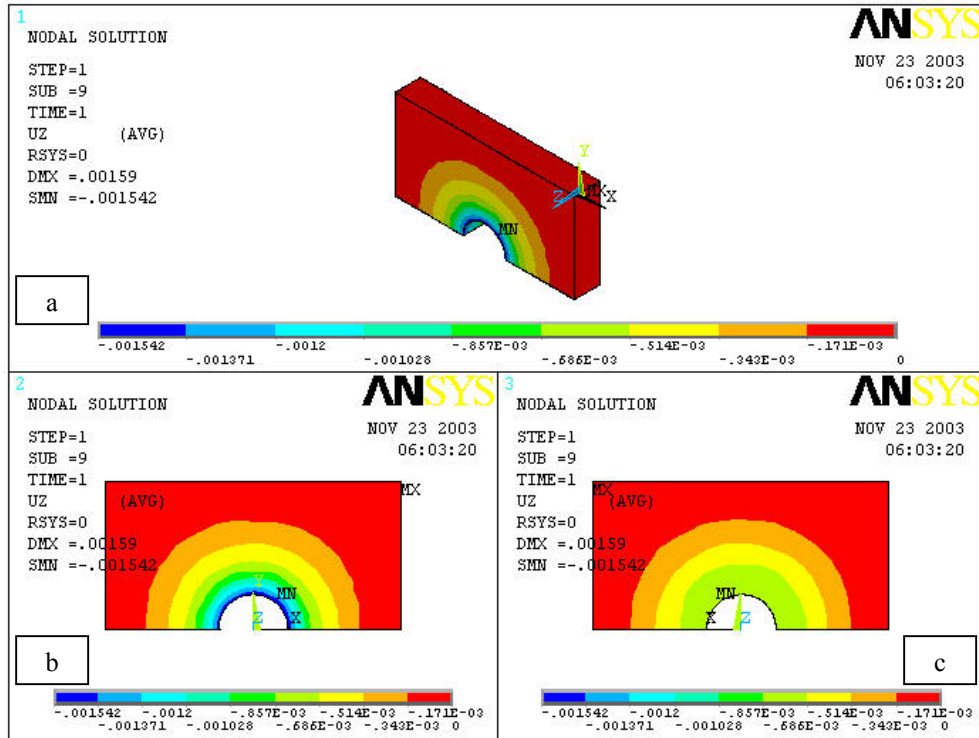
Figure 2.51: *z*-displacement at 2,500 N of SP (a) isometric (b) boltside (c) interface side
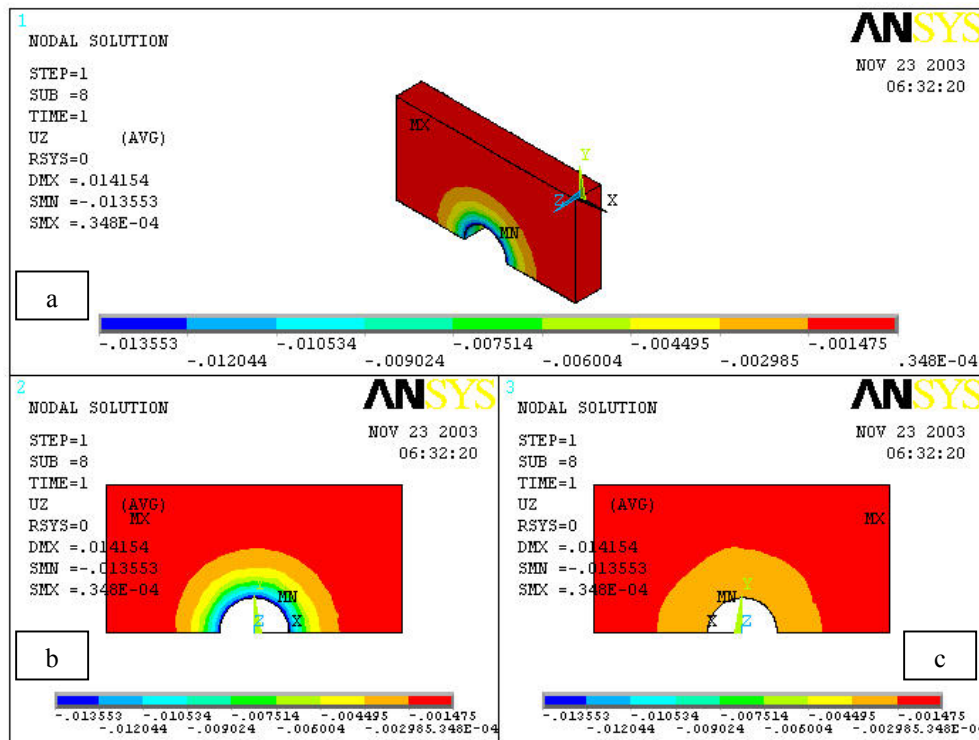
Figure 2.52: *z*-displacement at 30,000 N of SP (a) isometric (b) boltside (c) interface side
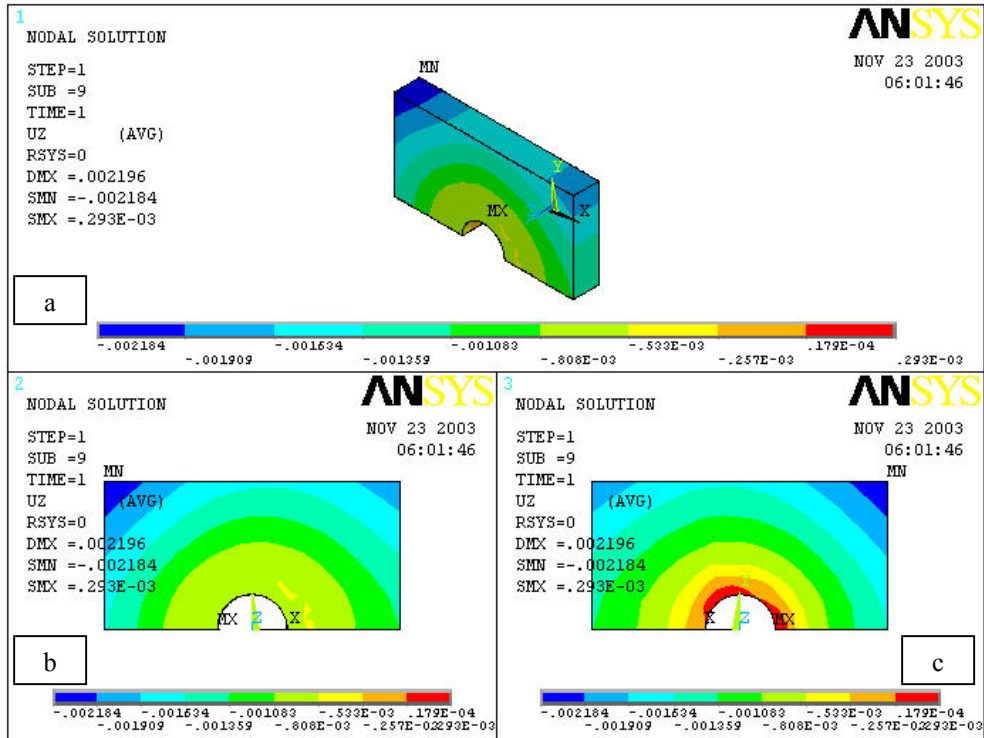
Figure 2.53: *z*-displacement at 2,500 N of LP (a) isometric (b) interface side (c) nutside
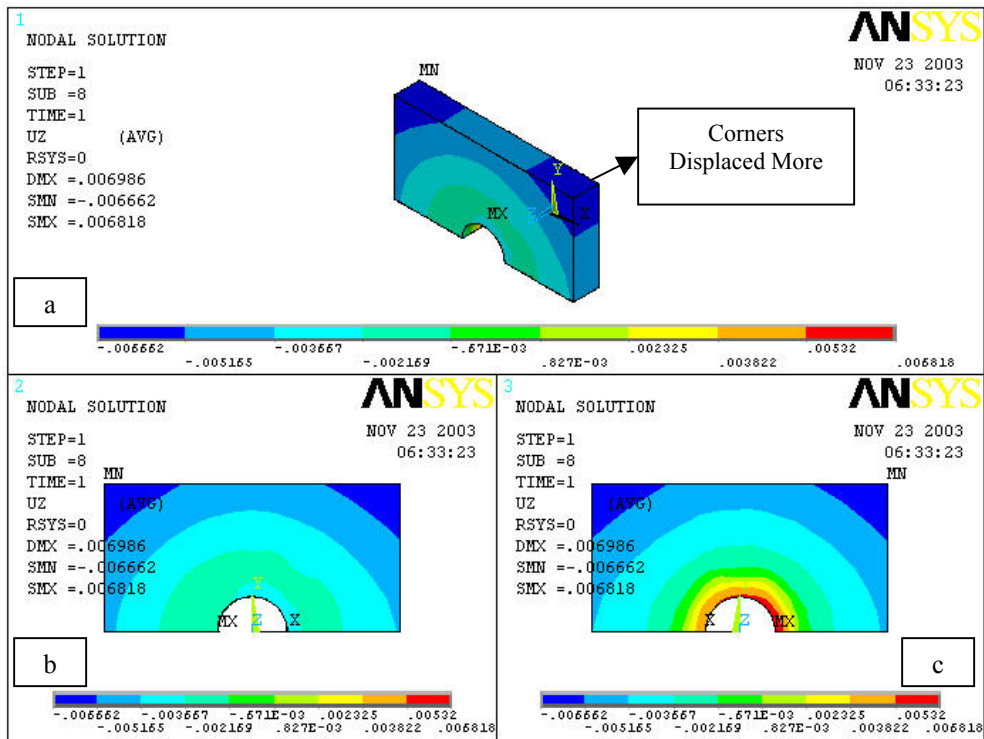
Figure 2.54: *z*-displacement at 30,000 N of LP (a) isometric (b) interface side (c) nutside
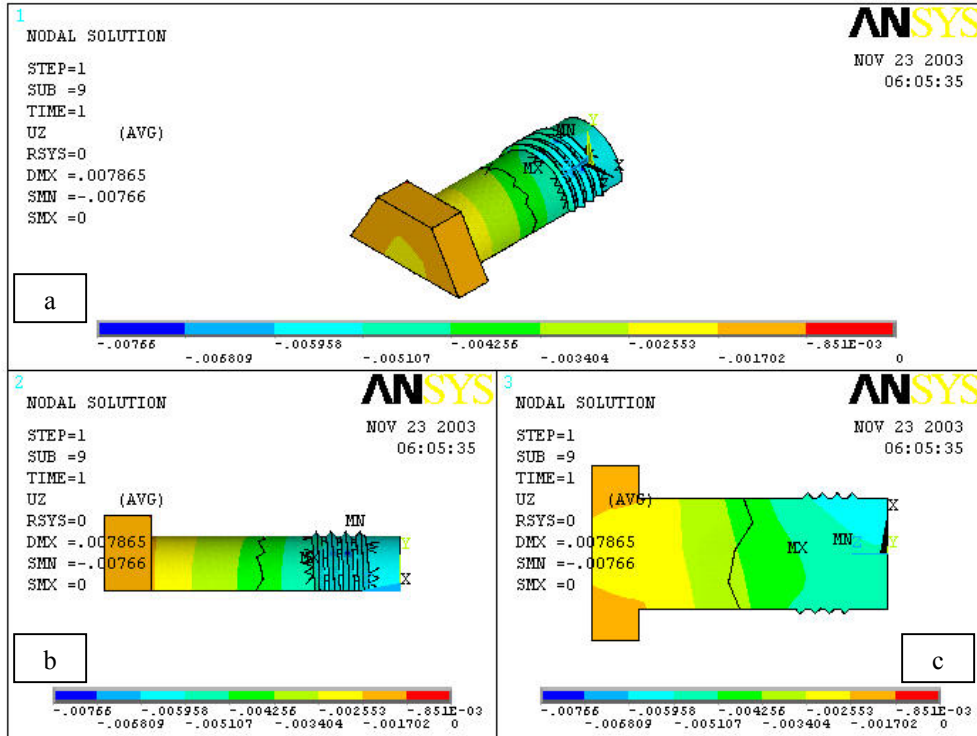
Figure 2.55: *z*-displacement at 2,500 N of bolt
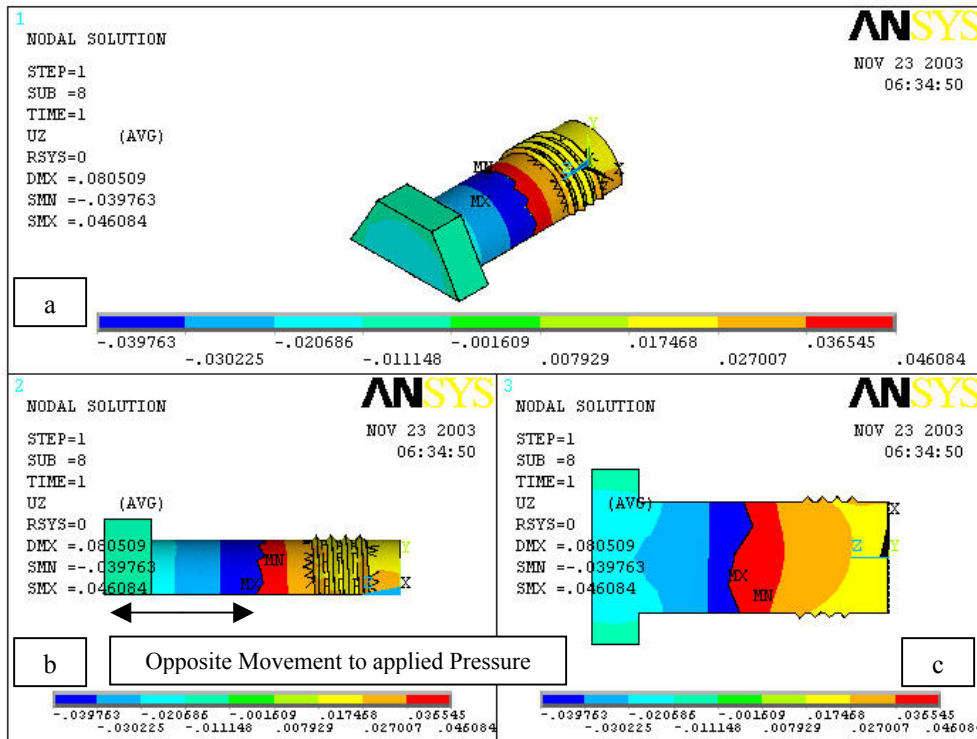
Figure 2.56: *z*-displacement at 30,000 N of bolt

Table 2.13: Maximum *z*-displacement under increasing pretension (tensile)

Pre Tension	*Bolt (mm)*	*SP (mm)*	*LP (mm)*
2,500 N	-0.00766	-0.001542	-0.002104
5,000 N	-0.00786	-0.002618	-0.002424
30,000 N	-0.03976	-0.013553	-0.006662
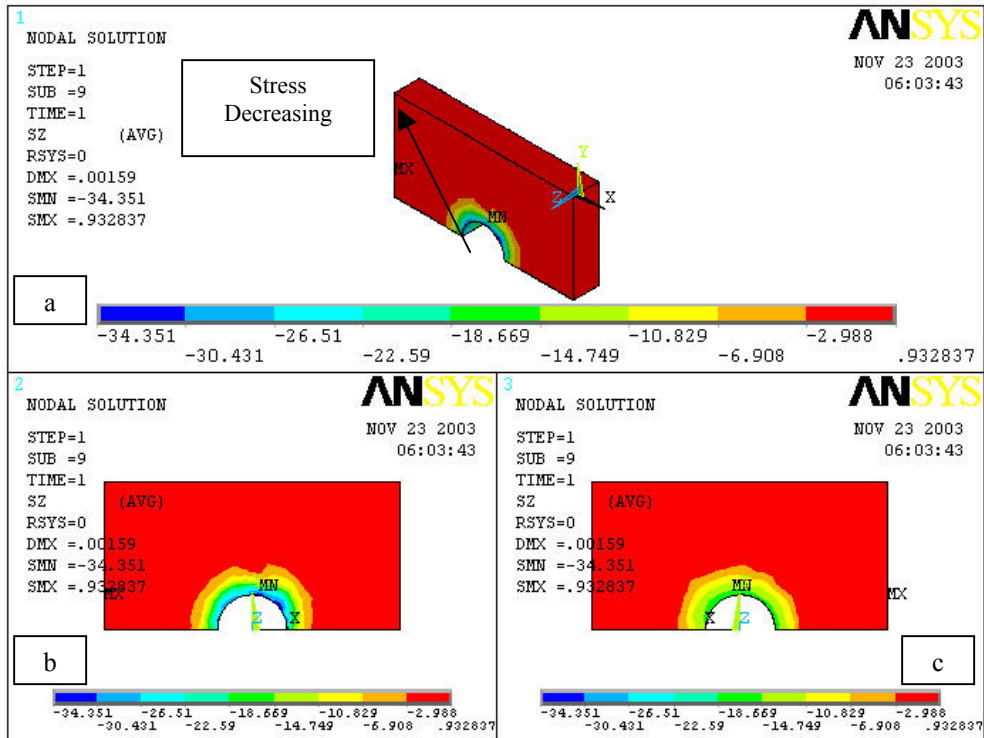
Figure 2.57: Stress σ_z at 2,500 N of SP (a) isometric (b) boltside (c) interface side
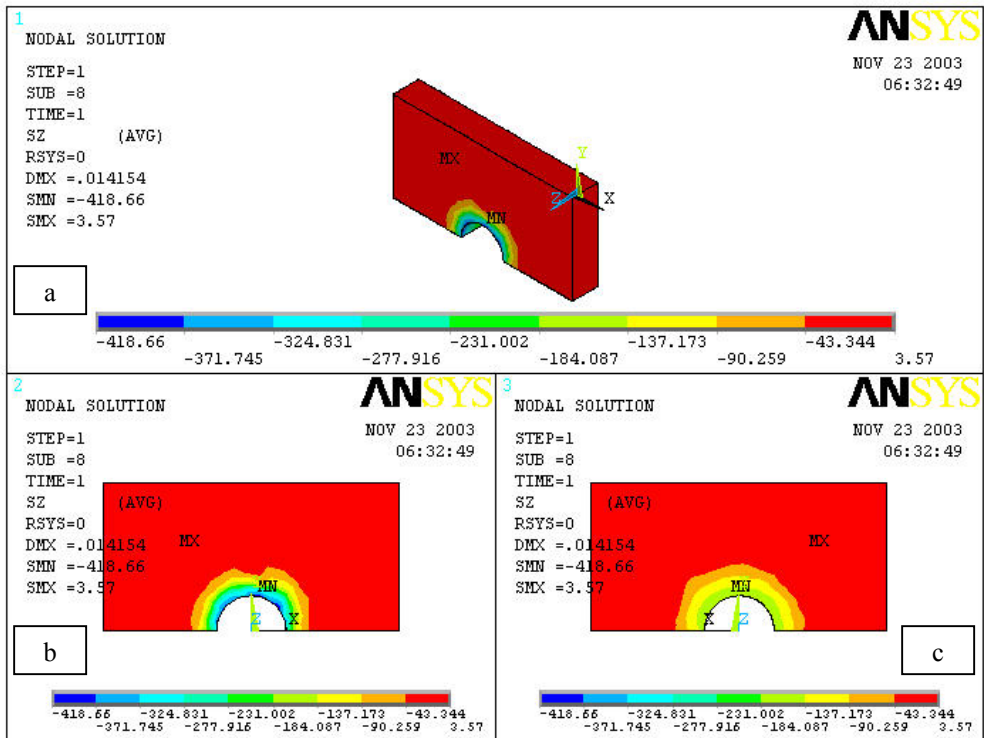
Figure 2.58: Stress σ_z at 30,000 N of SP (a) isometric (b) boltside (c) interface side
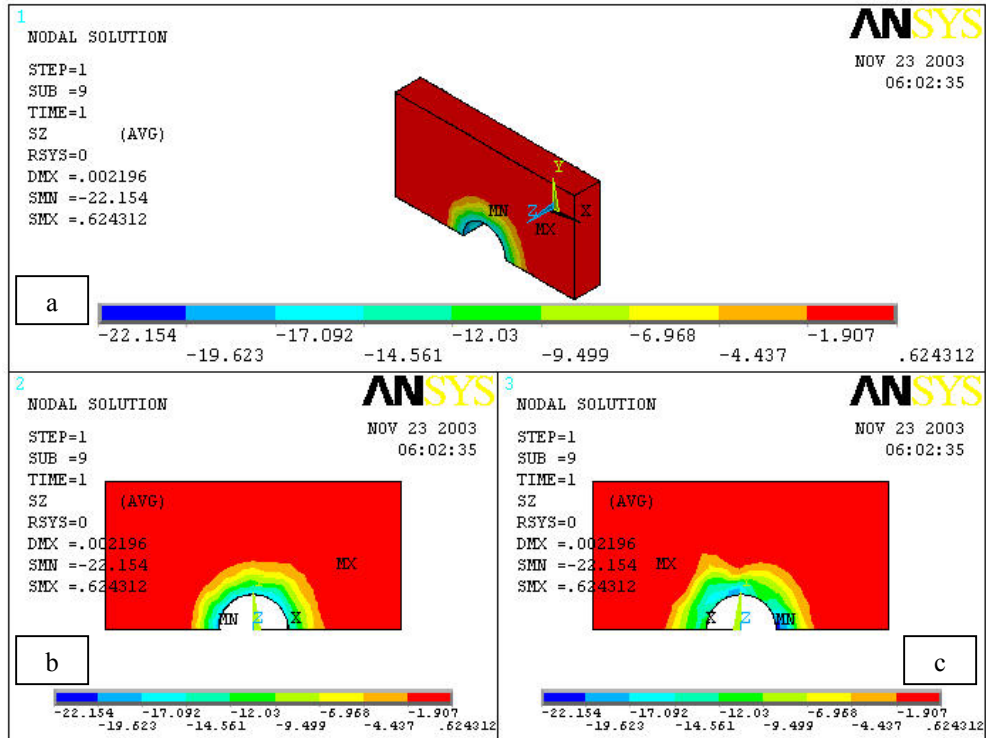
Figure 2.59: Stress σ_z at 2,500 N of LP (a) isometric (b) interface side (c) nutside
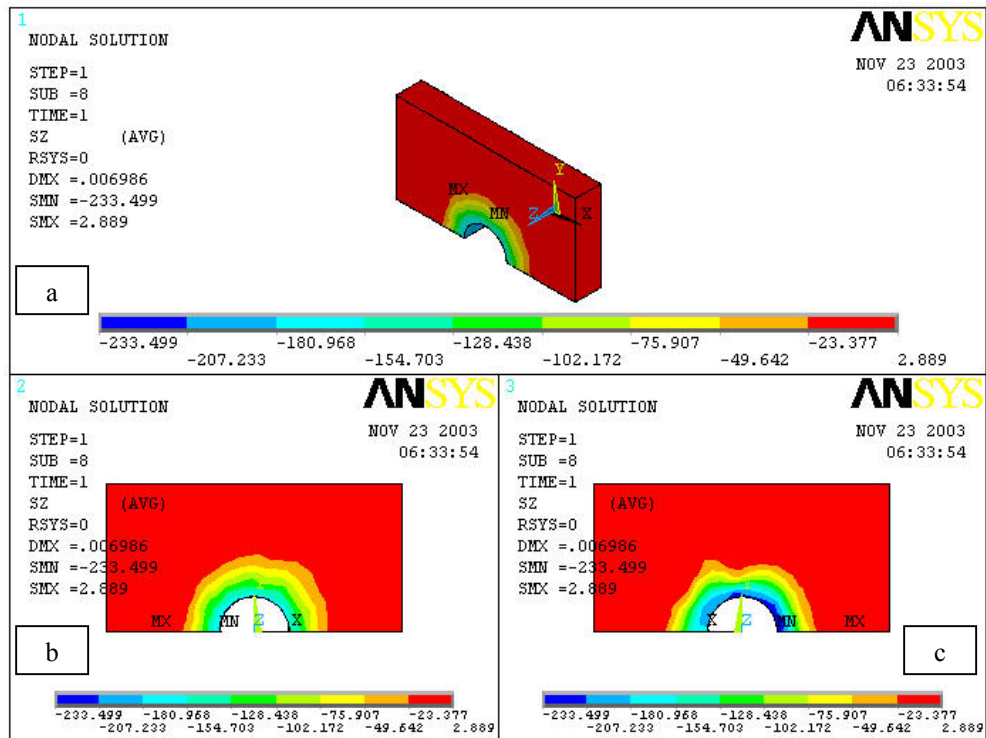
Figure 2.60: Stress σ_z at 30,000 N of LP (a) isometric (b) interface side (c) nutside
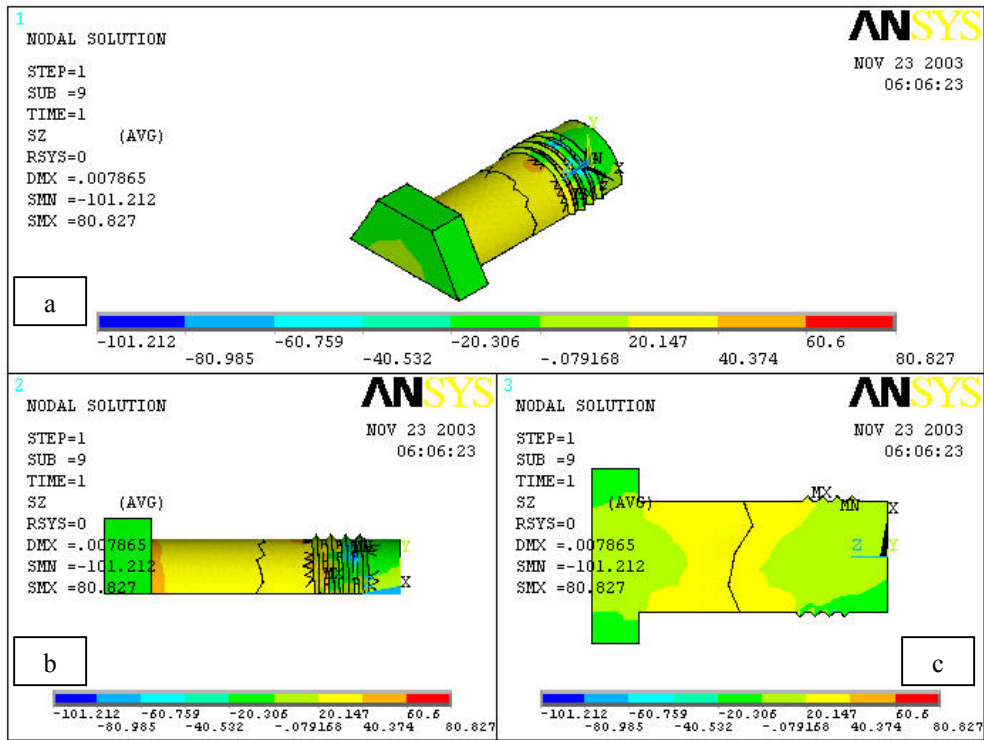
Figure 2.61: Stress σ_z at 2,500 N of bolt
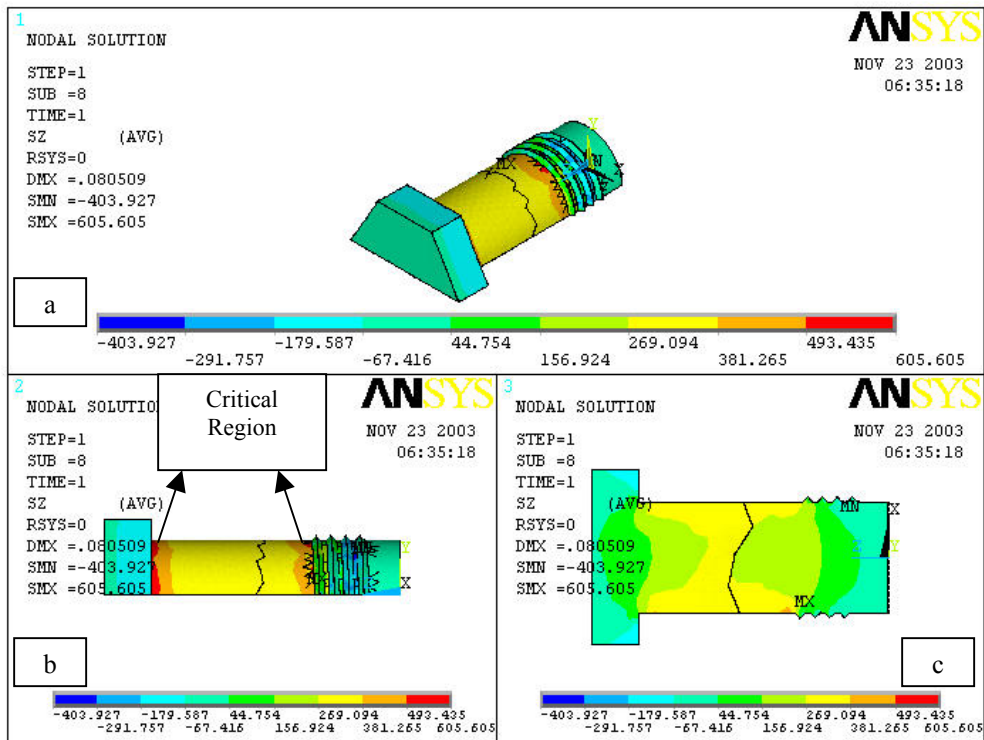
Figure 2.62: Stress σ_z at 30,000 N of bolt
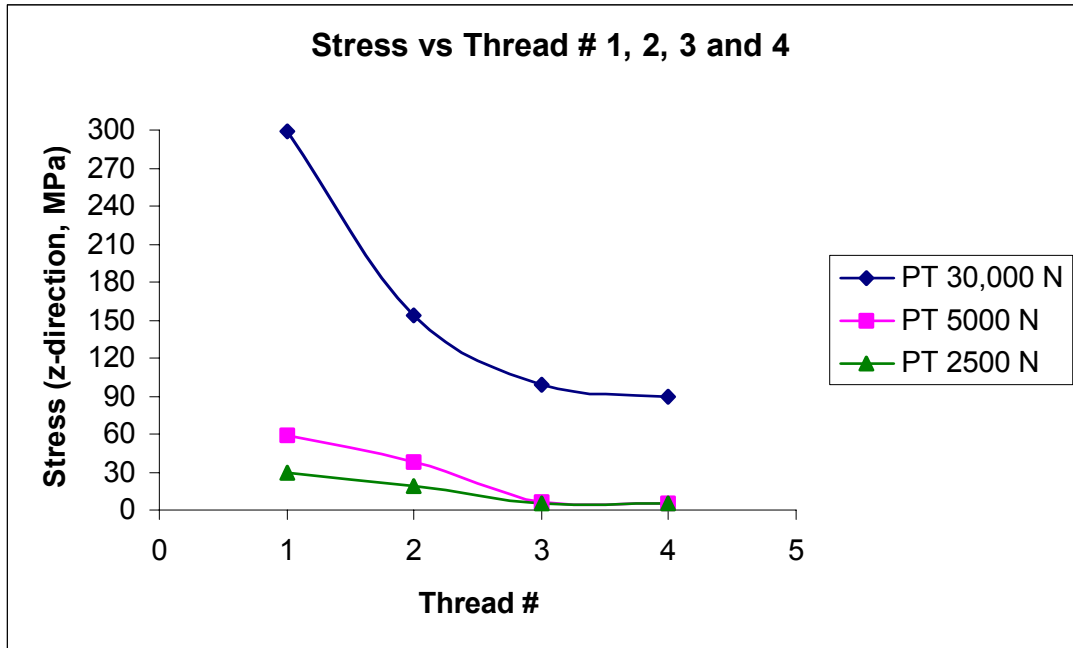
Figure 2.63: Stress variation at the root along the threads 1, 2, 3 and 4
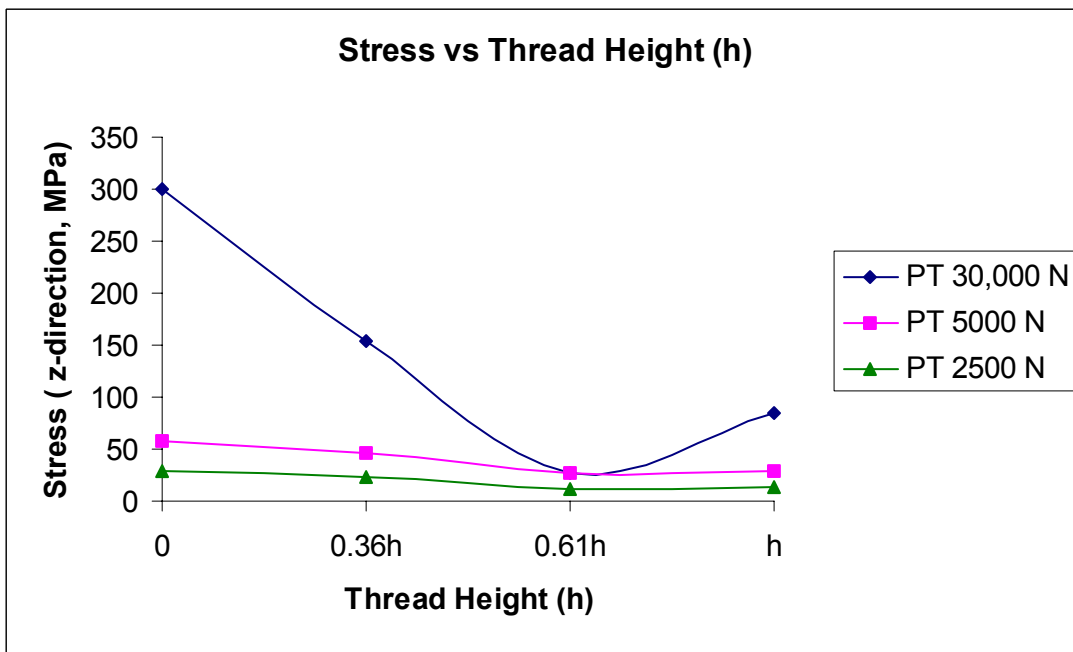
Figure 2.64: Stress variation along thread 1, from root to tip of the thread

a) Pretension = 2500 N

b) Pretension = 5000 N

c) Pretension = 30000 N
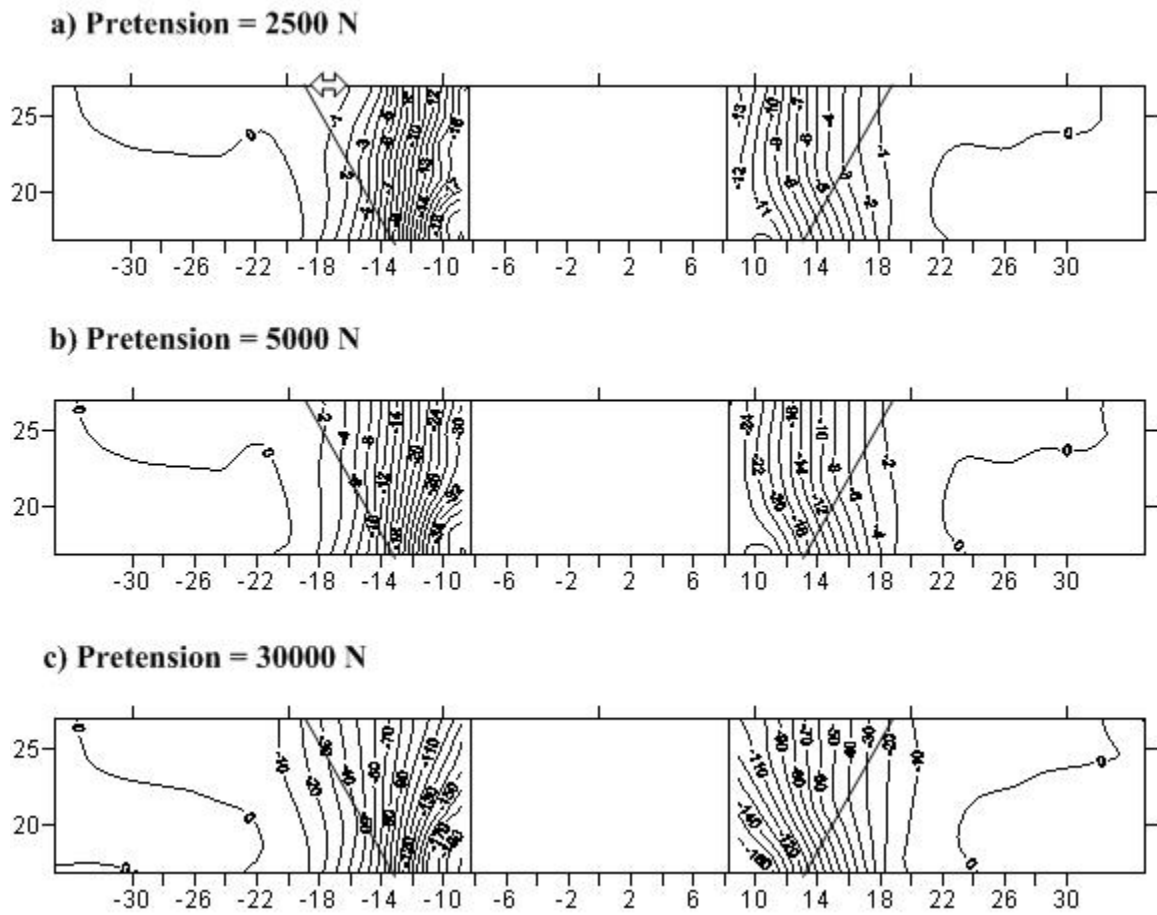
Figure 2.65: Stress distribution on LP in xz plane at pretension (a) 2,500 N (b) 5,000 N

and (c) 30,000 N

Table 2.14 Maximum Stress σ_z under increasing pretension (tensile)

Pre Tension	Bolt (MPa)	SP (MPa)	LP (MPa)
2,500 N	80.827	-34.351	-22.154
5,000 N	178.85	-69.451	-42.008
30,000 N	605.05	-418.66	-233.499

2.5   CONCLUSION

From the numerical results of shear type and tensile type loading following conclusions are drawn.

1. Effect of loading, coefficient of friction pretension and clearance is there when joint is loaded in shear.

2. In all the cases for SP maximum value of displacement and stress is at the interface side and critical point is the upper region of the bolthole where the bolt is hitting the surface.

3. In all the cases for LP maximum value of displacement and stress is at the interface side and critical point is the lower region of the bolthole where the bolt is hitting the surface.

4. The upper portion of SP is in compression and lower half is in tension. The effect is opposite in case of LP. Upper half portion of LP is in tension as it is being loaded in that direction.

5. There is slight bending in the bolt due to the applied boundary condition in shear type of loading.

6. The value of maximum compressive stress increase as pretension increases.

7. Critical regions in the bolt are the regions just below the head of bolt and around first engaged thread.

8. The threads share different loads when loaded in tension. First thread taking the highest of the load.

CHAPTER 3

FOUR BOLT MODEL

3.1   INTRODUCTION

Literature survey clearly indicates that there is not much work reported on studying the effect of layout on bolted joints. Some limited experimental work is reported. Two dimensional and axisymmetric models are reported in some papers but the work is not extended to study the layout effect. Tan et al [22] studied the effect of bolts in rows. Experiments confirm that there is reduced effective capacity per bolt with any increase in the number of bolts placed in a row. Hockey et al [20] investigated the behavior of truss plate reinforced by single and multiple bolted connections in parallel strand lumber under static tension loading were investigated. Their effect on the ultimate tensile strength of the connection was observed.

Work that is reported in this layout study area is mostly experimental. This chapter discusses four-bolted joint in shear type loading. Four different arrangements of four bolts are analyzed. The schematic of these layouts are shown in figure 3.1. Displacement pattern and stress distribution is studied on all the four arrangements. Experiment is conducted to validate the numerical results. This work is helpful in fortifying the basic idea that the load is not shared equally on all the bolts.
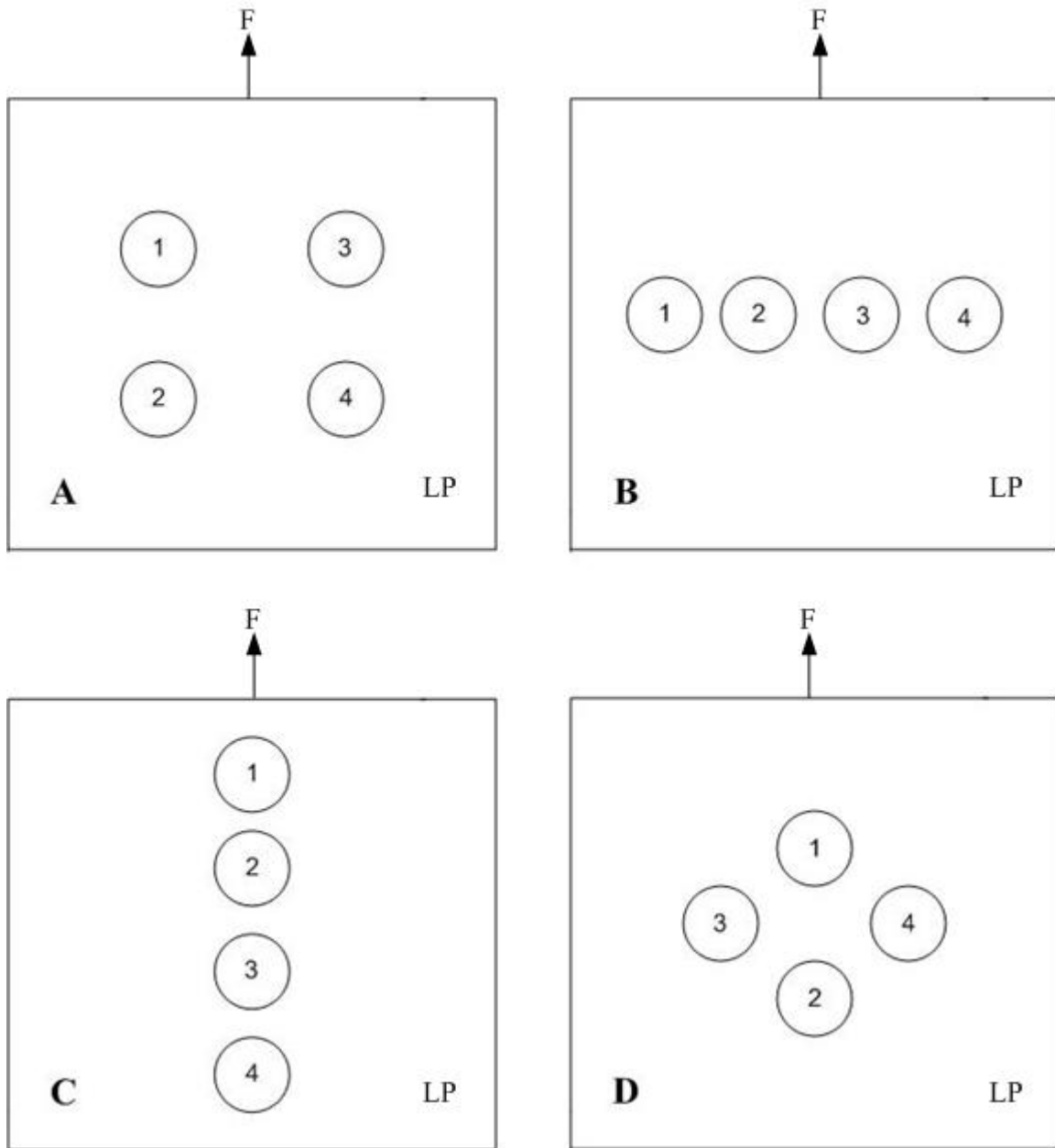
Figure 3.1: Schematics of four bolted joint layouts (A, B, C and D)

3.2   FE MODEL DESCRIPTION

The model is three-dimensional. For geometrical modeling same approach as that employed for one bolt model is used. The procedure to make the threads on the bolts is also the same. Finite element modeling uses same type of element and material properties as used before. The boundary conditions applied in all the layouts are shown in figure 3.2. Lower surfaces of the supporting plates are constrained in all the layouts and displacement is given to the loading plate as a load (shear type loading). Contacts are used at the interacting surfaces and friction coefficient is there. The details being same as that of one bolt model in shear. The load of 0.06mm is applied with a pretension of 30,000 N. Clearance of 0.05 mm and 0.75 friction coefficient (steel to steel) is used. Symmetry is employed thus half models are used in the analysis. The number of nodes and elements in this four-bolt model are 97096 and 19762 respectively. Some of the numerical results are verified through an experiment.

3.3   RESULTS AND DISCUSSIONS

3.3.1   Layout A

_y_-displacement

Figure 3.3 shows the displacement pattern of supporting plate (SP) for layout A. (a) Isometric view, (b) boltside view and (c) interface side view are shown respectively. Isometric view shows that the displacement pattern is changing through out the thickness of the plate. This is very clear by looking at the different pattern on both sides. SP boltside shows that the sides and bottom region of the plate is not moving with the applied load because of the constraint applied and the displacement is higher around the bolt holes. For SP interface side lower surface is at zero displacement but there is more movement as
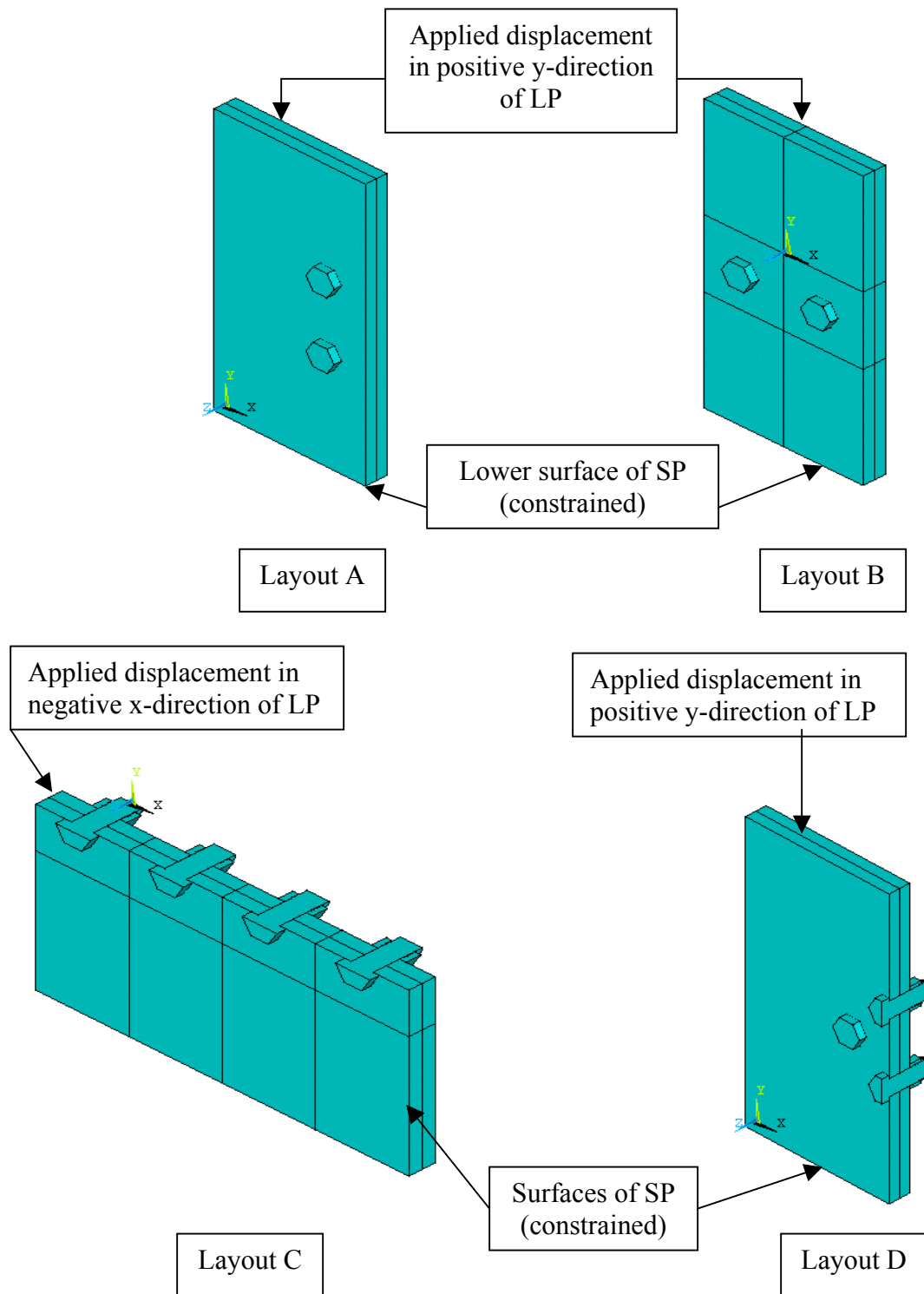
Figure 3.2: Boundary conditions for layout A, B, C and D

compared to the boltside in the upper region. In this case the maximum displacement region is around the bolt 1 which is near the applied load edge. Maximum value of displacement is 0.0311 mm. The upper edge on the interface side is not moving uniformly in the direction of the load. More movement is in the center of the surface. This is because of the arrangement of the bolts. Figure 3.4 gives the (a) isometric view, (b) interface side and (c) nutside view of loading plate (LP) for layout A. Displacement in y-direction is shown. Region close to the loading edge is approaching the applied load displacement value of 0.06mm. Displacement decreases moving away down. Minimum displacement region is around bolt 2. LP nutside shows that the region above the bolt 1 and the side of the surface is moving to the applied load value of 0.06 mm. So there is some upwards movement from the sides while the center being less displaced. Closely inspecting these figures, it is clear that the displacement pattern is vice versa the pattern obtained in SP.

Stress σ_y

Figure 3.5 shows the stress distribution σ_y of SP for layout A. Again (a) isometric view, (b) boltside and (c) interface side is shown in this figure. Stress distribution is not uniform through the thickness. SP boltside shows that the region above the bolt 1 is in compression. This is because when load is applied bolt is striking the upper contact surface of the plate depending on the clearance level thus compressing it. Region below the bolt becomes in tension. SP interface side also shows the similar pattern. The regions above the bolt 1 and bolt 2 are in compression and region below are in tension. In this case maximum value of stress is 111 MPa and it is at the interface side of the plate. Figure 3.6 shows the stress distribution σ_y of LP for layout A. isometric view, interface side and nutside is shown in the figure respectively. LP interface side shows the regions of tensile

Figure 3.3: *y*-displacement of SP for layout A (a) isometric (b) boltside(c) interface side
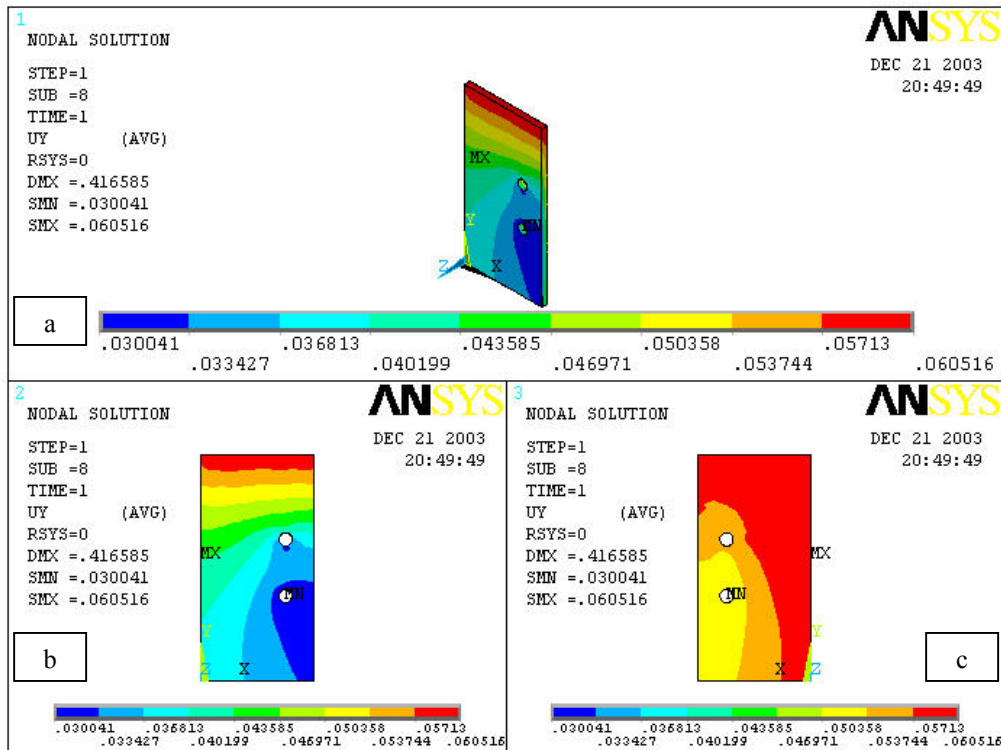
Figure 3.4: *y*-displacement of LP for layout A (a) isometric (b) interface side(c) nutside
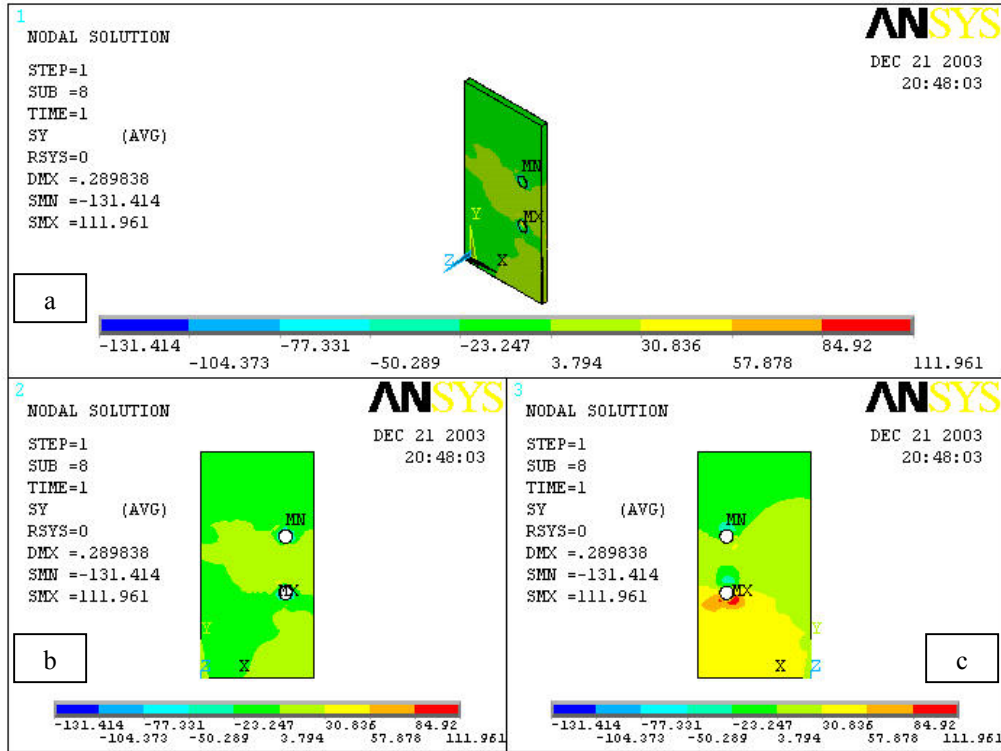
Figure 3.5: Stress σ_y of SP for layout A (a) isometric (b) boltside(c) interface side
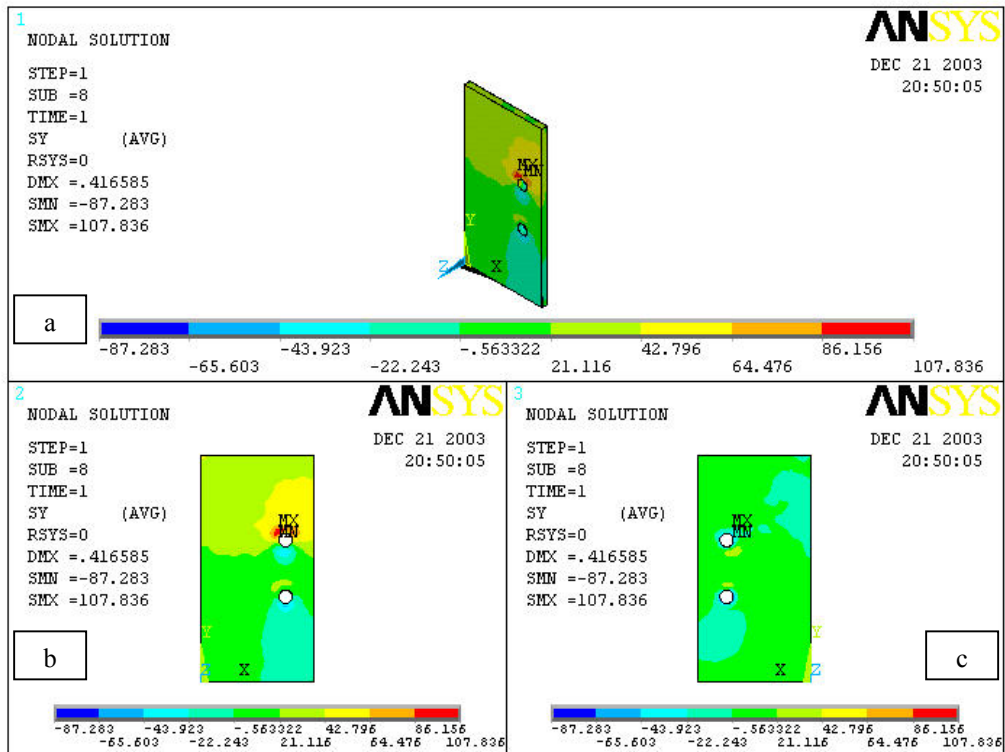
Figure 3.6: Stress σ_y of LP for layout A (a) isometric (b) interface side(c) nutside

stresses above the bolt 1 and bolt 2. Reason for this, is that the bolt is striking the lower portion and putting that in compression. The pattern is vice versa as it is seen in SP. The maximum value of stress on this interface side of the plate is given to be 107 MPa. Nutside of LP is mostly in compression. Small regions around the bolt hole are under tensile stress. Figure 3.7and 3.8 show the von Mises stress distribution on SP and LP. The maximum von Mises stress is 173 MPa in SP and 192 MPa in LP, which indicates that LP is more stressed at the critical region.

3.3.2 Experimental Validation

To verify the numerical results, an experiment is conducted in which tensile testing is used. Experimental set up is shown in the figure 3.9. Fixtures are used to clamp the bolted joint in the jaws of the machine. The locations of strain gages are shown clearly in figure 3.10 strain gages 1, 2, 3 and 4 are placed on LP and 5, 6, 7 and 8 are placed on SP. Three different displacements tests have been performed. The strain gage readings are recorded. For numerical analysis symmetry is employed and half model is used. Strains at location 1 and 3 on loading plate and at location 5 and 7 on the supporting plate are noted from the finite element model at the three displacement values used in the experiment. The graphs shown in figure 3.11 and 3.12 show the strain values at these locations that are recorded experimentally and numerically. The first observation by seeing the graph is that there are quite differences in the values of strains that are obtained experimentally and the values of strains corresponding to these locations obtained by the numerical model but still the order of magnitude is same. This big deviation may be due to several reasons. One of them is that the fixture is made up of same material as that of the specimen. This most probably leads to that the fixture experience some displacement too when the loading is

Figure 3.7: von Mises stress of SP for layout A (a) isometric (b) boltside(c) interface side
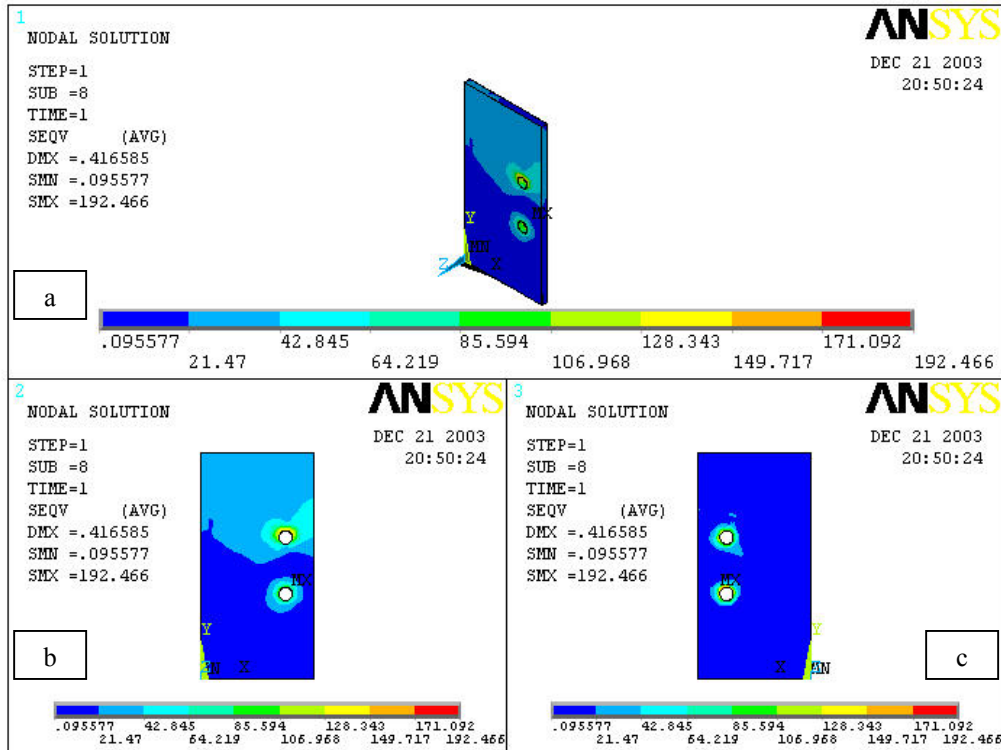
Figure 3.8: von Mises stress of LP for layout A (a) isometric (b) interface side(c) nutside

Figure 3.9: Four bolt joint experimental set up
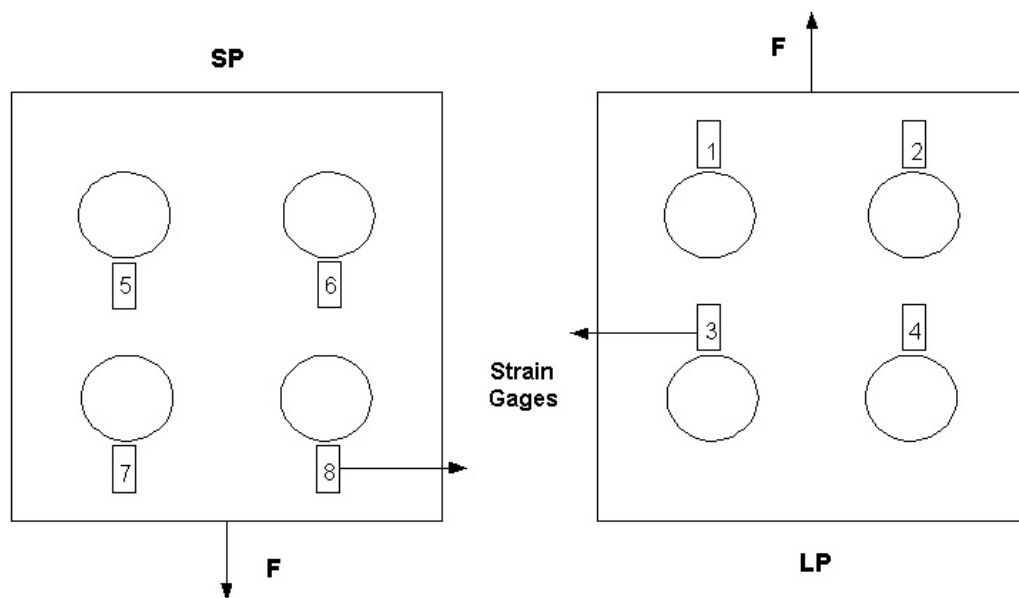
Figure 3.10: Location of strain gages
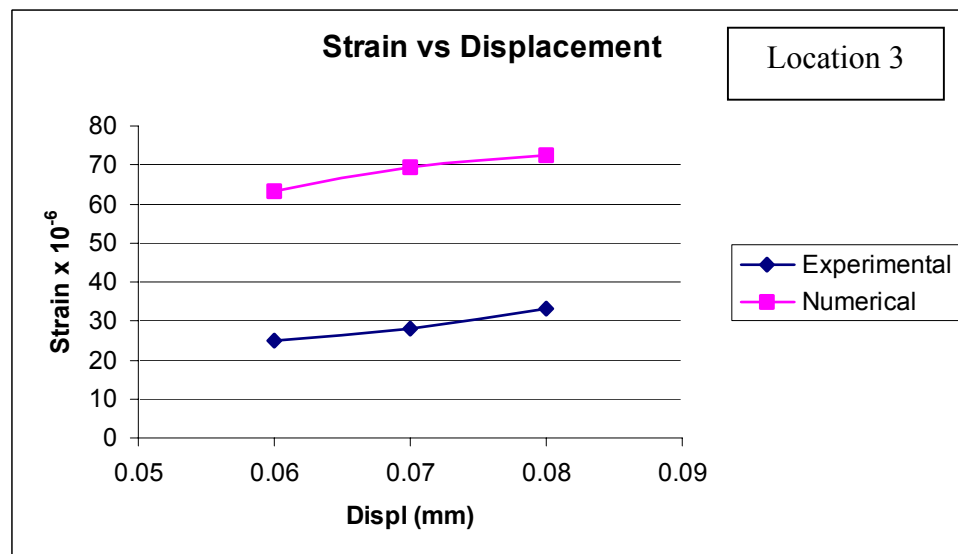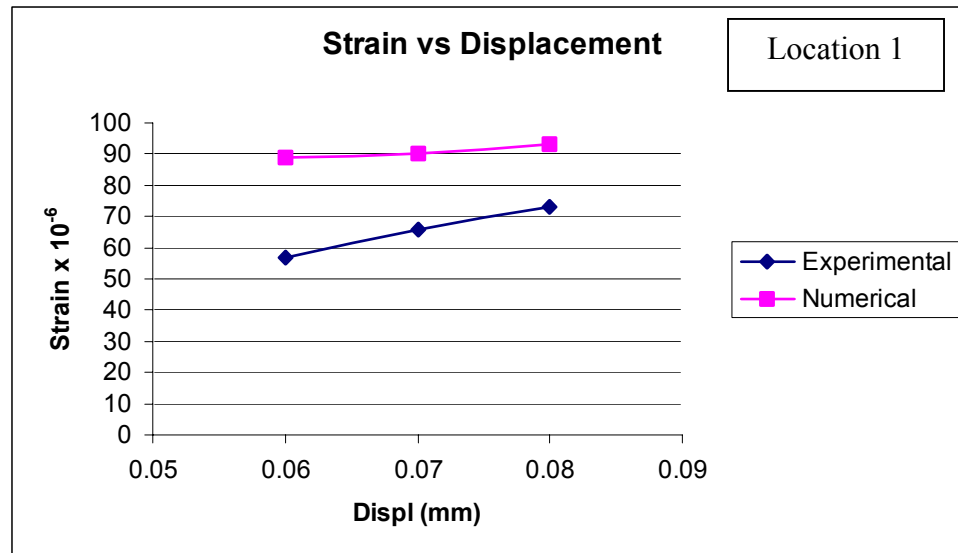
Figure 3.11: Comparison of strain values on LP at locations 1 and 3
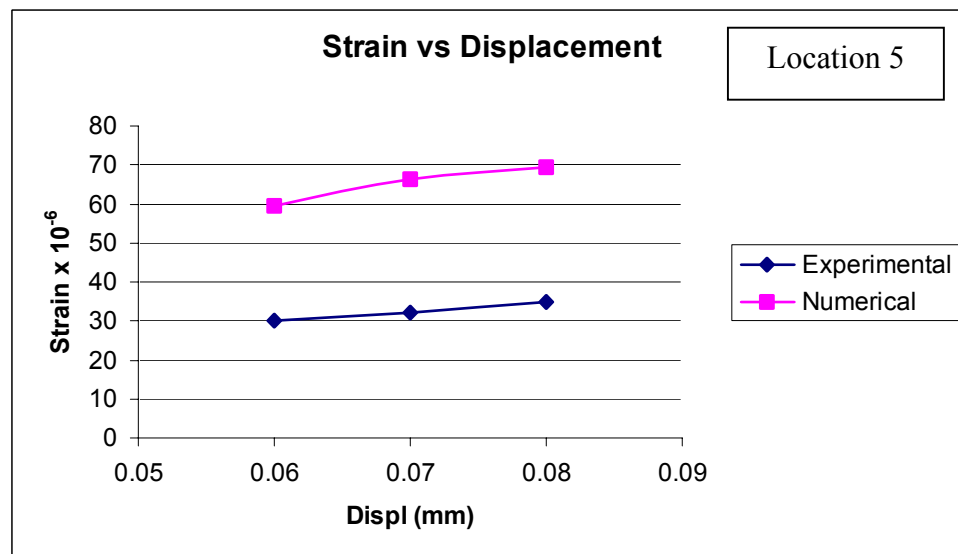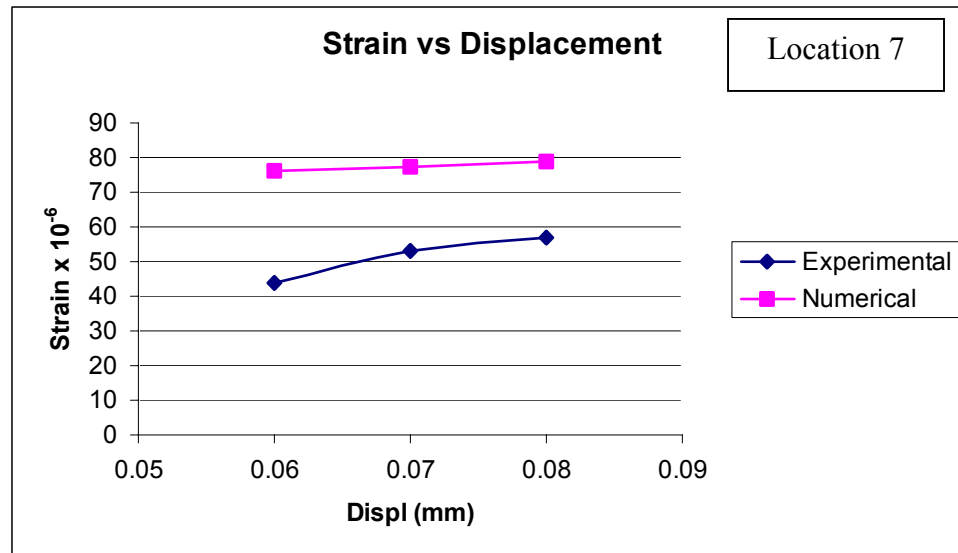
Figure 3.12: Comparison of strain values on SP at locations 7 and 5

done. Due to the fixture displacement the experimental value is always less than the numerical value because force applied by the machine is being distributed in the plate and the fixture. The trend is also same for the experimental and numerical results. The important conclusion of this experiment is that the strain produced in the vicinity of bolt, which is closer to the loading edge, is more than the other region. This observation can be seen in both the plates. Location 1 and 7 are closer to the loading edge while 5 and 7 are closer to the supporting edge. The range of numerical strain at location 1 is 55 x 10^{-6} to 75 x 10^{-6} and at location 3 the range is 25 x 10^{-6} to 35 x 10^{-6}. There is a reduction in the strain values around the bolt hole that is away from the loading edge.

3.3.3   Layout B
_y_-displacement

Figure 3.13 shows the _y_-displacement pattern of SP for layout B. (a) Isometric view, (b) boltside and (c) interface side is shown in the figure. Again the pattern of displacement is changing along the thickness. In this layout most of the surface on SP boltside is not moving with the load. Lower surface of interface side of SP is constrained. Due to the horizontal positioning of the bolts upper half portion as a whole is going to the maximum displacement value of 0.0308 mm. Figure 3.14 shows the displacement pattern in y-direction of LP for layout B. LP interface side shows that upper half region is moving more while lower half region is showing less movement. Region very close to the loading edge is going up to 0.06mm. The value decreases as we move away towards the bolts in the center. This pattern is because of the positioning of bolts in the horizontal arrangement.
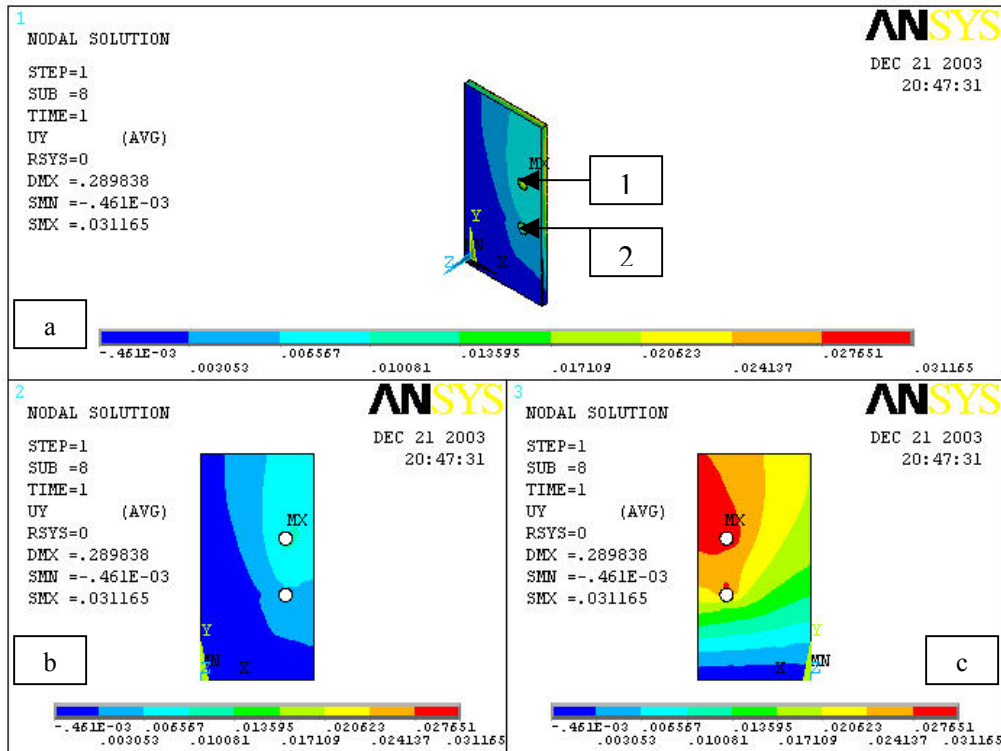
Figure 3.13: *y*-displacement of SP for layout B (a) isometric (b) boltside(c) interface side
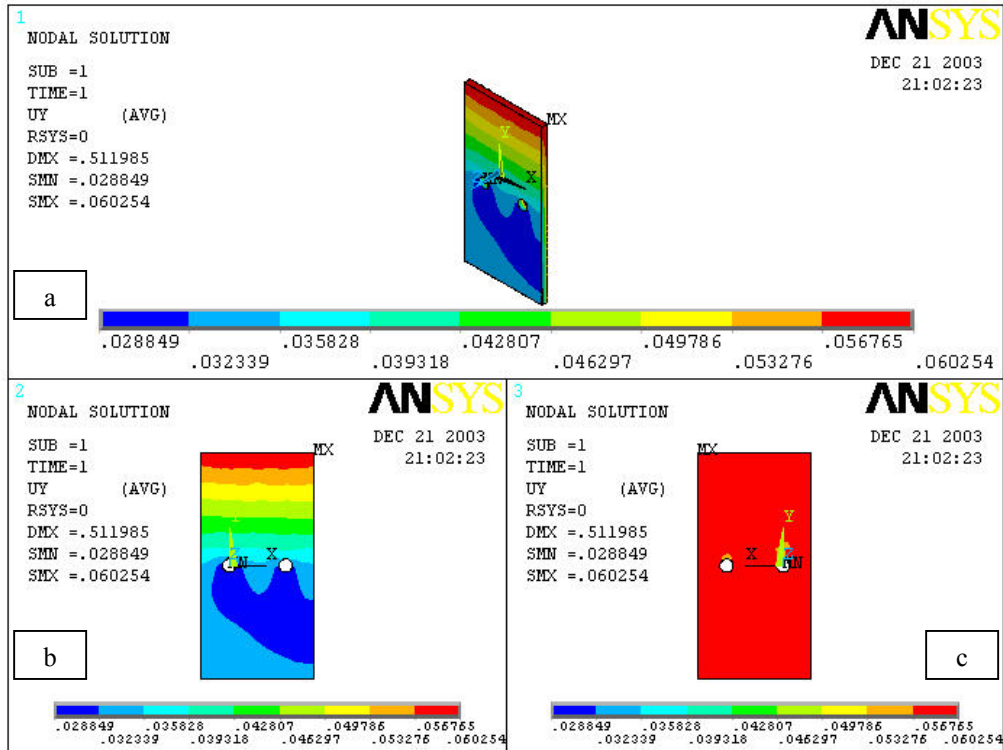
Figure 3.14: *y*-displacement of LP for layout B (a) isometric (b) interface side(c) nutside

Stress σ_y

Figure 3.15 shows the stress distribution σ_y with three views of SP for layout B. Due to the horizontal positioning of the bolts SP boltside is now in compression as whole. The half region above the bolts is all in compression on the interface side. Uniform distribution of stress is there. Right below the bolts high stress region is present. in this case maximum value of stress is 108 MPa. Figure 3.16 shows the stress distribution σ_y of LP for layout B. Hence upper half region of LP interface side is under tensile stress with a maximum stress value of 97 MPa located near bolt 1 on the interface side. Nutside of LP is again not much stressed. Figure 3.17 and 3.18 show the von Mises stress distribution on SP and LP. The maximum von Mises stress is 157 MPa in SP and 153 MPa in LP, which indicates that due to the horizontal position of the bolts the stress is almost the same in both plates.

3.3.4   Layout C

x-**displacement**

Figure 3.19 shows the isometric view, boltside, and interface side of SP for layout C. Boltside of SP shows that the surface is constrained till above bolt 4. Rest of the region is moving with the load. Side of the surface is also at zero displacement. SP interface side shows that only a little region above bolt 1 is moving to the displacement of 0.04522 mm. The value of displacement decreases as we move down to the bottom of the plate. Figure 3.20 shows x-displacement pattern of LP for layout C. Boltside of LP shows that the surface is moving from the sides more. The effect is that there is movement in direction of applied force from the sides while the movement decreases as we move to the center. This is because of the vertical positioning of the bolts. SP interface side shows that region around bolt 4 is moving with the least displacement which is along the loading direction

Figure 3.15: Stress σ_y of SP for layout B (a) isometric (b) boltside(c) interface side

Figure 3.16: Stress σ_y of LP for layout B (a) isometric (b) interface side(c) nutside
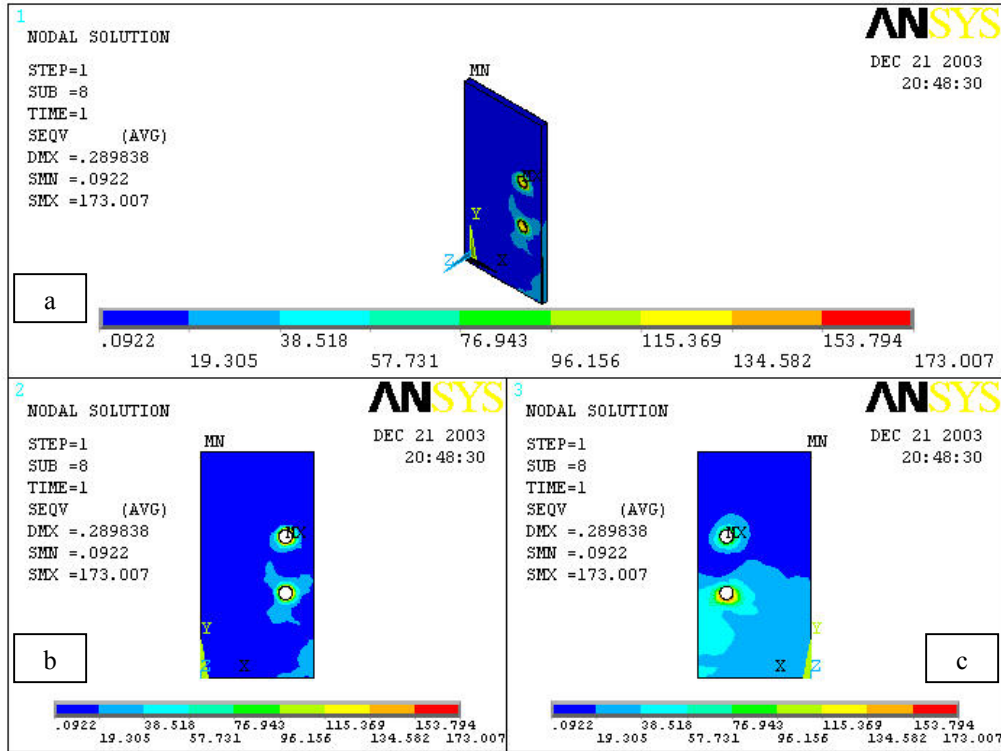
Figure 3.17: von Mises stress of SP for layout B (a) isometric (b) boltside(c) interface side

Figure 3.18: von Mises stress of LP for layout B (a) isometric (b) interface side(c) nutside
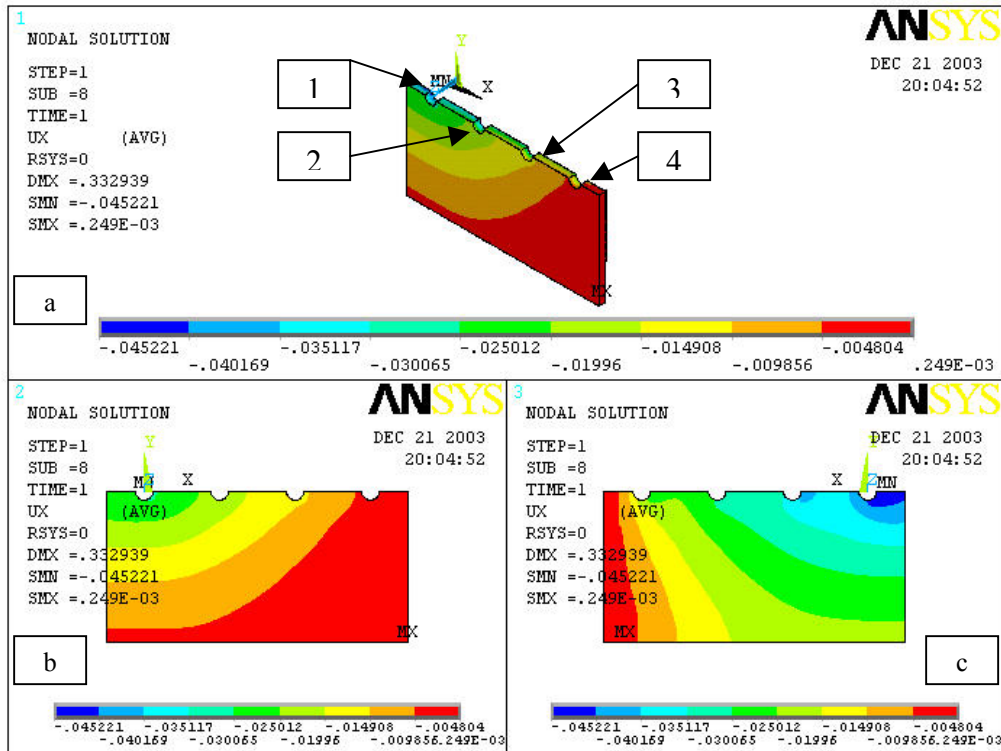
Figure 3.19: *x*-displacement of SP for layout C (a) isometric (b) boltside(c) interface side
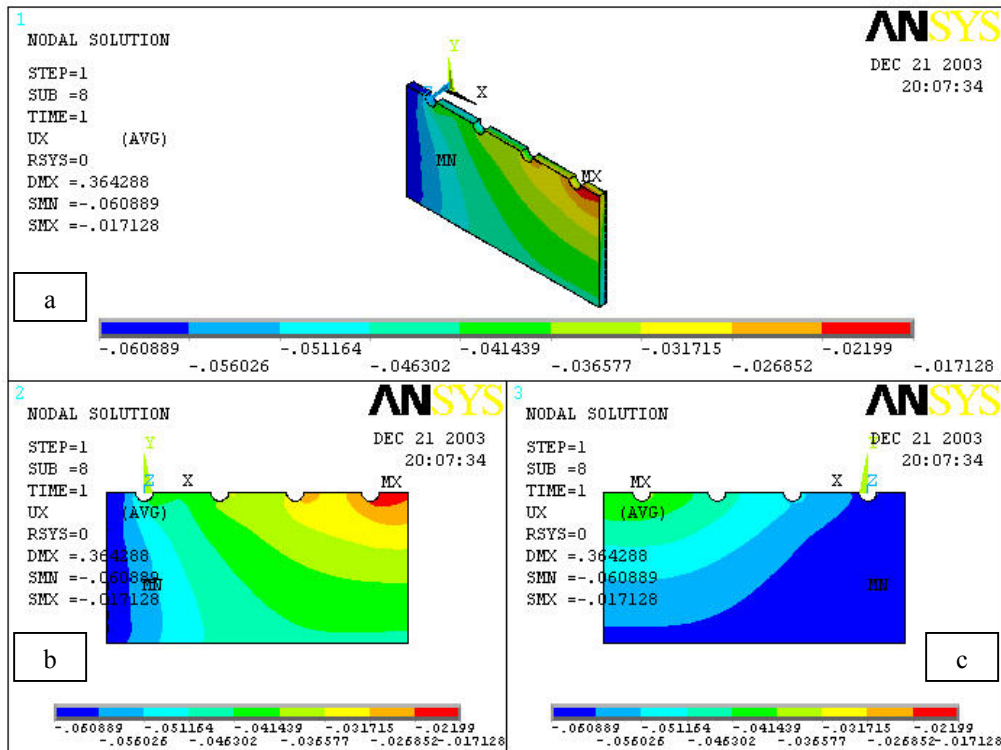
Figure 3.20: *x*-displacement of LP for layout C (a) isometric (b) interface side(c) nutside

Stress σ_x

Figure 3.21 shows the stress σ_x distribution with (a) isometric view, (b) boltside and (c) interface side of SP for layout C. SP boltside is mostly under compressive stress but there are small regions of tensile stress around bolt holes. On interface side of SP tensile stress region is increased. The maximum value of stress is very high that is 203 MPa. The sudden change in stress value is because of the vertical bolts position. Figure 3.22 shows the stress distribution σ_x on LP for layout C. LP interface side shows more stressed surface. In this case maximum value of stress is around bolt 1. Upper half region up till bolt 2 is in tension and the other half is in compression. On LP nutside tensile stresses are around bolt holes. Hence the maximum value of stress reaches a value of 222 MPa. Figure 3.23 and 3.24 show the von Mises stress distribution on SP and LP. The maximum von Mises stress is 329 MPa in SP and 331 MPa in LP, which indicates that both plates are going in plastic deformation at the critical regions.

3.3.5 Layout D

***y*-displacement**

Figure 3.25 shows the three views of SP for layout D. The *y*-displacement pattern is almost same as in layout A but there is more displacement in the region between the bolts. SP interface side shows that the region of maximum displacement around bolt 1 is decreased if we compare it with layout A. Maximum value is again on the interface side and is 0.0325. Figure 3.26 gives the displacement pattern of LP for layout D. LP interface side shows more relative movement regions as compared to the nutside due to the slipping phenomena. Minimum value of displacement is in the region around the bolt 2. LP nutside region near the loading edge is moving with displacement value equal to the applied load.
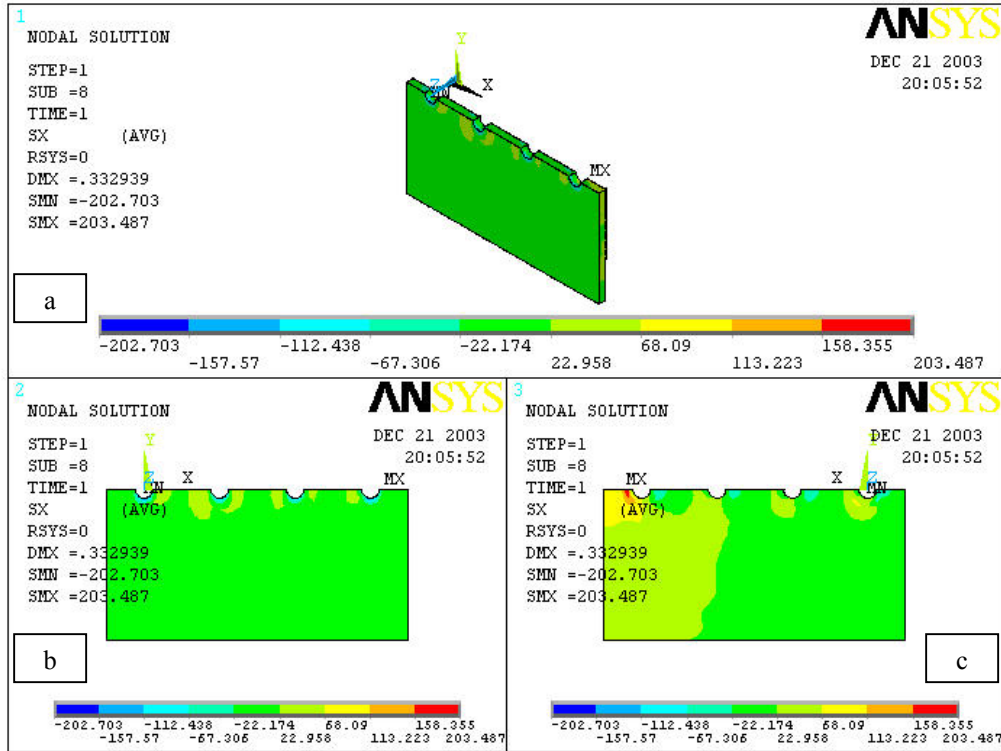
Figure 3.21: Stress σ_y of SP for layout C (a) isometric (b) boltside(c) interface side
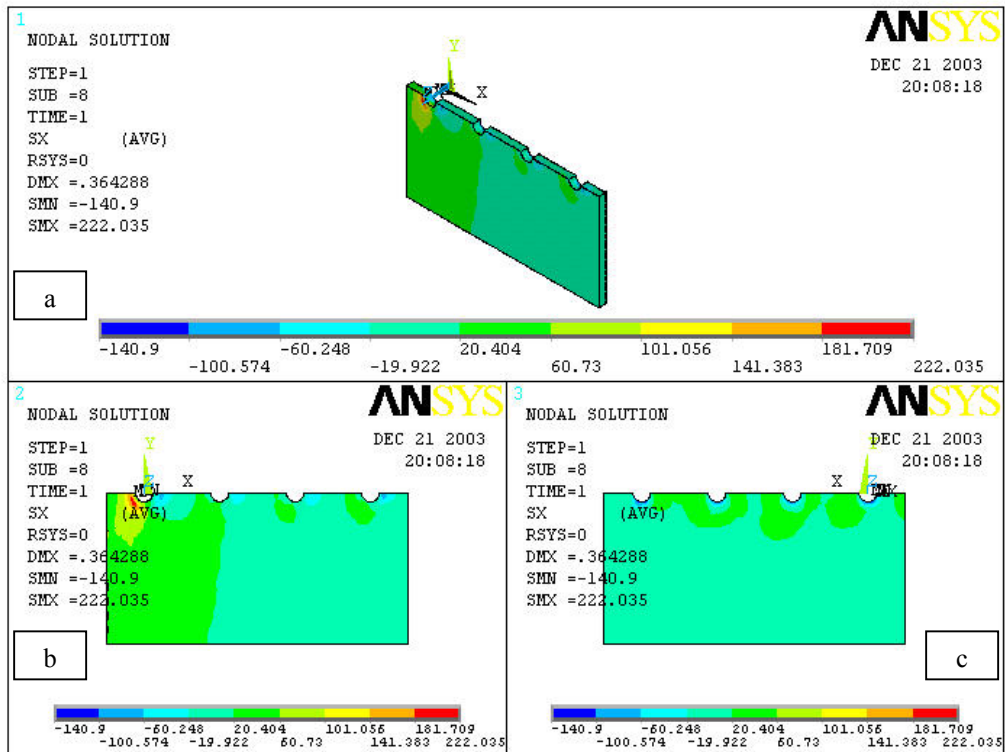
Figure 3.22: Stress σ_y of LP for layout C (a) isometric (b) interface side(c) nutside
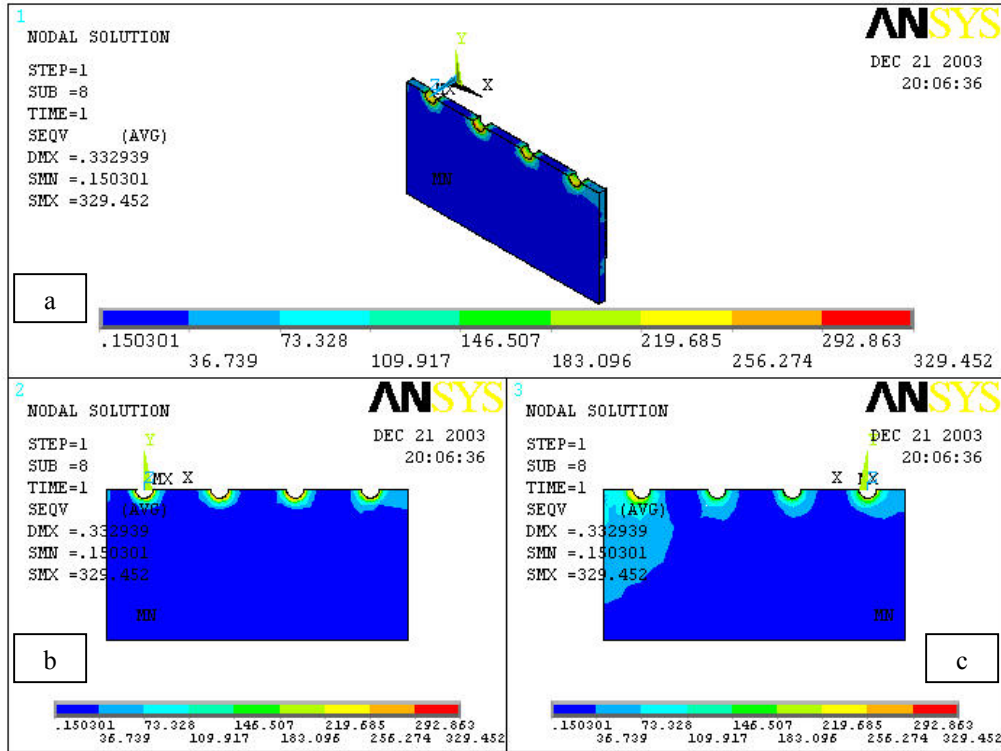
Figure 3.23: von Mises stress of SP for layout C (a) isometric (b) boltside(c) interface side
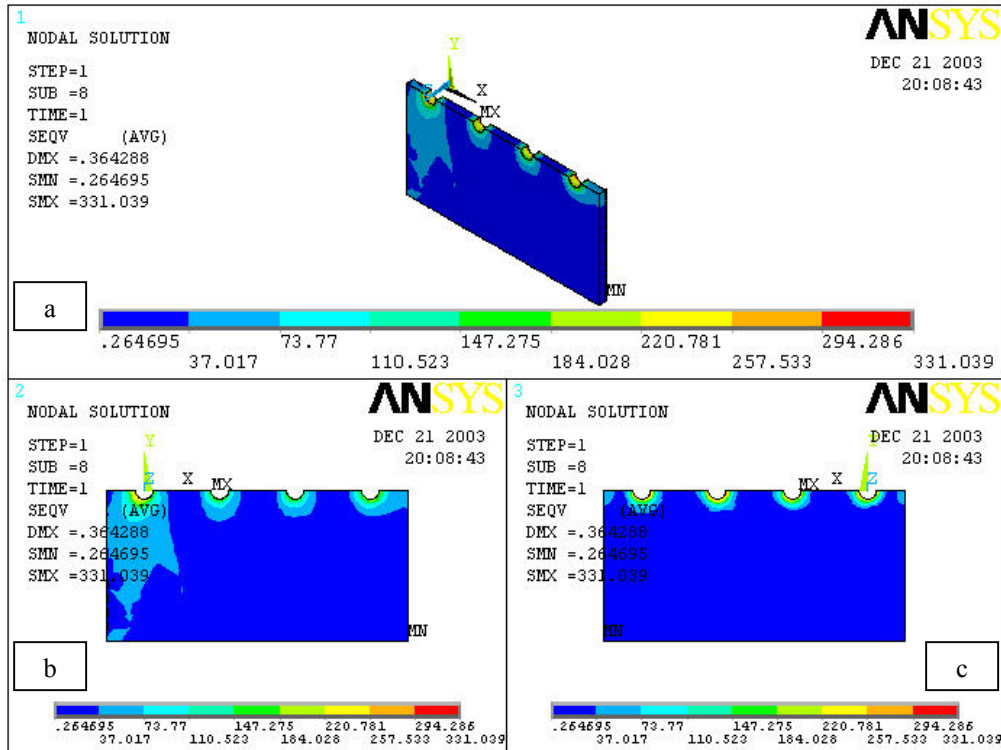
Figure 3.24: von Mises stress of LP for layout C (a) isometric (b) interface side(c) nutside
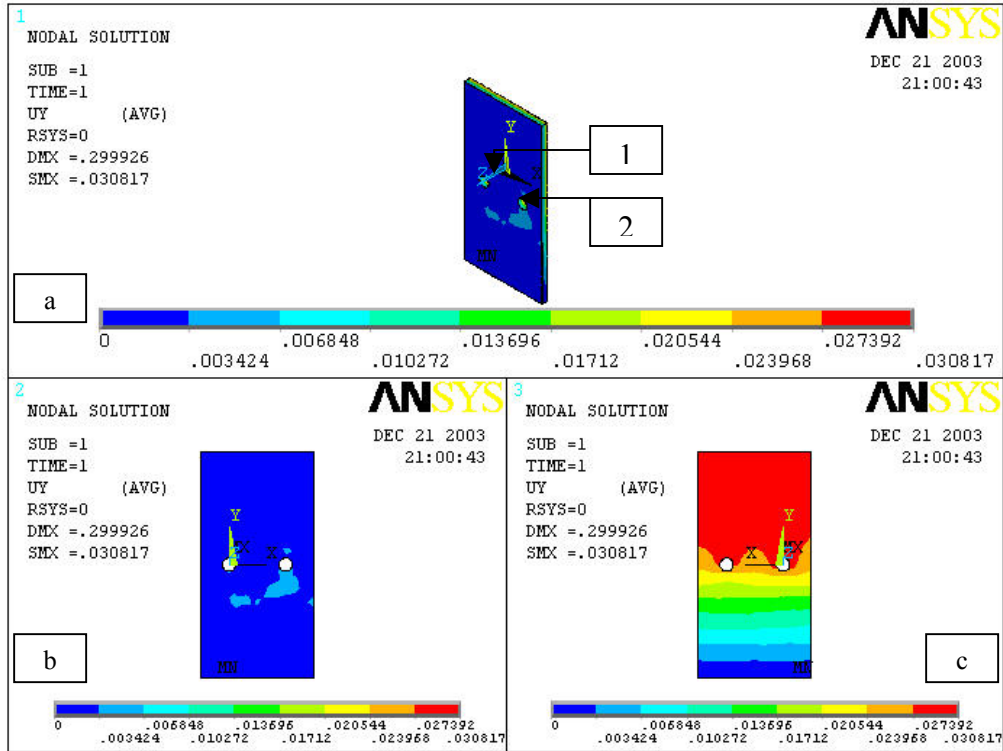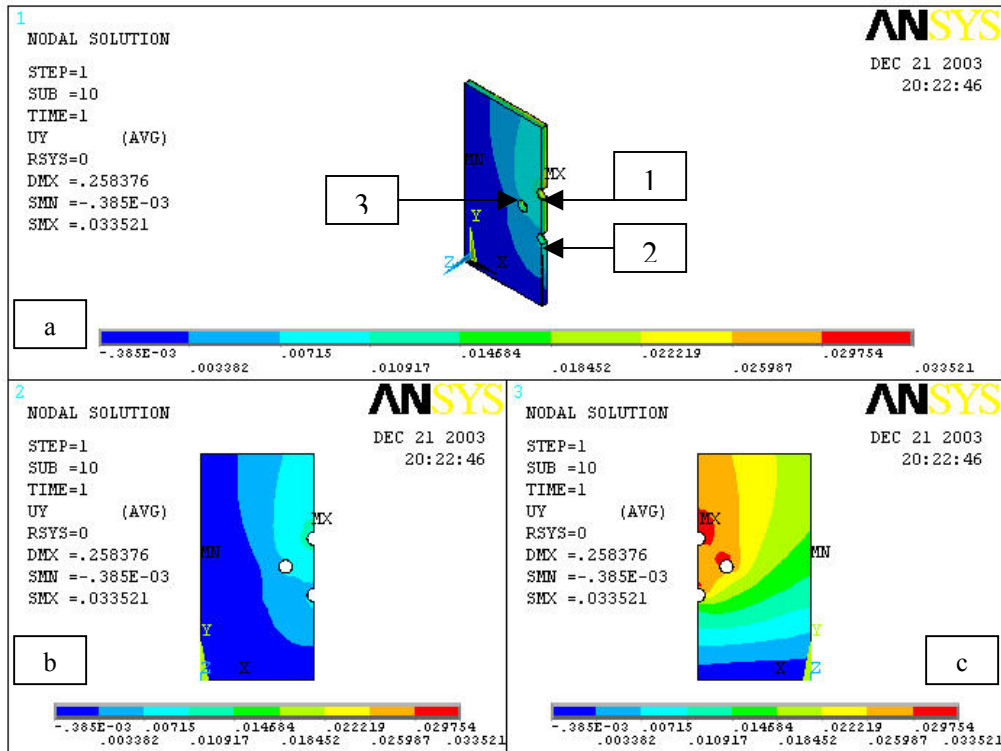
Figure 3.25: *y*-displacement of SP for layout D (a) isometric (b) boltside(c) interface side
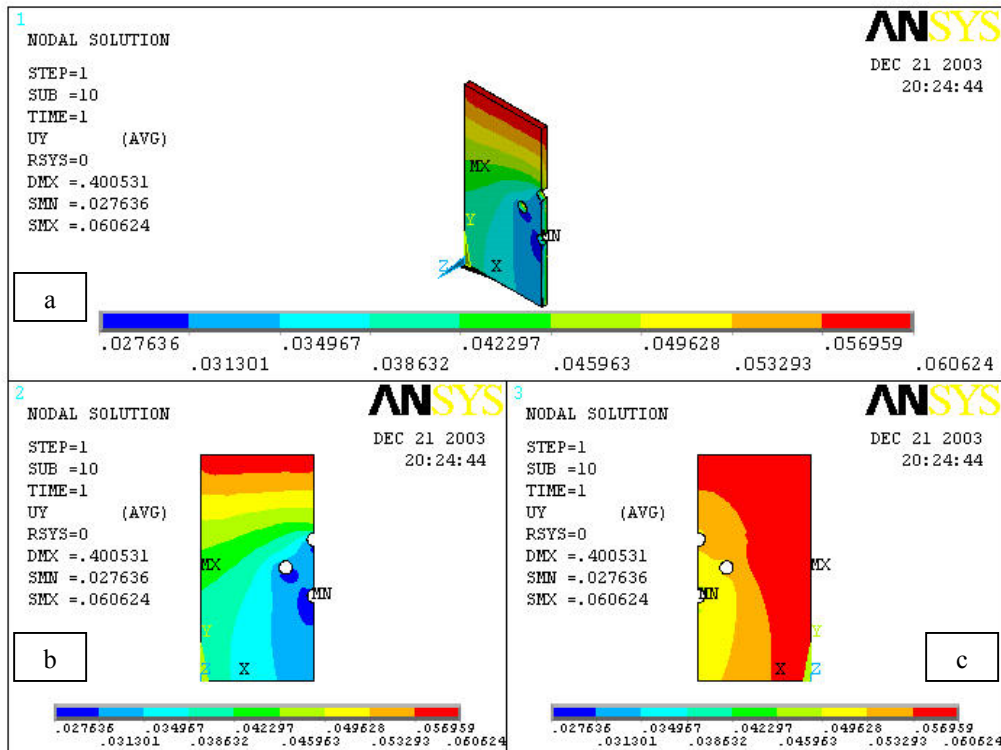
Figure 3.26: *y*-displacement of LP for layout D (a) isometric (b) interface side(c) nutside

Sides of this surface also show this movement thus it can be said that due to the positioning of the bolts plate is moving in upward direction from the sides.

Stress σ$_y$

Figure 3.27 shows the stress σ$_y$ distribution of SP for layout D. Regions of compressive stresses are present above the bolt holes on SP boltside. Maximum stress as in all the plates is on the SP interface side. It is near bolt 2. In this case maximum value 103 MPa. Figure 3.28 shows the stress distribution on LP for layout D. Three views are shown. Upper half portion of the interface side is in tension. The High stress regions are around the bolt holes. The maximum stress value is 104 MPa and is on the interface side of the LP. Small regions of tensile stresses are there on LP nutside. Figure 3.29 and 3.30 show the von Mises stress distribution on SP and LP. The maximum von Mises stress is 348 MPa in SP and 308 MPa in LP, which indicates that SP is more stressed at the critical region. The critical region in both plates is going into plastic deformation.
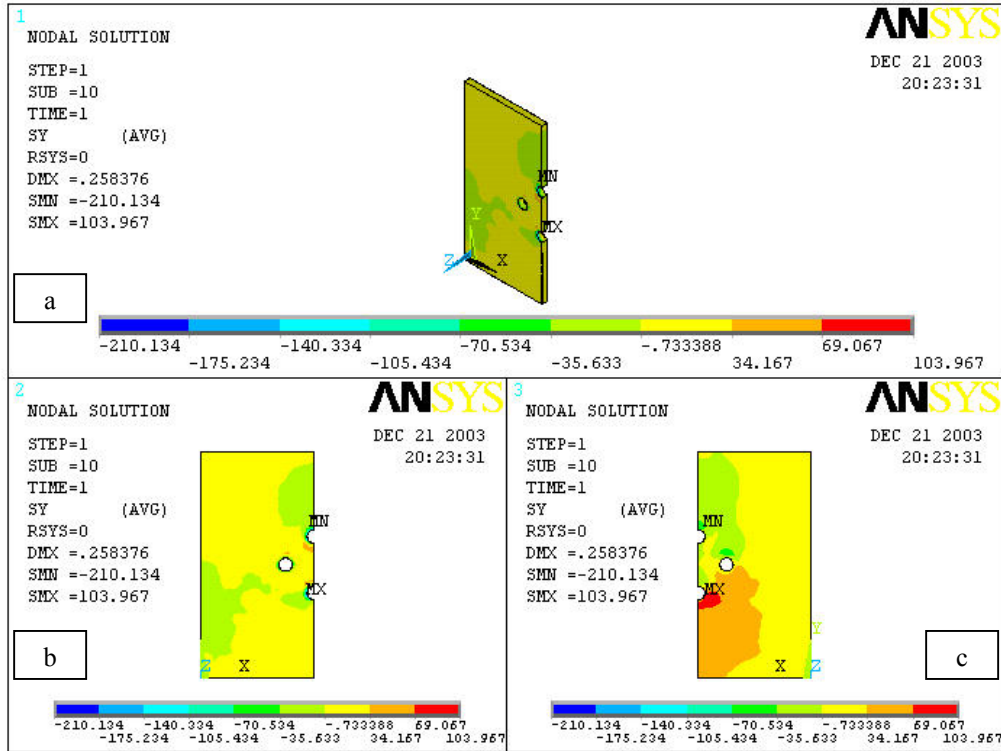
Figure 3.27: Stress σ_y of SP for layout D (a) isometric (b) boltside(c) interface side
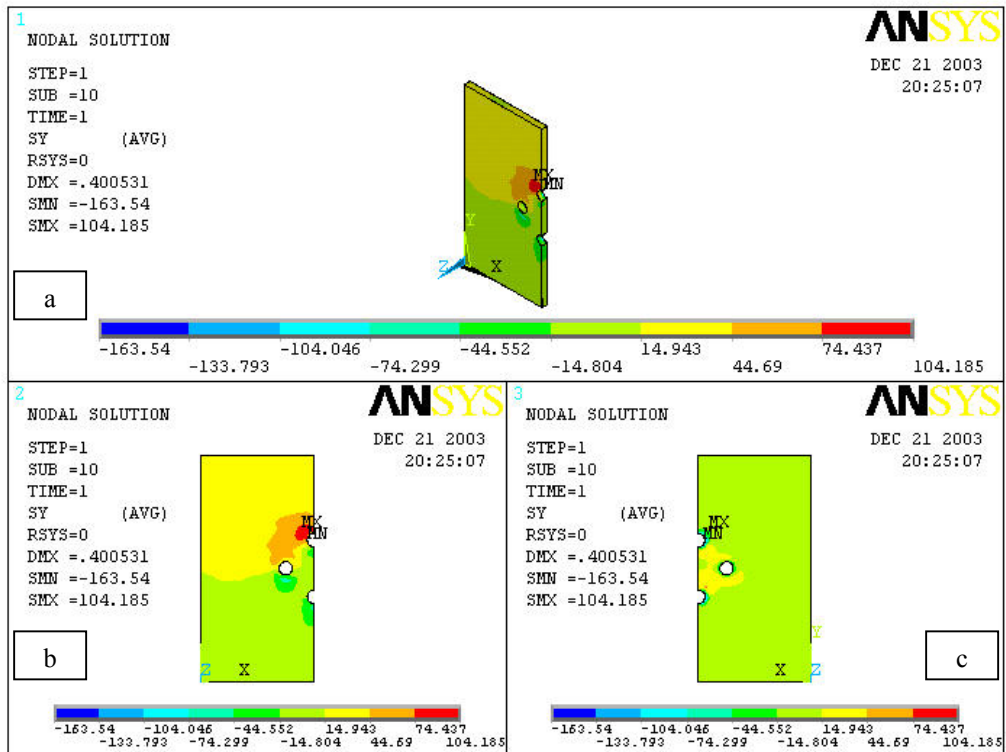
Figure 3.28: Stress σ_y of LP for layout D (a) isometric (b) interface side(c) nutside
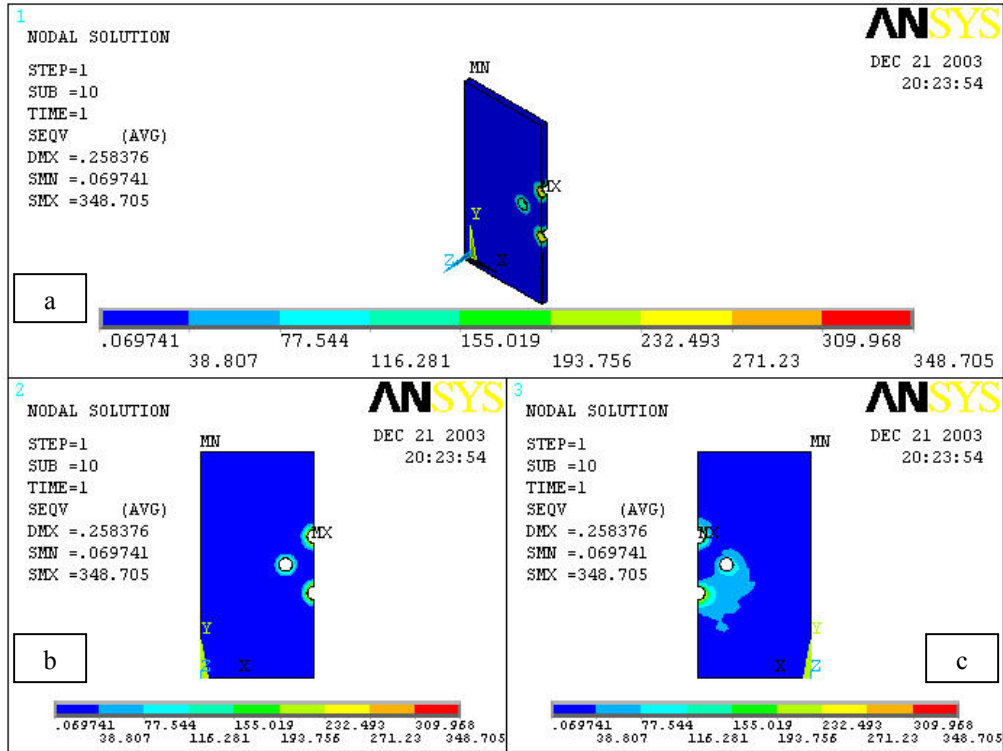
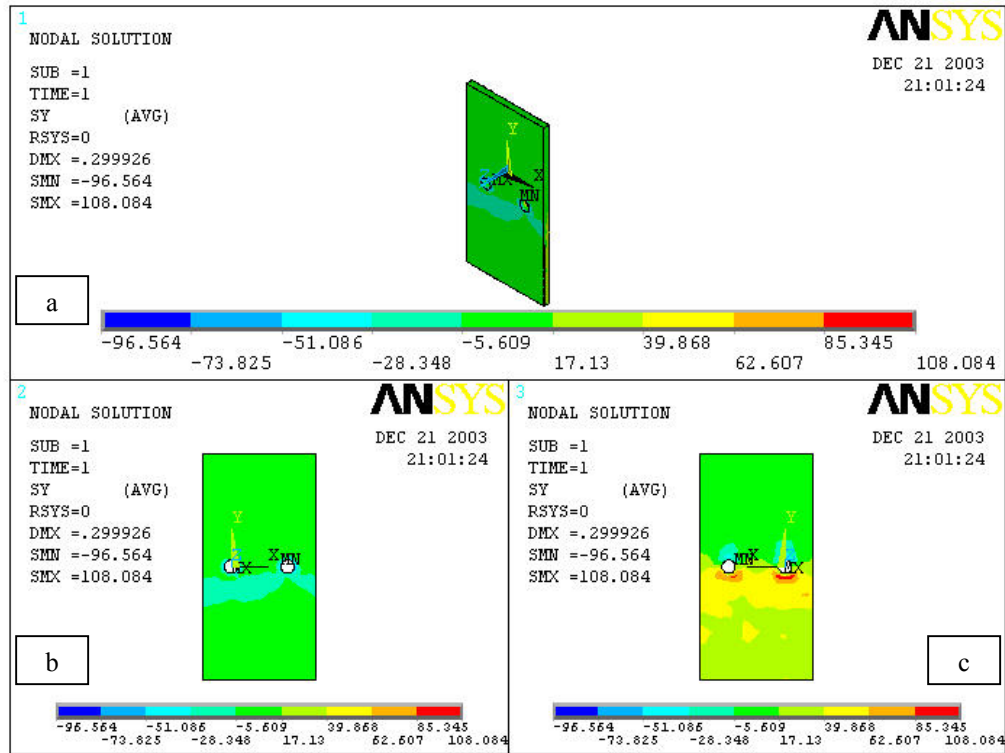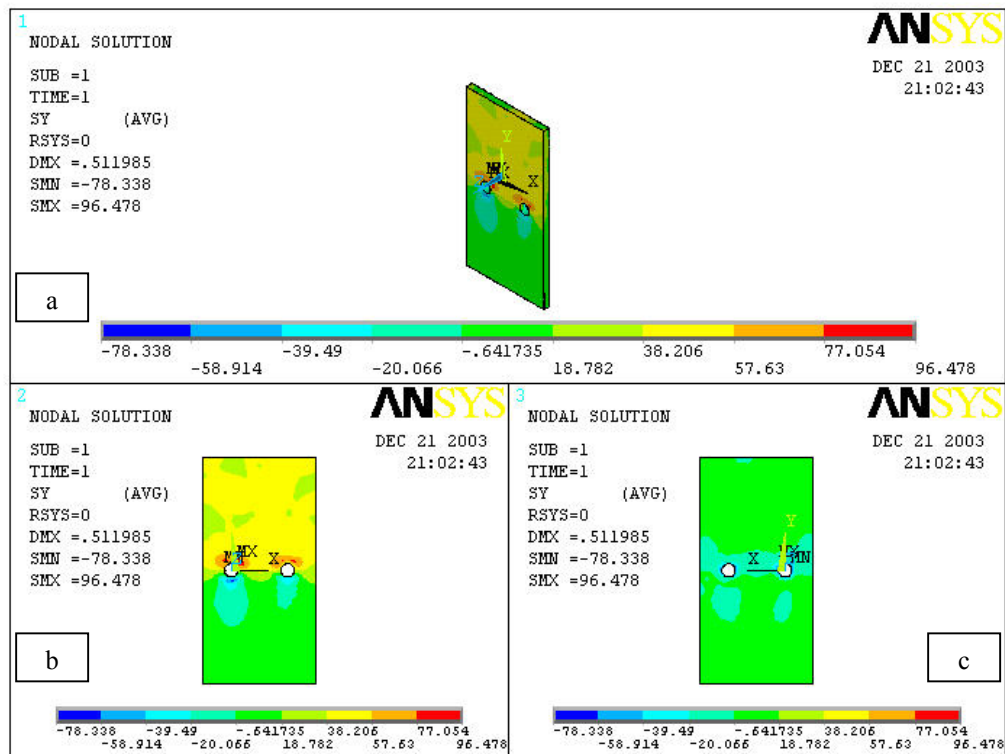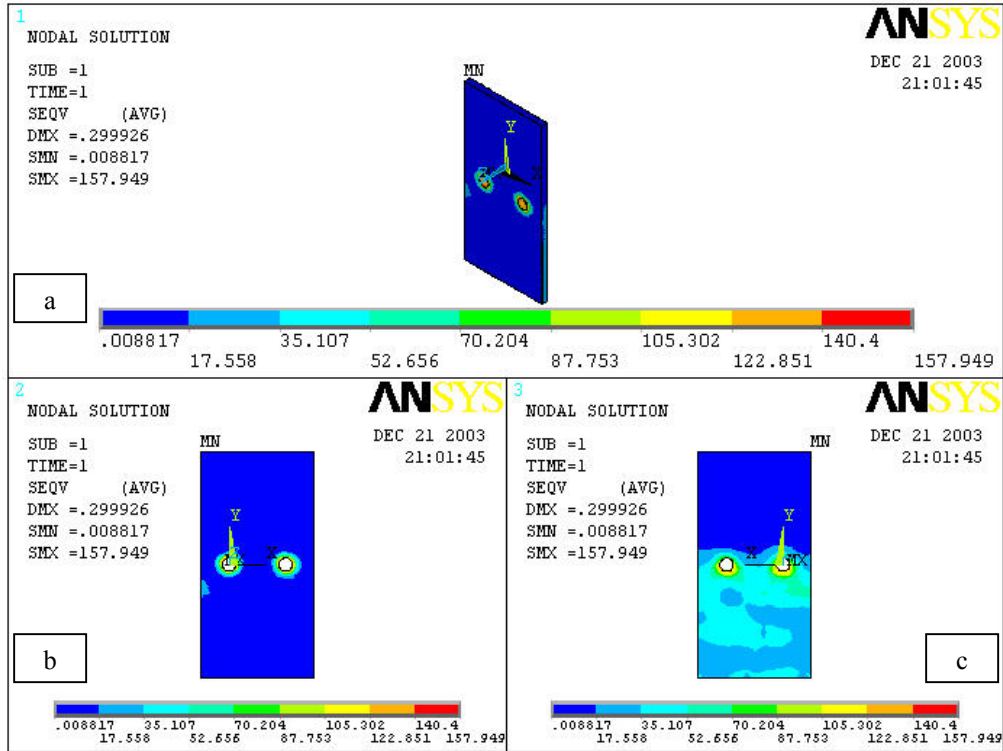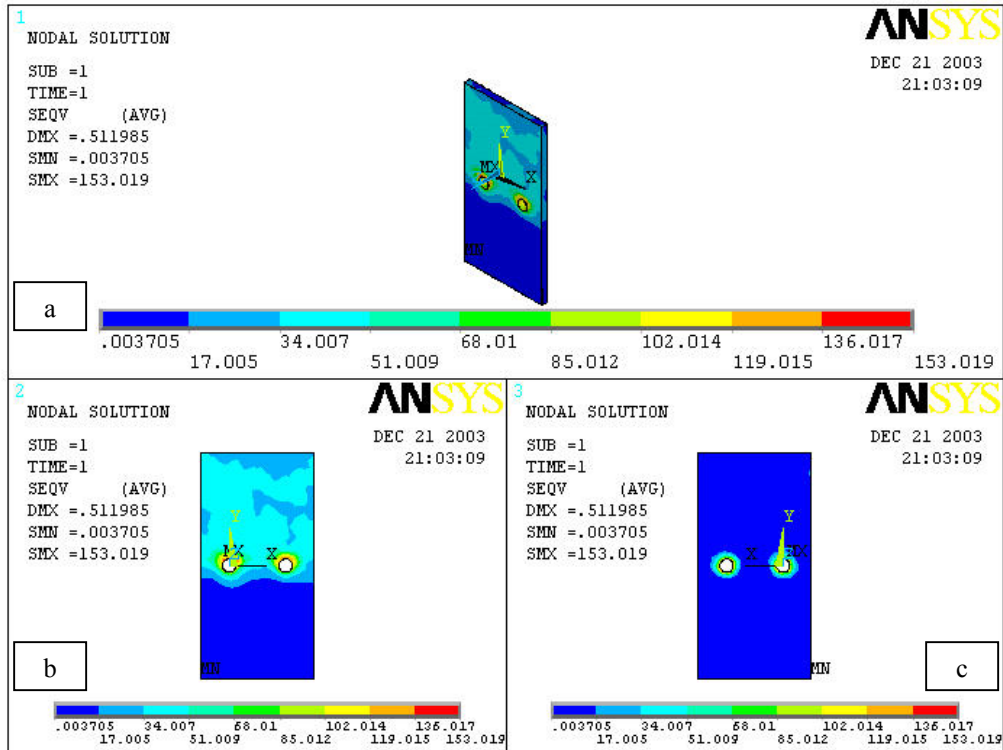Figure 3.29: von Mises stress of SP for layout D (a) isometric (b) boltside(c) interface side
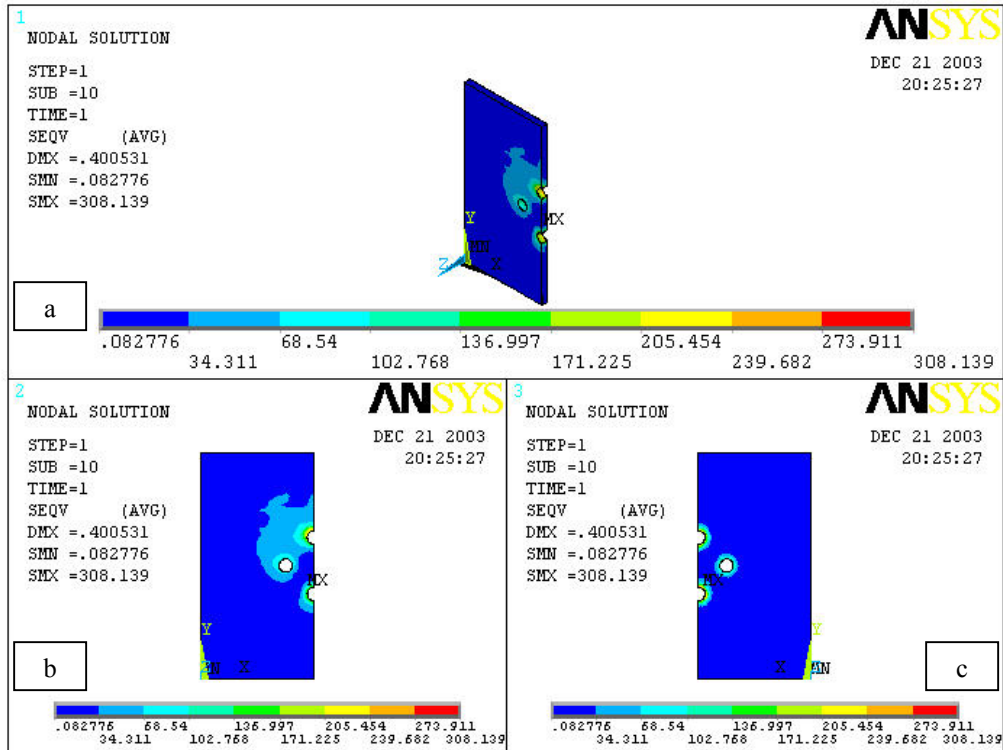
Figure 3.30: von Mises stress of LP for layout D (a) isometric (b) interface side(c) nutside

3.4 COMPARISON

After analyzing the layouts individually Table 3.1 lists the maximum von Mises stress values on SP and LP. It is clear from this table that layout C and D are showing the highest stress value for loading and supporting plate, respectively. While the layout B has the minimum stress values. Stress values for layout A and layout B are comparable. So layouts A and B are better than layouts C and D. Table 3.2 lists the maximum stress values in the direction of applied load in the bolts. It is clear that the highest stress is in the critical bolt of layout C. The minimum stress is again in the layout B. It is clear from these two tables that there is a relationship between the high stress regions of loading plate with the critical bolt experiencing high stress in a specific layout.

3.5 CONCLUSIONS

1. The values of maximum von Mises stress in lay out C and D is higher in both SP and LP than the values for lay out A and B. It is concluded that the last mentioned layouts are better.

2. Looking at the layouts individually LP and SP interface sides are more critical as compared to the LP and SP bolt and nut sides because the value of stress is higher at these surfaces.

3. For lay out A, LP, stress σ_y value is more in the region around the bolthole 1. For SP the critical region is around bolthole 2. For layout D, LP, stress value is more around the bolt hole 1 as compared to the bolt hole 2 and bolt hole 3. For SP, region around bolt hole 3 is more critical than the other two regions. For lay out C, LP, stress has higher value around bolthole 1. For SP the maximum value of stress is at bolt hole 4 thus being more critical region. For lay out B, on LP stress around

bolt hole 1 is more. But in SP, bolt hole region 2 is more stressed. This is due to the boundary condition and holding of the plate at one position.

4. For lay out A, critical bolt is bolt 1 as it has higher stress σ_y value. For lay out D, bolt 1 is critical than the other two bolts. For lay out C bolt 1 has high value of stress means it has more yielded than the other three bolts. For lay out B bolt 1 is more critical, having slightly high stress value than bolt 2.

5. It can be concluded that the distribution of stress σ_y is not symmetric around every bolt hole in the member as usually assumed in design procedure calculations. The stress distribution changes with the change of arrangement of bolts.

6. It is also observed that the critical region in the LP is the same where the bolt is critical too.

Table 3.1: Maximum von Mises stress σ_v on SP and LP

	σ_v at SP (MPa)	σ_v at LP (MPa)
Layout A	173	192
Layout B	157	153
Layout C	329	331
Layout D	348	308

Table 3.2: Maximum stress σ_y in the Bolts for different layouts

	σ_y at Bolt#1 (MPa)	σ_y at Bolt#2 (MPa)	σ_y at Bolt#3 (MPa)	σ_y at Bolt#4 (MPa)
Layout A	105.725	93.745	105.725	93.745
Layout B	94.767	94.151	94.151	94.151
Layout C	197.93	185.32	182.12	156.758
Layout D	166.662	102.943	159.374	159.374

CHAPTER 4

LAY OUT FACTOR

4.1   INTRODUCTION

The bolts do not share equal loads when the bolted joint is put in service. In a particular layout the bolt taking most of the load is the critical bolt. The distance from the group centeroid and loading edge, location of the bolt etc, are some factors that affect the load sharing capacity of the critical bolt in a layout. In this chapter a geometrical relationship is derived to compare the different layouts in terms of the critical bolt. This idea of developing a tool in terms of geometric parameters for design optimization and quick calculation is not new. For example in heat exchangers, ligament efficiency term is used. This relates the length and diameter of the tubes used in a boiler. The greater the length of the tube the greater is the ligament efficiency. Annubar factor is very common in fluid flow. This relates the annubar shape and size to the mass flow rate of fluid flowing in a duct. Annubars are very common to use in large size ducts where there is need to keep the energy loss and flow disturbance to a minimum. In extrusion process, complexity of a die is a function of the ratio of the perimeter to the crossectional area of the part, known as the complexity index. Thus a solid round extrusion is the simplest shape. The larger the perimeter the greater is the complexity of extrusion. In heat transfer field, shape factor for transient conduction is available. Shape factor is proportional to the characteristic time constant of the slowest eigenfunction of cooling or heating problem with temperature independent thermal properties and boundary conditions of first kind.

138

Size is universally defined as volume to surface area ratio. So shape factor is surely a geometrical parameter. This relates the shape with the heat fluxes. So sphere and cube have lower shape factors while the infinite slab has the highest.

Arif et al [30] developed the complexity factor on the basis of failures of dies in extrusion process. Bart et al [31] obtained shape factor for transient heat conduction in arbitrary objects for which no analytical solution exists. Such a shape factor is the dominant parameter in the prediction of heat transfer processes. V.Sheshdari et al [32] carried out a study around a circular pipe using computational fluid dynamics (CFD) code, fluent to establish the effect of body shape on the annubar factor. It is found out that the annubar factor for elliptical shape with high slenderness ratio has the highest annubar factor and minimum permanent pressure. Arif [34] analyzed different configurations using finite element analysis for four-bolted joint. He developed a layout effect prediction tool in terms of geometry. The prediction of the tool was quite effective for the four-bolted joint. The proposed layout factor is only limited to the four bolted joint and it is not for the layouts of other number of bolts.

In this chapter a layout factor in terms of geometry is developed for any number of bolts under shear loading. Most of the work done reported in the literature assumes that all the fasteners in the joint have an equal share of the applied loads. However it is clear from the previous chapter in which a four-bolt joint is tested in different configurations, that fasteners do not share equal loads. John Bickford [35] reports this unequal sharing too. This assumption leads to a more conservative design and lacks the optimization in terms of number, size and layout of bolts. From the previous study it is clear that geometric factors like the distance from the edge, center and sides affect the load bearing capacity of bolts in a particular lay out. In this chapter different layout of 2, 3 4, 6 and 8 bolts are

analyzed numerically. Maximum load on a fastener in the layout is identified. A lay out factor is then defined. It makes use of the geometric parameters that can predict the behavior of the critical fastener in a particular layout. The idea is that if we have two different types of layouts by calculating the lay out factor we can predict easily which lay out is better in terms of critical load.

4.2   COMPUTATIONAL MODEL

4.2.1   Geometric Idealization

Primary objective of this study is to predict the maximum load resulting in a fastener in a layout and then proposing a geometrical layout factor. For this purpose two-dimensional model is used. 2, 3, 4, 6 and 8 bolted joints are considered in the analysis. Different layouts are shown in the figures 4.1 to 4.5. The layouts considered are more common in civil engineering field like structures, girders, and beams. In mechanical engineering bolts are arranged more on the pitch circle in round form as in flanges. Designer does not have the liberty to choose between the shapes of layouts. However for preliminary study simpler layouts are considered. All the holes are of same diameter for different layouts. All the geometric dimensions and material properties are given in table 4.1. The dimension of the plate increases with the increase in the number of bolts.

4.2.2   Finite Element Model

Finite element model is developed using a commercial FE code ANSYS. For modeling purpose only the members having the applied shear load are considered. The fasteners are assumed to be rigid and fixed. A uniform pressure is applied on the top edge of the plate. Material behavior is idealized as linear isotropic. The member is idealized as plane stress problem. It is meshed with Plane 2 element. Plane 2 is a six-nodded triangular

Table 4.1: Modeling data for shear joint

Size of member plate (2, 3, 4, 6 and 8 bolted joint)	
Width	100 mm, 150 mm, 200 mm, 300 mm and 400 mm
Height	100 mm, 150 mm, 200 mm, 300 mm and 400 mm
Material of member plate	
Modulus of elasticity	210GPa
Poisson's ratio	0.3
Yield Strength	300 MPa
Diameter of the Fasteners	M16 x 2
Grade	8.8
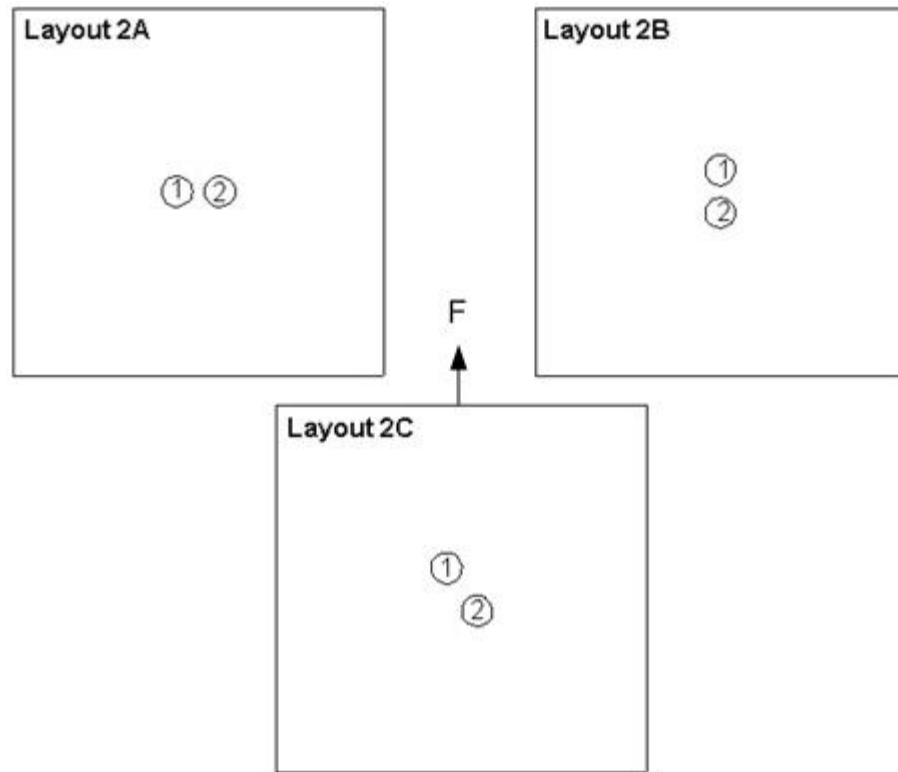
Figure 4.1: Two-bolted layouts
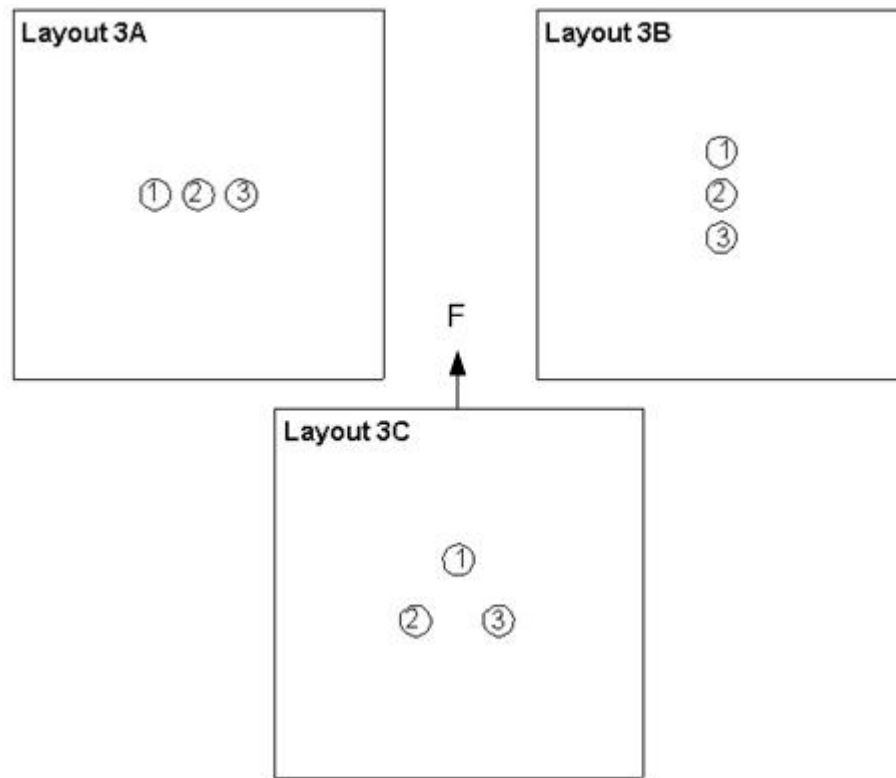
Figure 4.2: Three-bolted layouts
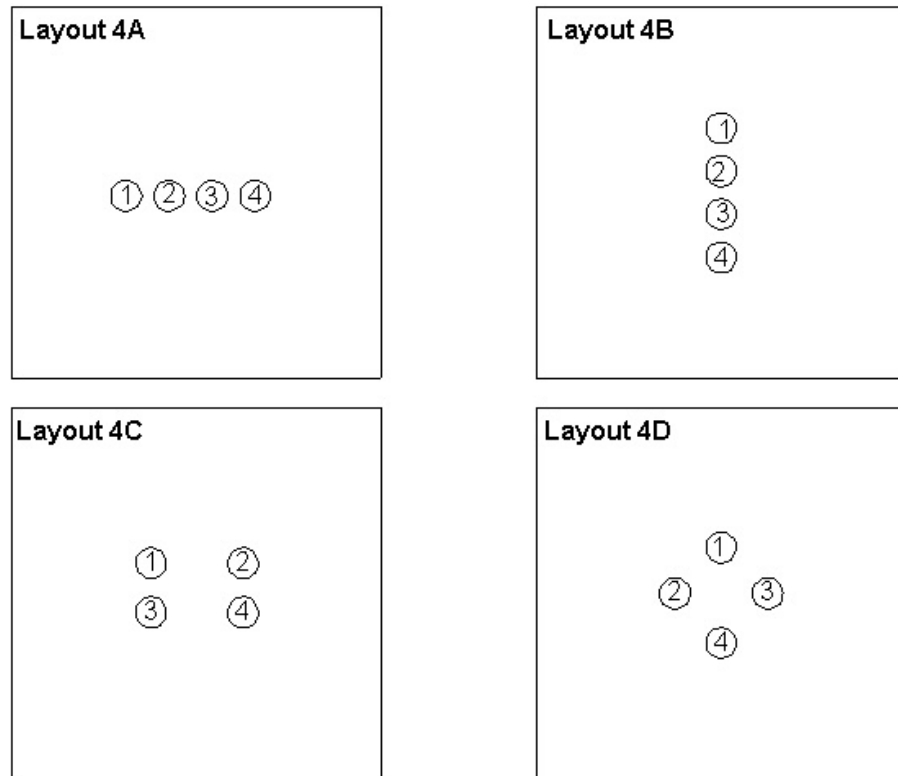
Figure 4.3 Four-bolted layouts
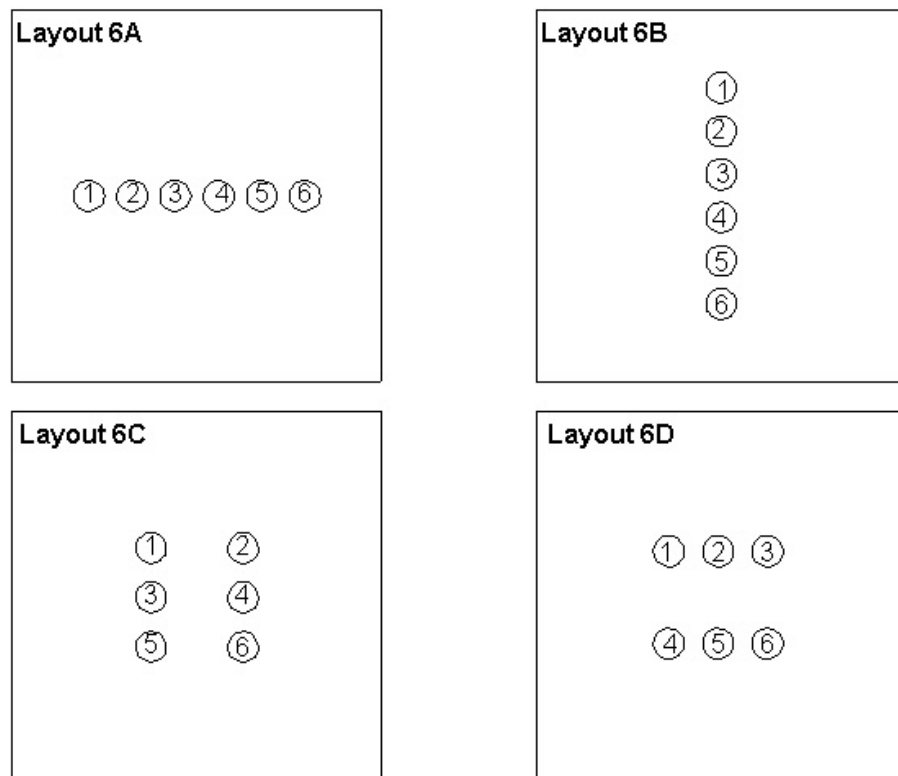
Figure 4.4: Six-bolted layouts
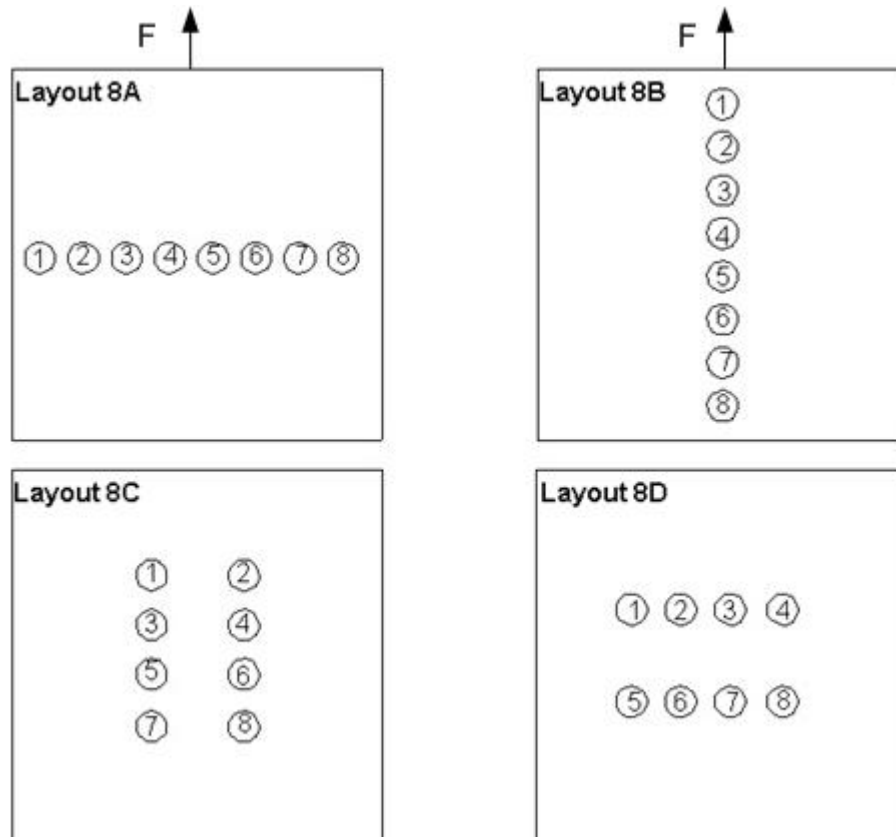
Figure 4.5: Eight-bolted layouts

element having a quadratic displacement behavior and is well suited to model irregular shapes. The element is defined by six nodes having two degrees of freedom at each point: translations in nodal X and Y directions. Figure 4.6 shows types of meshes used for the analysis. The element and node numbers increase from 2274 and 4598 in two bolted layouts to 10384 and 20738 in eight bolted layouts. Mesh refinement is done till the results obtained become constant. Contact elements are placed between the fasteners and the hole of the member. It is modeled using Targe169 and Conta172. The member hole edges are constrained as contact surfaces and the fastener is modeled as rigid target. Conta 172 are used to represent contact between 2-D target surfaces and a deformable surface, defined by this element. Targe169 is used to represent various 2-D target surfaces for the associated contact element. The contact elements themselves over lay the solid elements describing the boundary of a deformable body. Figure 4.7 shows the contact surfaces with their normals. There is no clearance between the hole and the fastener to do a preliminary study although this is not the case in reality. Friction coefficient used is 0.75.

4.3   RESULTS AND DISCUSSIONS

4.3.1   Load Shared by Fasteners

The load shared by each fastener in different layouts for a total applied load corresponding to 20 MPa is given in table 4.2 to 4.6. Lay out number 2A30 refers to layout A of 2-bolted joint at fastener spacing (h) of 30 mm. The maximum fastener load is high lighted in the table and sum of all the fastener loads is approximately equal to the total applied load. The values are obtained by numerical runs performed on ANSYS for different layouts. In order to get the force on the fasteners nodes are selected that are in a
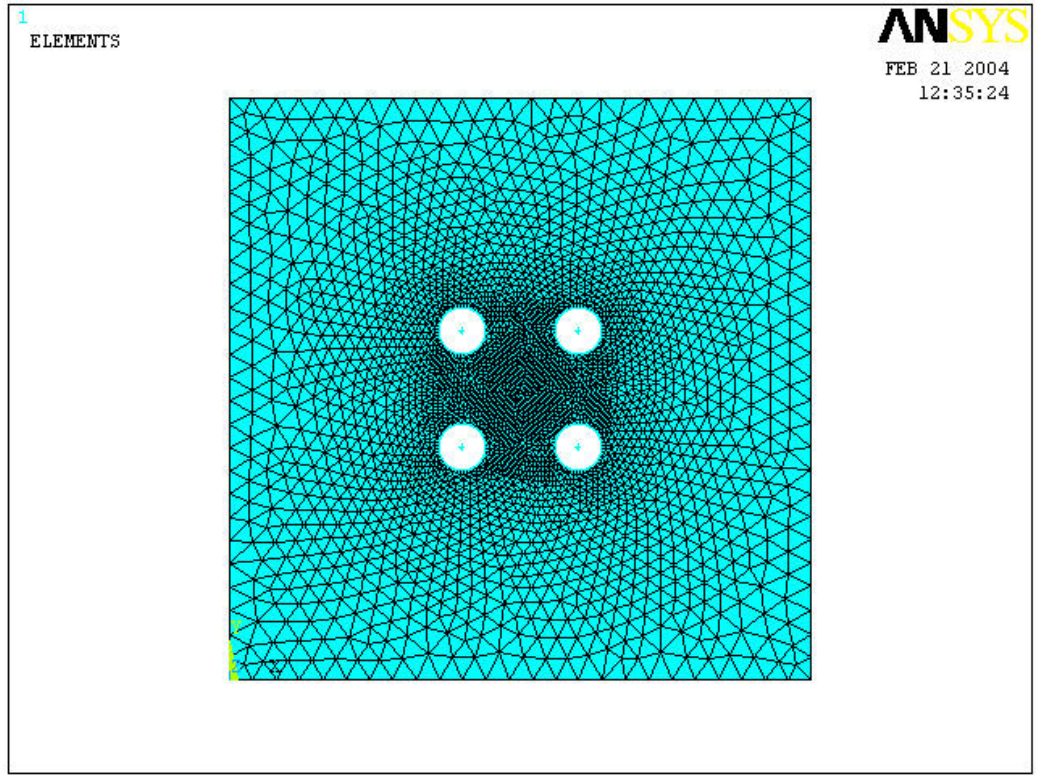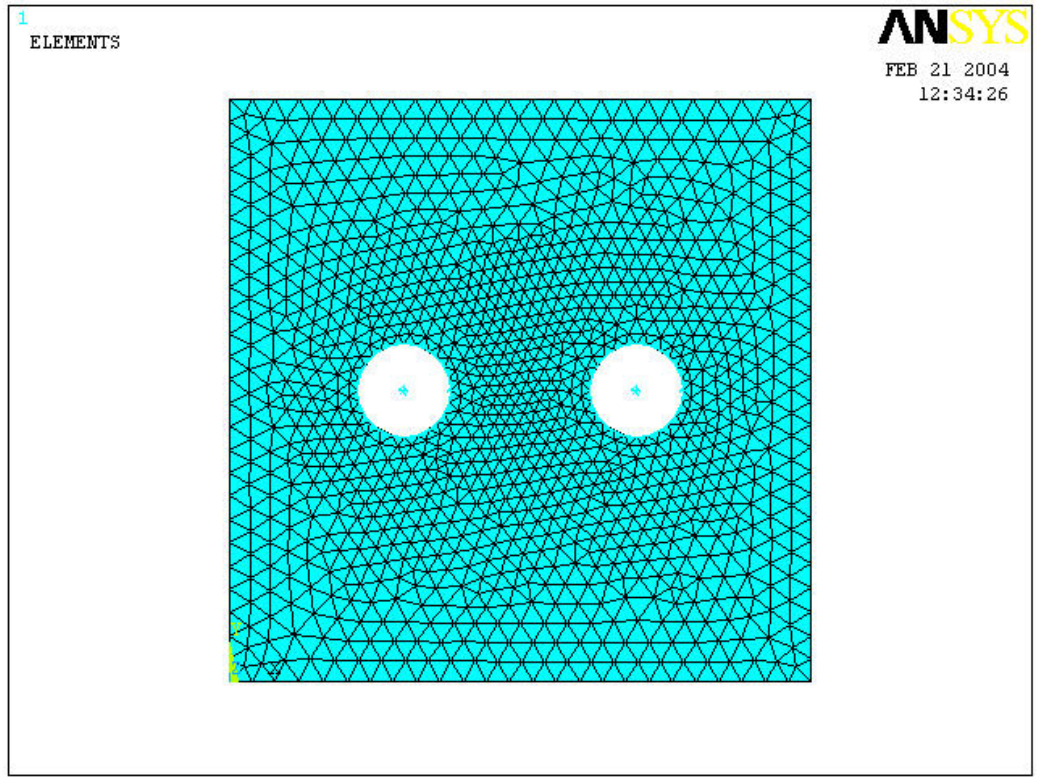
Figure 4.6: Mesh of two and four bolted layouts
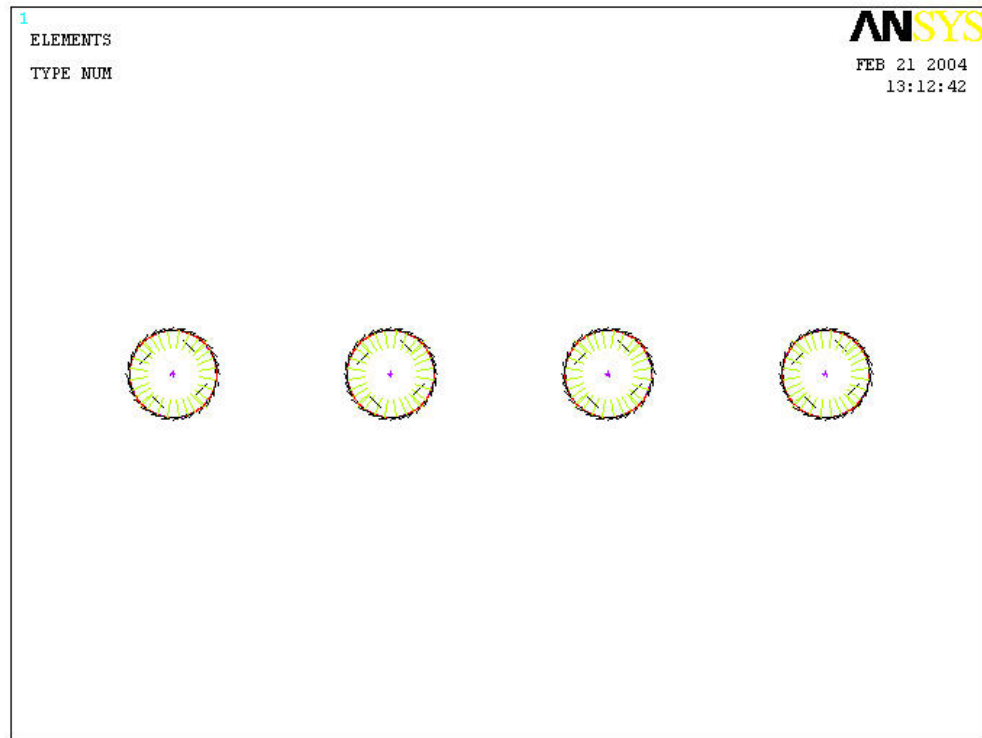
Figure 4.7: Contact elements at the interface of fastener and member hole

Table 4.2: Load shared by each fastener in two bolted layouts

Layout	F1(N)	F2(N)	FM(N)
2A30	1000.97	999.12	1000.97
2A40	1000.74	999.39	1000.74
2A50	1000.85	999.28	1000.85
2B30	1391.59	608.42	1391.59
2B40	1331.70	665.0299	1331.70
2B50	1261.44	738.816	1261.44
2C30	1119.59	880.02	1119.59
2C40	1124.84	871.23	1124.84
2C50	1079.24	920.76	1079.24

Table 4.3: Load shared by each fastener in three bolted layouts

Layout	F1(N)	F2(N)	F3(N)	FM(N)
3A30	1106	784	1109	1109
3A40	1065	866.62	1065	1065
3A50	1017	965.32	1019	1019
3B30	1523	782	694	1523
3B40	1601	818	558	1601
3B50	1662	782	464	1662
3C30	1266	870	869	1266
3C40	1334	834	831	1334
3C50	1376	811	813	1376

Table 4.4: Load shared by each fastener in four bolted layouts

Layout	F1(N)	F2(N)	F3(N)	F4(N)	FM(N)
4A30	1190	811	811	1187	1190
4A40	1121	876	877	1121	1121
4A50	1033	966	966	1033	1033
4B30	1631	905	704	758	1631
4B40	1713	970	722	594	1713
4B50	1767	1030	753	448	1767
4C30	1201	1202	798	796	1201
4C40	1262	1264	735	734	1262
4C50	1301	1301	698	696	1301
4D30	1047	1107	1107	731	1047
4D40	1173	1102	1103	619	1173
4D50	1238	1098	1096	566	1238

Table 4.5: Load shared by each fastener in six bolted layouts

Layout	F1(N)	F2(N)	F3(N)	F4(N)	F5(N)	F6(N)	FM(N)
6A30	1917	1075	825	700	631	832	1917
6A40	1919	1155	879	729	627	616	1919
6A50	2012	1220	951	781	648	404	2012
6B30	1353	877	770	770	877	1353	1353
6B40	1232	921	840	840	921	1232	1232
6B50	1064	979	956	956	980	1064	1064
6C30	1427	1427	681	681	891	891	1427
6C40	1500	1500	734	734	768	768	1500
6C50	1550	1550	764	764	687	687	1550
6D30	1360	840	1360	967	506	967	1360
6D40	1396	947	1396	886	487	884	1396
6D50	1419	1018	1419	837	475	832	1419

Table 4.6: Load shared by each fastener in eight bolted layouts

Layout	F1(N)	F2(N)	F3(N)	F4(N)	F5(N)	F6(N)	F7(N)	F8(N)	FM(N)
8A30	2163	1218	933	786	697	646	647	906	2163
8A40	2174	1303	1052	839	732	652	596	649	2174
8A50	2191	1361	1086	917	793	684	567	389	2191
8B30	1500	947	804	748	748	804	947	1500	1500
8B40	1336	969	867	823	823	867	969	1336	1336
8B50	1092	994	963	947	947	963	994	1092	1092
8C30	1636	1636	738	738	613	613	1012	1012	1636
8C40	1710	1710	810	810	632	632	852	852	1710
8C50	1763	1763	860	860	634	634	740	740	1763
8D30	1502	861	861	1502	1118	524	524	1118	1502
8D40	1527	950	950	1527	1021	500	500	1021	1527
8D50	1540	1012	1012	1540	958	487	487	958	1540

contact at the interface for every fastener. Values of force in the applied direction of pressure are then noted from the result window of ANSYS general post processor.

First observation is that there is different load share on each fastener. For layout 2B, the critical fastener (fastener1) load share increases from 63% at h=30 to 70% at h=50. It is observed that critical fastener is the one that is near to the loading edge. For layout 4C, the critical fasteners are the two upper ones close to the loading edge and their load share increases from 30% at h=30 to 33% at h=50. For layout 4B, the load share of the critical fastener (fastener 1) increases from 40% at h=30 to 45% at h=50, whereas it decreases for the least loaded fastener from 18% to 11%. The distribution is worst in this case. In the case of horizontal layouts i.e. 2A, 3A, 4A, 6B and 8B, the fasteners located, near the edges of the plate share more load than the fasteners in the middle. Load sharing capacity decreases towards the center of the bolt group. Load share at these critical fasteners at the edges increases with the increase in pitch.

For vertical layouts i.e. 2B, 3B and 4B, load sharing capacity decreases moving in downward direction away from the loading edge. For 6A and 8A, there is slight deviation from this decreasing load share trend. For 6A when the pitch is smallest the load share on the bottom most fastener (fastener 6) increases from fastener 4 and 5. Same is true for layout 8A30 and 8A40. By changing the pitch it is observed that load share on fastener 1 increases and the fastener located at the bottom in every layout decreases.

In layouts 4C, 4D, 6C, 6D, 8C and 8D fasteners are arranged around the group centroid in the form of rows. In 4C, 6D and 8D in which there are two rows around the group centroid, as the pitch increases, the load sharing increases in the fasteners located near the loading edge. It is also true for the rows, which are nearer to the loading edge. The load sharing decreases in the row that is away from the loading edge.

4.3.2 Stresses in the Member

In order to get confidence about the values obtained for each fastener, stress distribution on the member is also obtained. von Mises stress distribution in the member for different layouts of four bolt at fastener spacing of 40 mm is shown in figure 4.8. The von Mises stress distribution shows that higher stress regions are localized around the fasteners, but the magnitude varies with the arrangement. The most uniform distribution of stress around the four holes is observed in layout 4D ranging from 100 to 90 MPa. Layout 4C results in the most severe loading of the member with a maximum stress of 150 MPa around the top fastener hole. For layout 4A the critical regions are just below the upper two holes (fastener 1 and 2) with a maximum value of 130 MPa. The maximum stress around the bottom holes (fastener 3 and 4) is 60 MPa. The maximum stress value in layout 4D is 140 MPa. There is a shift in the stress level from the lower most (fastener 4) to the middle row fasteners (fastener 2 and 3). As a result the stress value in the region around the fastener 4 has dropped to 50 MPa. It appears to be a viable conclusion that the stress distribution in the member around the holes close to the loading edge has higher magnitudes than the stresses around the lower holes. Also from the table 4.3 and figures 4.8 it is clear that the fastener that carries highest load is in the region of the member where the stress is also high in the member. So we can say that there is a relationship between the highly stressed member region and the critical fastener. Figure 4.9-11 shows the stress pattern for layout of two bolts. Again it is clear that uniform distribution is in the case of layout 2A when bolts are in line horizontally. For layout 2B the maximum stress is around the fastener 1 that is close to the loading edge. Same is true for the layout 2C. Figure 4.12-14 shows the stress pattern for layout of three bolts. In layout 3A the stress distribution is almost uniform on the fasteners 1 and 2. Slightly lower in the fastener
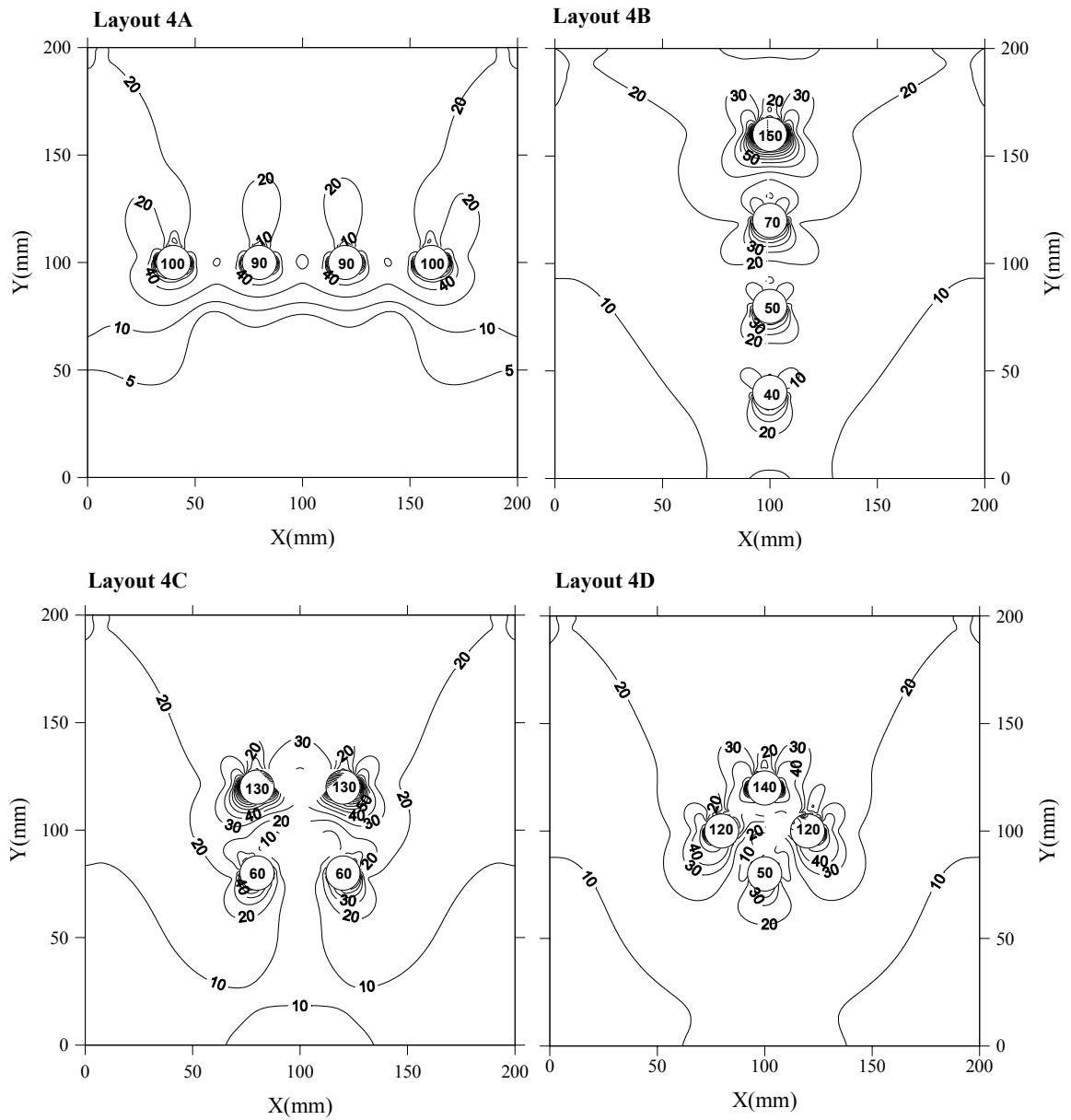
Figure 4.8: von Mises stress distribution for four bolted Layouts
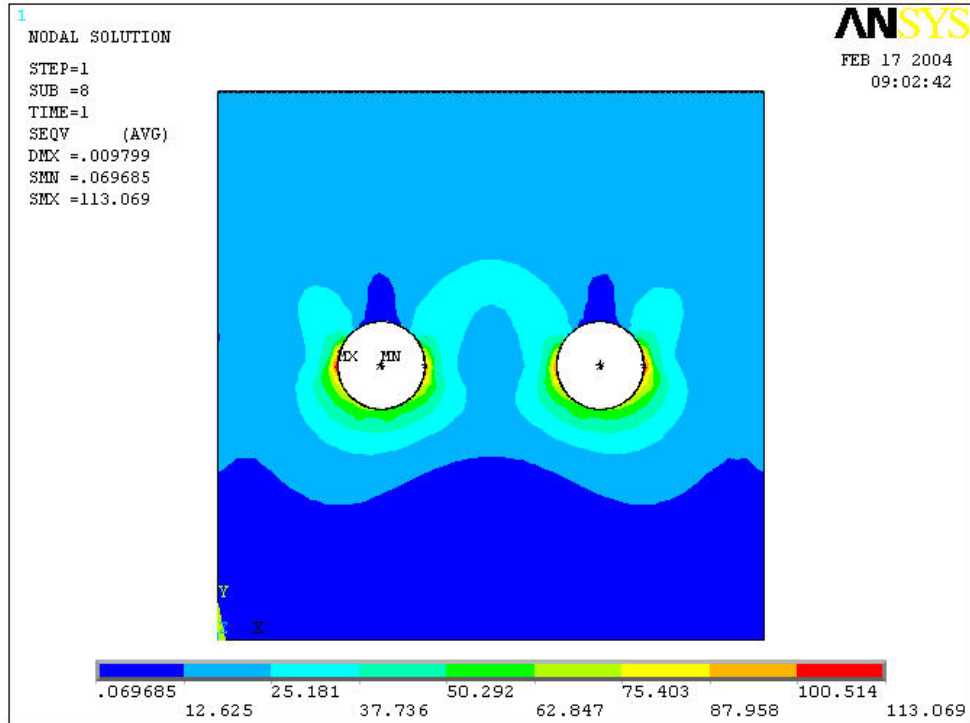
Figure 4.9: Stress pattern in layout 2A
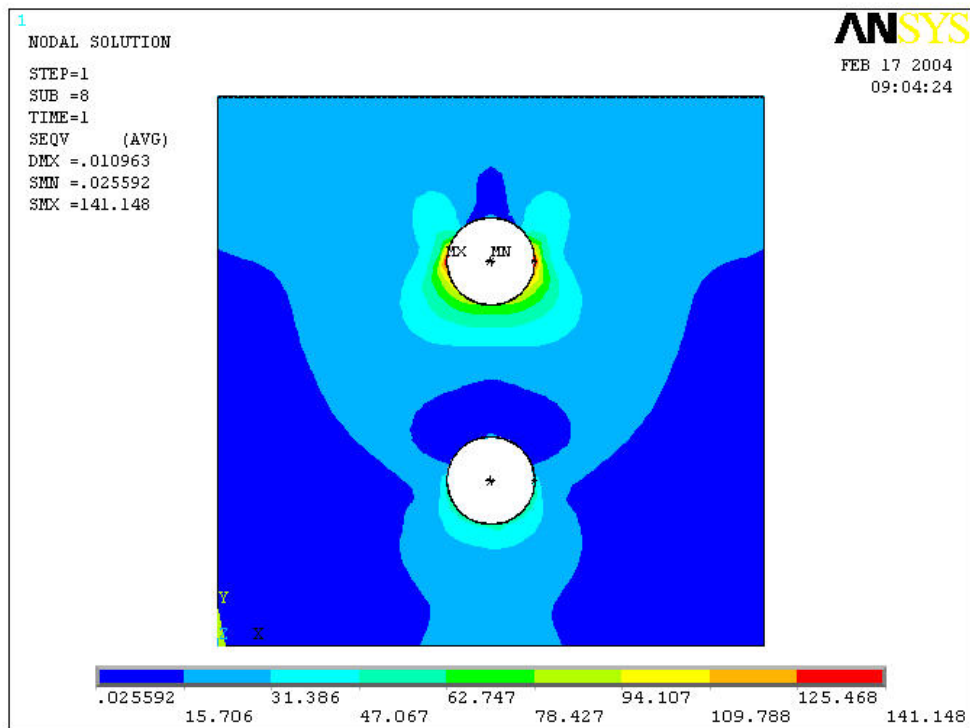
Figure 4.10: Stress pattern in layout 2B
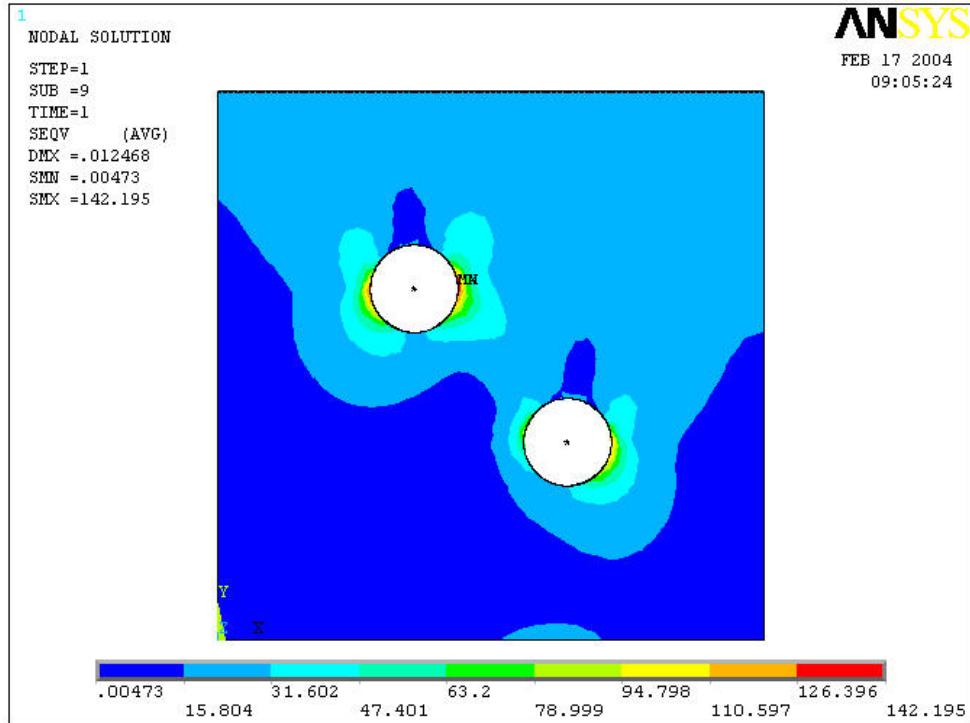
Figure 4.11: Stress pattern in layout 2C
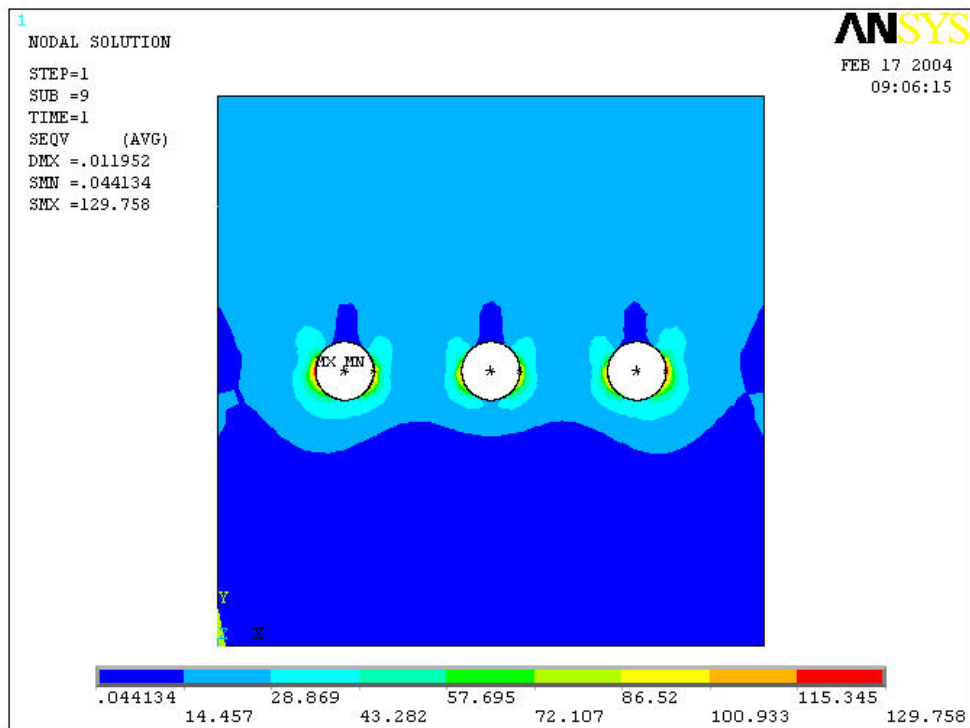
Figure 4.12: Stress pattern in layout 3A
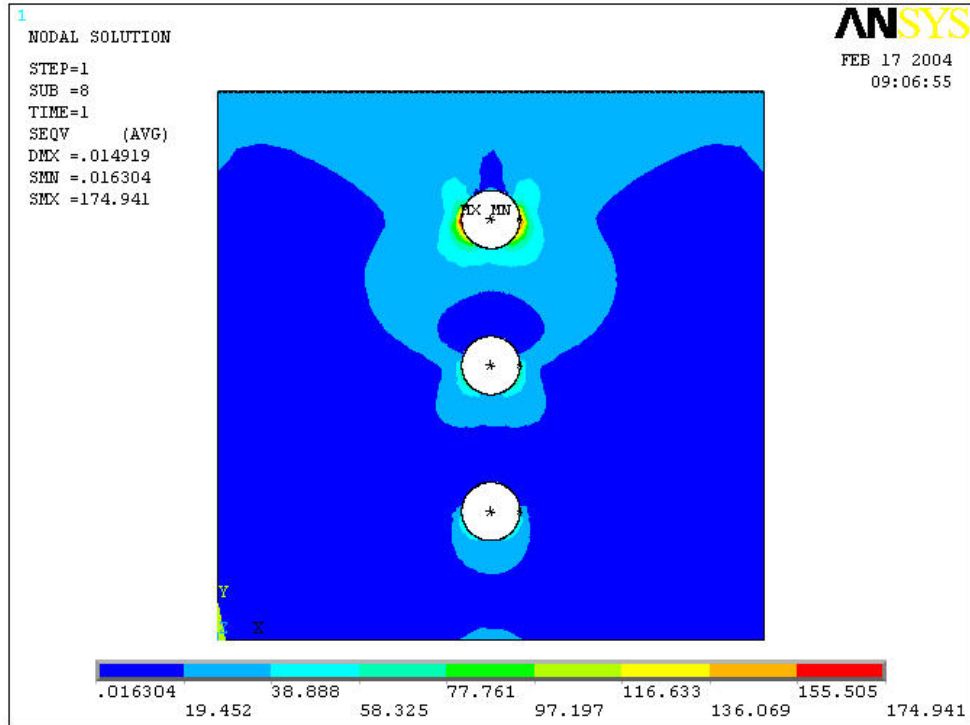
Figure 4.13: Stress pattern in layout 3B
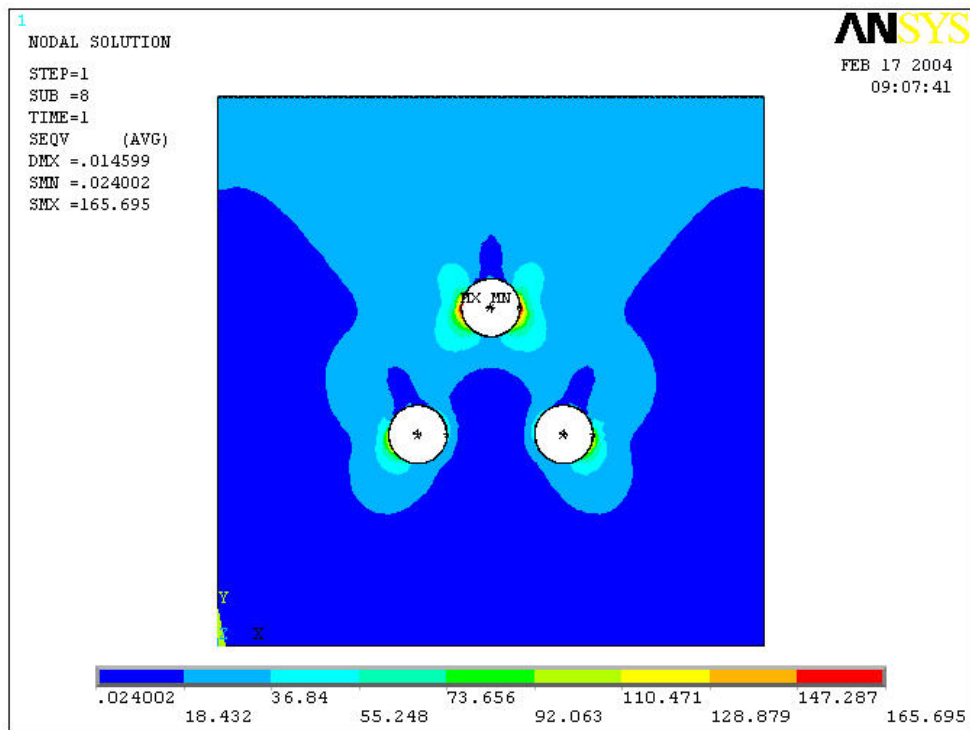
Figure 4.14: Stress pattern in layout 3C

2. Fastener 1 is critical from observation both in layout 3B and 3C. These results are again in agreement with the conclusion that the critical region in the members is same where the critical fasteners are located.

4.4   Layout Factor

On the basis of this different types of load sharing and stress distribution few parameters are identified that are affecting this load share. This include the position vector R of fastener that is close to the loading edge from the centroid, maximum horizontal distance X of the fastener from the centroid, maximum vertical distance Y of the fastener from the centroid, minimum distance e from the loading edge to the fastener. Combinations of these individual parameters are also checked for RSQ value. RSQ returns the square of the Pearson product moment correlation coefficient through the given points. It is the correlation coefficient and it shows the strength of linear relationship between two variables A and B. Statistically RSQ can be given by formula

$$RSQ = \frac{\sum AB - n\overline{A}\,\overline{B}}{\sqrt{(\sum A^2 - n\overline{A}^2)(\sum B^2 - n\overline{B}^2)}} \qquad (4.1)$$

Figure 4.15 helps to identify these factors on the layout of four-bolted joint. Before checking for the RSQ value the parameters are non-dimensionalised. $\overline{F}$, $\overline{X}$ and $\overline{Y}$ are used for this purpose and are defined below

$$\overline{F} = \frac{F}{Ft} \qquad (4.2)$$

Where $\overline{F}$ is the non-dimensional force, F is the force value on critical fastener from the numerical simulation and F_t is the total force that is applied on the edge of the member. Similarly
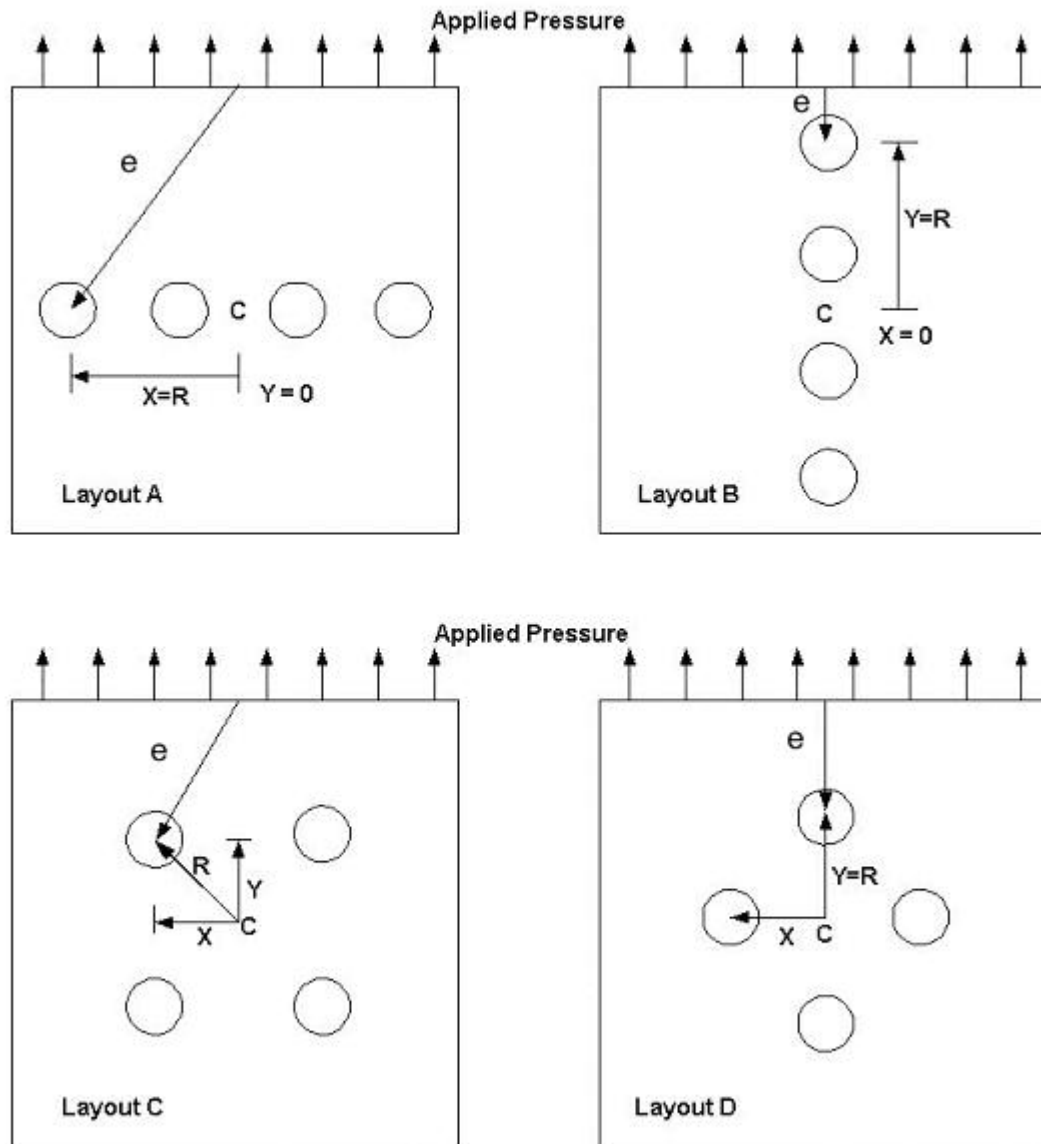
Figure 4.15: Geometric parameters shown on a four-bolted joint

$$\overline{X} = \frac{X}{X_{\lim it}}\left(\frac{\pi}{2}\right) \qquad \text{and} \qquad \overline{Y} = \frac{Y}{Y_{\lim it}}\left(\frac{\pi}{2}\right) \tag{4.3}$$

where X_{limit} and Y_{limit} respectively are half the width and height of the particular layout. This changes with the change of the bolt numbers, as length is different for different numbered fasteners. $\overline{X}$ and $\overline{Y}$ are the normalized coordinates scaled from 0 to $\left(\frac{\pi}{2}\right)$.

The non-dimensional value $\overline{e}$ is defined as follows

$$\overline{e} = \frac{e}{e_{\lim it}} \tag{4.4}$$

where $\overline{e}$ is the edge distance defined in the figure and e_{limit} is the total length of any layout that changes with the change in the number of bolts.

Table 4.7 shows the value of RSQ against the $\overline{F}$ for different geometric parameters for all the layouts. From this it is clear that $\overline{e}$ and $\overline{Y}$ are the parameters that have the highest dependence on $\overline{F}$. Rests of the parameters are weak. $\overline{e}$ and $\overline{Y}$ both have dependence more than 80 percent on $\overline{F}$ so these parameters are selected to develop a layout factor that can satisfy all the layouts of any number of bolts. After doing a detailed analysis and checking different combinations of these two parameters following relationship for layout factor β is developed.

$$\beta = \frac{A^{(\cos\overline{Y})^{0.3}}}{f} \tag{4.5}$$

where,

$$A = -\ln(\overline{e})^{\psi} \tag{4.6}$$

$$\psi = -0.0035n^2 - 0.0445n + 1.0823 \tag{4.7}$$

$$f = 1.5684\ln(n) + 0.7288 \tag{4.8}$$

Table 4.7: *RSQ* values of various geometric parameters with $\overline{\overline{F}}$

Parameters/Bolts	2	3	4	6	8
e	**0.879**	**0.989**	**0.857**	**0.939**	**0.946**
X	0.816	0.888	0.587	0.495	0.763
Y	**0.819**	**0.969**	**0.915**	**0.812**	**0.883**
(R/e)^n	0.589	0.382	0.369	0.292	0.211
ln (R/e)	0.613	0.413	0.675	0.563	0.448
R/e	0.618	0.484	0.641	0.503	0.377

where *n* is the number of bolts used in a particular lay out

How close the relationship predicts the value of load on the critical fastener can be noted from the following discussion. However the idea is not to predict accurately but the idea is to catch the trend of the variation of $\overline{F}$ in a layouts of same number of bolts. Table 4.8 shows clearly that as the value of $\overline{F}$ increases, β also increases. This means that we can identify which layout is better by calculating β from geometry. The layout with high value of β has more load on the critical fastener and vice versa. An approximate guess for the value shared by the critical fastener can also be identified by this relationship. The graphs in figure 4.16-17 show the capturing of trend of $\overline{F}$ with the layout factor derived β. The different layouts of a specific number of fasteners are arranged in ascending order of their respective critical normalized force on the critical fastener. The predicted force from the definition of Arif [34] is also shown in 2 and 3 bolted layouts. He has worked for the four-bolt layout. But it is clear that his definition cannot be applied to other layouts. The predicted force line is not showing the increasing trend and also not predicting the force correctly.

In order to check the limitations of the equation derived more layouts are tested numerically. In study A layouts with equally spaced fasteners are simulated. Four-bolted joint and six-bolted joint are considered. The bolt arrangement is different from the arrangements that we have used before while deriving the equation. Layout factor is calculated using the same correlation. In study B layouts with variable spacing between the fasteners are tested. Three-bolted joint and four-bolted joint are considered. Layouts that are used in these two studies are shown in figure 4.14 and 4.15.

Table 4.8: Comparison of β with $\overline{F}$

2Bolt		3Bolt		4Bolt		6Bolt		8Bolt	
β	$\overline{F}$	β	$\overline{F}$	β	$\overline{F}$	β	$\overline{F}$	β	$\overline{F}$
0.515	0.5	0.293	0.254	0.271	0.258	0.199	0.177	0.155	0.136
0.507	0.50037	0.302	0.266	0.282	0.280	0.209	0.205	0.164	0.167
0.498	0.50049	0.310	0.277	0.292	0.297	0.218	0.225	0.186	0.187
0.569	0.53962	0.346	0.316	0.323	0.300	0.238	0.226	0.1866	0.190
0.578	0.5624	0.355	0.333	0.325	0.309	0.240	0.232	0.1867	0.192
		0.398	*0.342*	*0.335*	*0.3102*				
0.587	0.563	0.363	0.344	0.329	0.315	0.252	0.236	0.202	0.204
0.594	0.6307	0.377	0.380	0.334	0.325	0.251	0.238	0.209	0.213
				0.348	*0.336*				
0.613	0.6668	0.390	0.400	0.364	0.407	0.258	0.25	0.217	0.220
						0.261	*0.2581*		
0.629	0.6958	0.397	0.415	0.377	0.428	0.264	0.2583	0.233	0.270
				0.381	0.441	0.283	0.319	0.248	0.271
						0.295	0.32	0.254	0.274
						0.298	0.335		
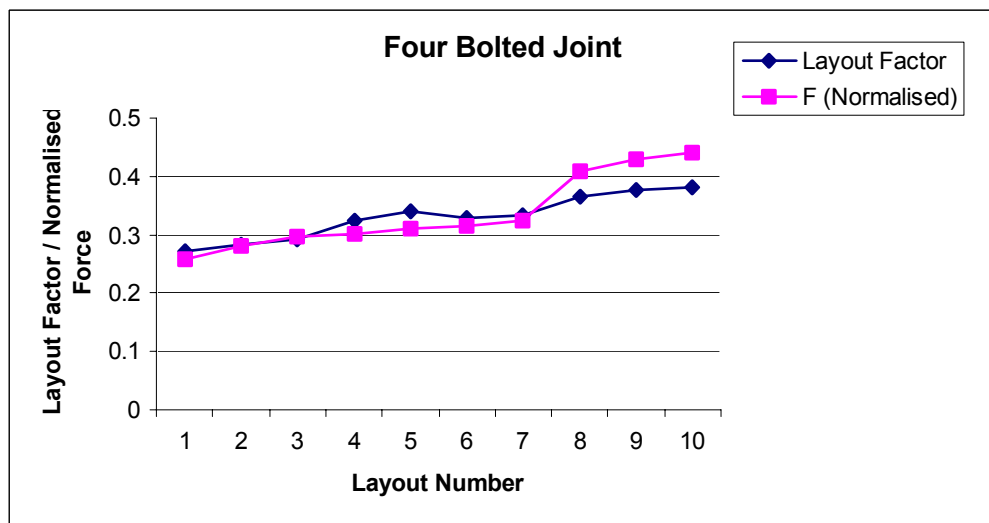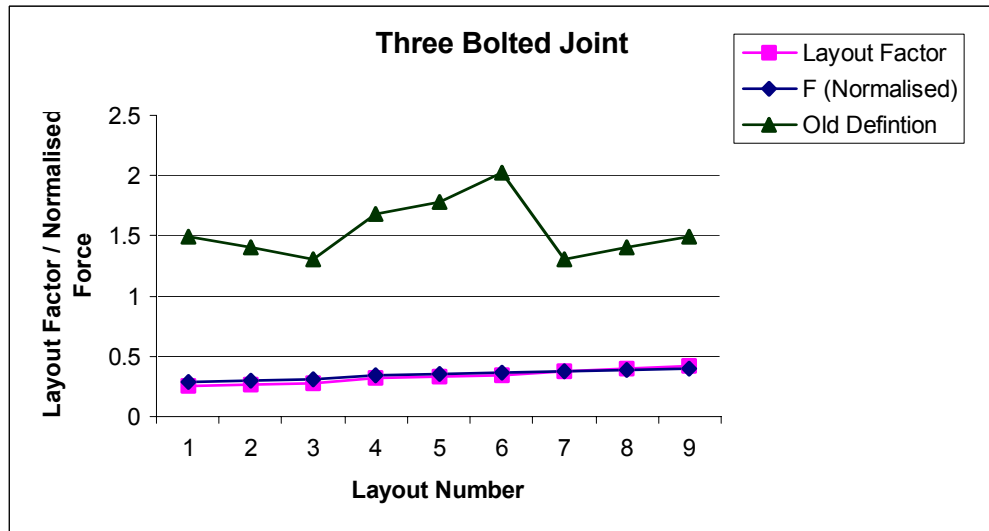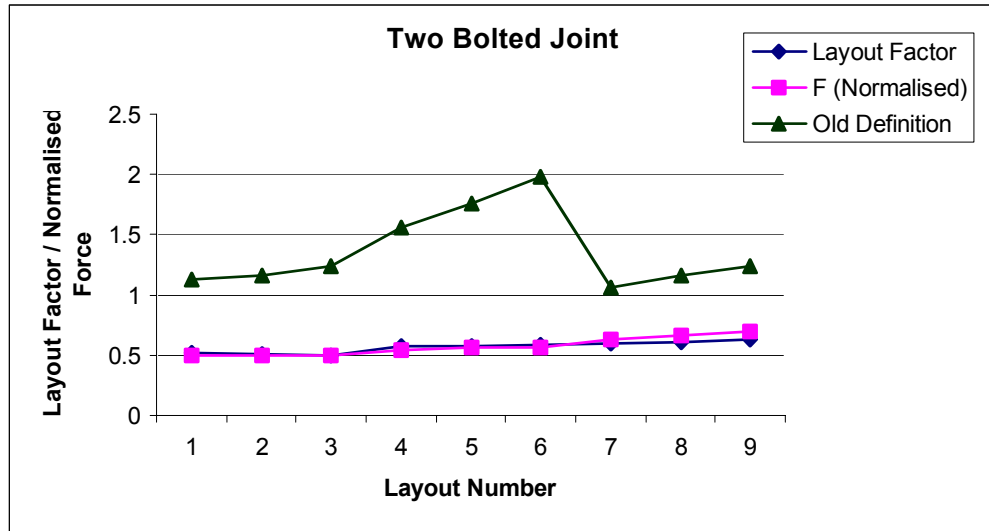
Figure 4.16: Graphs for $\overline{\overline{F}}$ and β for 2,3 and 4 number of bolts
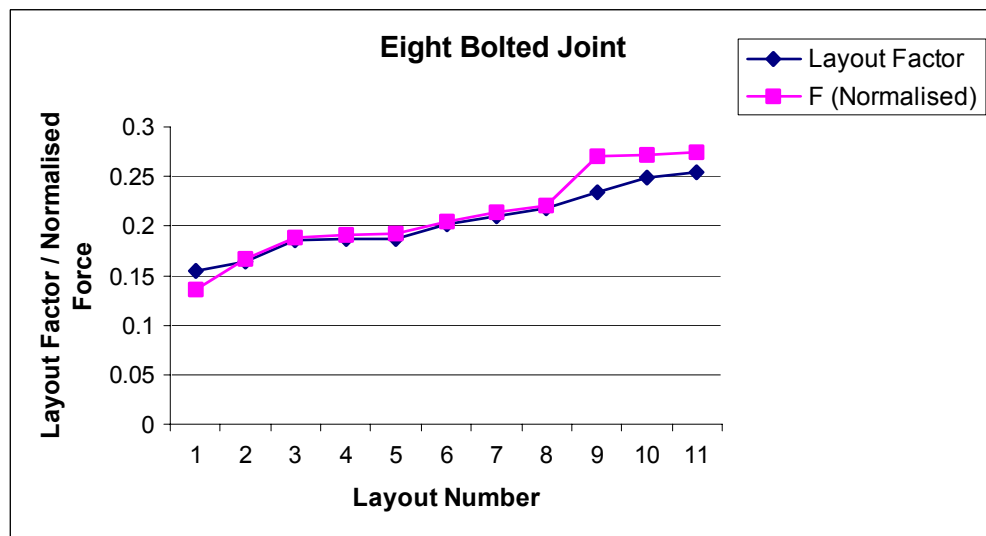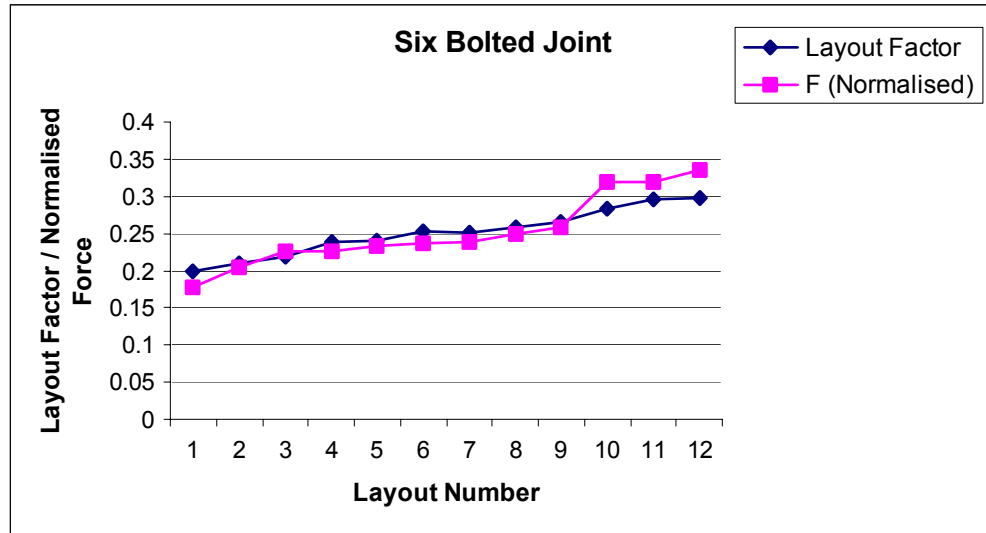
Figure 4.17: Graphs for $\overline{F}$ and β for 6 and 8 number of bolts
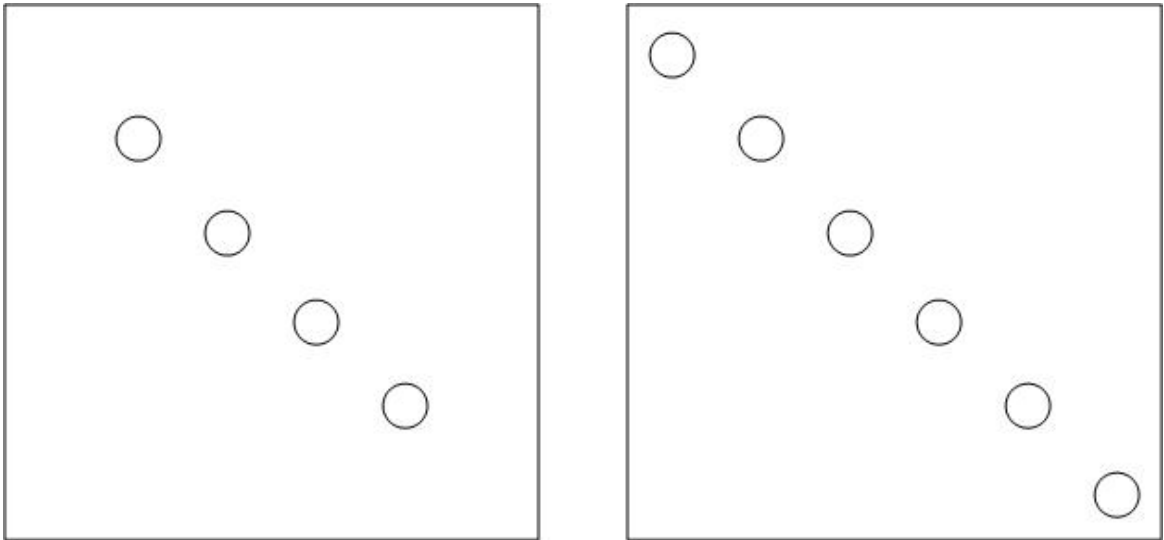
Figure 4.18: Four and six bolted layout (equal spacing)
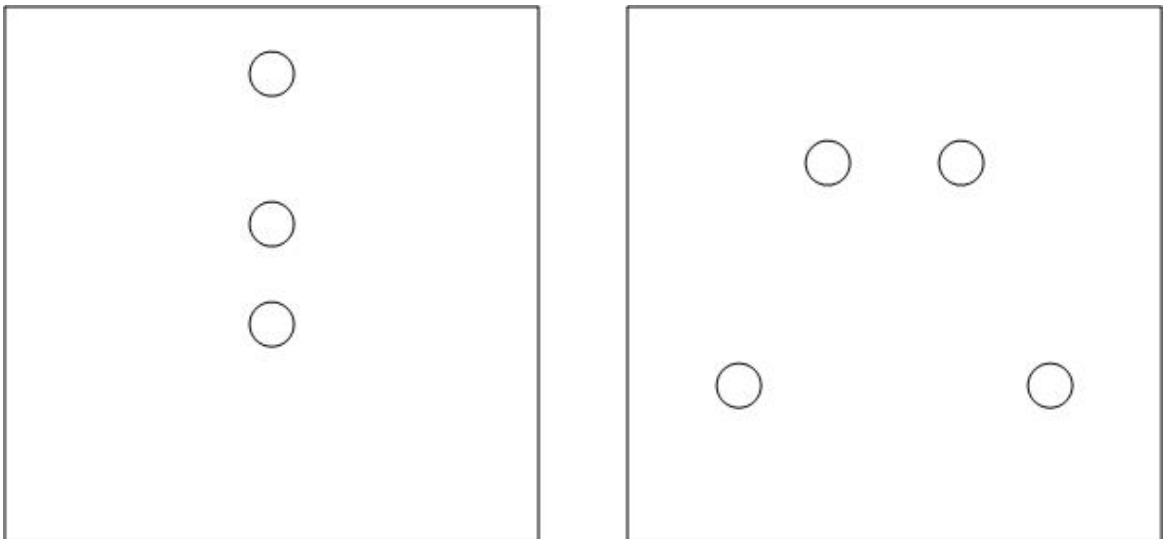
Figure 4.19: Three and four bolted layout (variable spacing)

Highlighted values in table 4.8 indicate the results of these special tests. It is observed that when the fasteners are equally spaced the values of $\overline{F}$ and β value are in harmony with the trend of the rest of layouts for four and six bolted joints. The value of $\overline{F}$ and β for four-bolted joint is 0.336 and 0.348 respectively. The row above has the lower values and the row below has higher values than this special test result. Same thing can be seen in six-bolted joint. Values of $\overline{F}$ and β being 0.258 and 0.261 respectively. This result also follows the ascending trend of all the six-bolted layout result.

The results of study B show us that when the bolts are not equally spaced then the values deviate from the usual ascending order trend. For three-bolted joint the $\overline{F}$ value is 34% while the relation is telling that 40% load of the applied force is being shared by the critical fastener. For four-bolted joint the difference between the predicted value of load and the actual load is not much but when compared with the other values of layout, it does not follow the ascending order trend.

It can be concluded that the correlation is good for the equally spaced fasteners but cannot be applied when the spacing is not equal.

CHAPTER 5

CONCLUSIONS AND RECOMMENDATIONS

The work includes the analysis of bolted joint under shear and tension loading. Single bolted joint is analyzed by changing the pretension value, clearance between the bolt and bolt holes and coefficient of friction. Effect of bolt layout is studied using a three dimensional four bolted joint analyzed under shear loading. A tool is developed in terms of geometric parameter to identify the critical arrangement. Important conclusions and recommendations for future work derived from this study are given below.

5.1   CONCLUSIONS

5.1.1   One Bolt Model

From the numerical results of shear type and tensile type loading on one bolt model, the following conclusions are drawn.

1.   Pretension, coefficient of friction and clearance, affect the displacement pattern and stress distribution of bolted joint in shear type of loading.

2.   When loaded in shear for supporting plate, maximum value of displacement and stress is at the interface side and the critical point is the upper region of the bolt hole where the bolt is hitting the surface.

3.   When loaded in shear for loading plate, maximum value of displacement and stress is at the interface side and critical point is the lower region of the bolt hole where the bolt is hitting the surface.

4. In shear type of loading maximum displacement and stress value decreases as the clearance is increased.

5. The value of maximum compressive stress increase in case of increasing pretension. This is valid for both tension and shear type of loading.

6. The maximum displacement value decreases as the friction coefficient increases because high value results in more restriction for the motion of the plate.

7. Pretension has dominant effect on the stress in z direction when the joint is loaded in tension. (this is in agreement with the results of experimental studies).

8. Critical regions in the bolt are the regions just below the head of bolt and around first engaged thread.

9. The threads share different loads when loaded in tension. First thread taking the highest of the load.

10. Results of experiment conducted are in agreement with the trend of the numerical results. The region closer to the applied load has high stresses.

5.1.2   Four Bolt Model

Four-bolted joint is analyzed in shear and effect of different arrangements is observed. Conclusions are as follow:

1. The stress distribution and displacement pattern is changed when the arrangement of bolts is changed.

2. The three dimensional analysis helps us to visualize that the stress distribution is not uniform throughout the thickness of the plate.

3. Diamond shape and vertical arrangement show higher stress value. It is concluded that the horizontal and two-row arrangement are better.

4. For all layouts on loading plate, maximum stress region is around the bolthole that is closest to the applied load. This trend is vice versa in case of supporting plate.

5. For all layouts, the bolt that is closest to the applied load has the highest stress. This means that this is the critical bolt.

6. It is also observed that the critical region in the loading plate is the same where the bolt is critical too. So there is relationship between the loading plate and bolts.

7. Experiment verifies the behavior of stress on the plates. The regions around the two bolts that are closer to the applied load have high values of stress as compared to the other two bolts. Same trend is observed in the numerical test. It can be concluded that the load is not equally shared on the bolts.

5.1.3 Other Bolt Layouts

Two-dimensional models are tested by changing the arrangement of bolts. 2, 3 4, 6 and 8 bolted joints are analyzed. Conclusions are drawn.

1 With the increase in the distance from the centroid, the load on the fastener increases in the upper half of the plate (moving towards the loading edge).

2 The load on the fastener decreases as we move away from the centroid in lower half.

3 When arranged horizontally the bolts near the edge share highest loads, and as we move to the center the load decreases.

4 The spread and position of the bolt effects its load sharing capacity.

5.1.4 Layout factor

1   A tool in terms of geometric parameters is developed to predict the maximum load shared by the critical bolt in a layout.

2   The relationship is valid for regular arrangement of bolts in different layouts.

3   The geometric relationship is valid for the non-eccentric loading only. Relationship does not apply to eccentric loading and non regular arrangement of the bolts

5.2   RECOMMENDATIONS

Following are some recommendations for the future work to be carried out on the bolted joint analysis.

1   In the FE model bolt size is remained fixed. It can be changed to see its effect on the mechanical behavior.

2   Two plates are used in current research. Same work can be done by considering three plates. Idea is to study the behavior change with the change in the number of plates.

3   Gasket can be included between the plates mating surface to investigate the gasket pressure. This study is useful in preventing the leaks through the joint.

4   Failure modes are not studied in current work. By investigating the plastic deformation different modes can be studied.

5   Mainly shear and tensile type loading is used in the current study. In bolted joints sometimes forces produce torque. Detailed study incorporating the moment with shear force can be done.

6   In tensile type of loading one-bolt model is analyzed only by changing the pretension. Effect of changing clearance can be investigated.

7   Three dimensional layout effects can be studied by increasing the number of bolts from 4 to higher number of bolts in future. Tensile type of load can also be included in the study.

8   Layout factor is derived for regular and non-eccentric loading. This can be extended to find a geometric factor in case of non-regular and eccentric loading.

Nomenclature

T Torque, N-m

C Empirical coefficient

F_i Pretension force, N

d Outer diameter of the bolt, mm

δ_b Absolute value of the bolt displacement

δ_b' Bolt displacement at nut side of the bolt

δ_b'' Bolt displacement at bolt head side

δ_c Absolute value of the displacement of the members

δ_c' Upper member compression

δ_c'' Lower member compression

Δ_{bc} Grip displacement

k Stiffness, N/mm

k_b Stiffness of the bolt, N/mm

k_c Stiffness of the member, N/mm

F_p Outer applied force, N

F_b Tensional force in the bolt, N

F_c Compressive force acting on the member, N

A_b Major diameter area of the bolt, mm^2

l_b Length of unthreaded portion of bolt in grip, mm

A_c Nominal cross section that is equal to the mean cross section of the two cones, mm^2

l_c Length of the member, mm

E Young's Modulus

E_b Young's Modulus of the bolt

E_c Young's Modulus of the member

α Cone frusta angle, degree

SP Supporting Plate

LP Loading plate

ν Poisson's ratio

μ Coefficient of friction

τ_{max} Maximum shear stress, MPa

σ_z Stress in z-direction, MPa

σ_y Stress in y-direction, MPa

σ_{xy} Shear stress in xy-direction, MPa

D Diameter of the washer, mm

l Length of grip, mm

t Thickness of the frusta, mm

RSQ Correlation coefficient

X Maximum horizontal distance of the fastener from the centroid, mm

Y Maximum vertical distance of the fastener from the centroid, mm

e Minimum distance from the loading edge to the fastener, mm

$\overline{F}$ Normalized force

$\overline{X}$ Non-dimensional X

$\overline{Y}$ Non-dimensional Y

$\overline{e}$ Non-dimensional e

R Position vector

β Layout factor

ψ Power factor

f Dividing factor

n Number of bolts

BIBLIOGRAPHY

[1]   Niemann, G., Maschinenelemente, Vol. 1, Springer Verlag, Berlin, 1975 (in german)

[2]   J. E. Shigley and C. R. Mischke, " Mechanical Engineering Design", Fifth Edition, McGraw Hill, New York, 1989.

[3]   Y. Ito, J. Toyoda and S. Nagata "Interface Pressure Distribution in a Bolted Flange Assembly", ASME paper no.77-WA/DE-11, 1977.

[4]   N. Motosh," Determination of Joint Stiffness in Bolted Connections", ASME Journal of Engineering for Industry, Vol.198, No.3, pp.858-861, 1976.

[5]   Terry F.Lehnhoff and Bradley A.Bunyard, "Effects of Bolt Threads on Stiffness of Bolted Joints", ASME Journal of Pressure Vessel Technology, Vol. 123, pp.161-165, May 2001

[6]   Terry F.Lehnhoff and Bradley A.Bunyard, "Bolt Thread and Head Fillet Stress Concentration Factors", ASME Journal of Pressure Vessel Technology, Vol.122, pp.180-185, May 2000.

[7]   T. Sawa, N. Hugorashi and T. Hiros, "Stress Analysis of Taper Hub Flange With a Bolted Flat Cover", ASME Journal of Pressure Vessel Technology, Vol.119, pp.293-299, August 1997

[8]   M. Tanaka and T. Aoike, "Behavior of Bolted Joints Tightened in Plastic Region", PVP-Vol. 367, Analysis of Bolted Joints, pp.89-95, 1998.

[9]   T. Fukuoka and T. Takaki, "Mechanical Behavior of Bolted Join in Various Clamping Configurations", Journal of Structural Engineering, Vol.120, pp.226-231, August 1998.

[10]   K. Varadi and L. Joanovics, "Non Linear Finite Element Analysis of the Contact, Strain and Stress of a Bolted Nut Washer Compressed Sheet Joint System", Reliability, Stress Analysis and Failure Prevention Issues in Fastening and Joining, Composite and Smart Structures, Numerical and FEA Methods, Risk Minimization, DE-Vol.92, pp.31-36, ASME 1996.

[11]   T. Fukuoka and T. Takaki, "Mechanical Behaviors of Bolted Joint During Tightening Using Torque Control", JSME International Journal, Series A, Vol.41, No.2, pp.185-191, 1998.

[12]   H. Lin, "Three Dimensional Finite Element Analysis of a Bolted Joint", PVP-High Pressure Technology, Vol. 297, pp.93-98, ASME1995.

[13]   N. Andreason, C.P. Mickenley and C. Soutis, "Failure Analysis of Bolted Joints in CFRP Woven Laminates", The Aeronautical Journal, Royal Institute of Aeronautics, pp.393-398, December 1998.

[14]   Abdel Hakim Bouzid and Michel Derenne, "A Simple Method for Analyzing the Contact Stress in Bolted Flange Joints With Non Linear Gaskets", PVP-ASME. Analysis of Bolted Joints, Vol. 382, pp.103-111, 1999.

[15]   J. J. Chen and Y. S. Shih, "A study of the Helical Effects on the Thread Connection by Three Dimensional Finite Element Analysis", Nuclear Engineering and Design, Vol.191, pp.109-116, 1999.

[16]   B. Cao, C. Duang and H. Xu,"3-D Finite Element Analysis of Bolted Flange Joint Considering Gasket Non linearity", Analysis of Bolted Joints, PVP-Vol. 382, pp.1221-126, ASME 1999.

[17]   A. M. Al Jefri, and Ahmed. K. Abdel Latif, "Characteristic of Bolted Joint Under Elastic Loading Conditions", Engineering System Design and Analysis Conference, PD-Vol. 80, pp.173-185, ASME 1996.

[18]   Bishwanath Bose, Zhi Min Wang and Susanta Sarkar, "Analysis of Unstiffened Flush End Plate Steel Bolted Joints", Journal of Structural Engineering, pp.1614-1621, December 1997.

[19]   E. Kerekes, B. Szabo and B. Unger, "Prestressed Bolt Joints Under Dynamical Load", 6th Mini Conference on Vehicle Dynamics, Identification and Anomalies, Budapest, ASME, pp.545-555, November 1998.

[20]   A.T. Wheeler, M. J. Clarke and G.J. Hancock, "FE Modeling of Four Bolt, Tubular Moment End Plate Connections", Journal of Structural Engineering, pp.816-822, July 2000.

[21]   Collin A. Rogers and Gregory J. Hancock, "Failure Modes of Bolted Sheet Steel Connections Loaded In Shear", Journal of Structural Engineering, pp.288-295, March 2000.

[22]   Jerome Montgomery, " Methods of Modeling Bolts in Bolted Joint"

[23]   C.C. Menzemer, L. Fei and T.S. Srivatsan, "Failure of Bolted Connections in an Aluminium Alloy", Journal of Material Engineering and Performance, Vol. 8, pp 197-204,1999.

[24]   B. Hockey, F. Lam and Helmut G.L. Prion, " Truss Plate Reinforced Bolted Connections in Parallel Strand Lumber", Canadian journal of Civil Engineering, Vol.27, pp.1150-1161, 2000.

[25]   C.C. Menzemer, L.Fei and T.S. Srivatsan, " Design Criteria for Bolted Connections Elements in Aluminum Alloy 6061", Journal of Mechanical Design, Vol.121, pp.348-358, September 1999.

[26]   D. Tan and I Smith, "Failure in the Row Model for Bolted Timber Connections", Journal of Structural Engineering, Vol.125, pp.713-718, July 1999.

[27]   N. Andreason, C.P. Mackinlay and C. Soutis, "Experimental and Numerical Failure Analysis of Bolted Joints in CFRP Woven Laminates", The Aeronautical Journal, Royal Institute of Aeronautics, pp.445-450, December 1998.

[28]   Camnho, Bowron and Matthews, " Failure Mechanisms in Bolted CFRP", Journal of Reinforced Plastics and Composites, Vol.17, 1998,

[29]   Swabson, James and Roberto, "Bolted Steel Connections: Tests on T stub Components", Journal of Structural Engineering, Vol.126, pp.50-56, January 2000.

[30]   A. F. M. Arif, A. K. Sheikh and S. Z. Qamar, "A Study of Die Failure Mechanisms in Aluminum Extrusion", Journal of Materials Processing Technology, Vol.134, pp 318-328, March 2003.

[31]   G. C. J. Bart and K. Hanjali, "Estimation of Shape Factor for Transient Conduction", International Journal of Refrigeration, Vol.26, pp 360-367 May 2003.

[32]   V. Seshadri, B. K. Gandhi, S. N. Singh and R K. Pandey, "Analysis of the Effect of Body Shape on Annubar Factor using CFD", Measurement, Vol.35, pp 25-32 , January 2004.

[33]   F. Osweiller, "French Rules for the Design of Fixed-Tubesheet Heat Exchangers", International Journal of Pressure Vessels and Piping, Vol.32, pp 335-354, 1988

[34]   Arif, "Effect of Fastener Layout on the Load Distribution of a Shear Joint using Finite Element Analysis", International Journal of Mechanics based design of Structures and Machines, (Submitted), 2003

[35]   John H. Bickford, "An Introduction to the Design and Behavior of Bolted Joints", Second Edition, Marcel Dekker, New York, 1990.

VITA

NAME: Hassan Khurshid

PLACE OF BIRTH: Wah Cantt, PAKISTAN.

ADDRESS: F-276, St # 27,

                          Officers Colony,

                          Wah Cantt,

                          PAKISTAN.

E-MAIL: hassankim@yahoo.com

                          hassankim77@hotmail.com

EDUCATIONAL QUALIFICATION:

M.S *(Mechanical Engineering)*
April 2004
King Fahd University of Petroleum and Minerals
Dhahran, Saudi Arabia.

B.S *(Mechanical Engineering)*
May 1998
Ghulam Ishaq Khan Institute
Topi, NWFP, Pakistan.